OPTIMIZATION OF IN-SITU GENERATED CO_2 USING CHELATING AGENTS FOR EOR FROM CARBONATE RESERVOIRS

BY

AMJED MOHAMMED HASSAN SHEIKH MOHAMMED

A Thesis Presented to the
DEANSHIP OF GRADUATE STUDIES

KING FAHD UNIVERSITY OF PETROLEUM & MINERALS

DHAHRAN, SAUDI ARABIA

In Partial Fulfillment of the
Requirements for the Degree of

MASTER OF SCIENCE

In

PETROLEUM ENGINEERING

DECEMBER 2015

KING FAHD UNIVERSITY OF PETROLEUM & MINERALS

DHAHRAN- 31261, SAUDI ARABIA

DEANSHIP OF GRADUATE STUDIES

This thesis, written by **AMJED MOHAMMED HASSAN SHEIKH MOHAMMED** under the direction his thesis advisor and approved by his thesis committee, has been presented and accepted by the Dean of Graduate Studies, in partial fulfillment of the requirements for the degree of **MASTER OF SCIENCE IN PETROLEUM ENGINEERING.**

Dr. Hasan S. Al-Hashim
(Advisor)

Dr. Abdullah S. Sultan
Department Chairman

Dr. Abdullah S. Sultan
(Member)

Dr. Salam A. Zummo
Dean of Graduate Studies

Dr. Mohamed A. Mahmoud
(Member)

31/1/16

Date

This work is dedicated to my lovely parents, sister, brother, and my wife.

ACKNOWLEDGMENTS

Glory and praise be to Allah the almighty, first and foremost, for every success I found, and knowledge been developed throughout this work.

Acknowledgement is due to King Fahd University of petroleum & minerals for the scholarship I have been given to complete my master degree in petroleum engineering.

My sincere gratitude goes to my thesis advisor, Dr. Hasan Salman Al-Hashim, for allowing me to join his research activities and for the trust he put on me and for his professional guidance during the course of my thesis work. I would like to extend my thanks to all of my committee members, Dr. Abdullah Sultan and Dr. Mohamed Mahmoud for their valuable comments and contributions.

I would like to thank the department of petroleum engineering represented by the chairman, Dr. Abdullah Sultan, for allowing me to use the department's laboratories and equipment to perform my work. I would also like to thank to Dr. Abdullah Sultan for his valuable support during ordering of the consumables and materials for my thesis work through the Center for Petroleum & Minerals of the Research Institute.

In KFUPM, I would like to express my special thanks to Mr. Abdulrahim Muhammadain for the precious time he spent with me on the core flooding system and for the professional comments he made on my laboratory experiments and the review of results. I would also like to thank Mr. Mr. Abdulsamad Iddrisu who was very helpful during the laboratory experiments

My sincere thanks go to Mr. Assad Barri from the Petroleum Department at KFUPM for his help during preparation and compatibility study of the chelating agent solutions and for Mr. Ahmed Kasha, graduate student from the Petroleum Department, for the time he spent with me on zeta-potential instrument.

I would like to express my special thanks to my friends Ahmed Abdulhamid, Bramasto Adam, Badr Salem Bageri and Ahmed Abdulazeem for their help during the laboratory experiments. Special thanks go my twin Anas Alsiddig Yousif who always stood by my side for more than 8 years.

And no words can ever express my sincere gratitude to my mother, my father, my brothers and sister, and my lovely wife who always stood by my side and gave me the courage to complete my degree.

TABLE OF CONTENTS

LIST OF FIGURES

LIST OF TABLES

LIST OF ABBREVIATIONS

CEOR : Chemical Enhanced Oil Recovery

DIW : De-ionized water

EDTA : Ethylenediaminetetraacetic Acid

EDL : Electrical-double-layer.

EOR : Enhanced Oil Recovery

ICP : Inductively Coupled Plasma

Na_2EDTA : Di-Sodium Ethylenediaminetetraacetic Acid

Na_2GLDA : Di-sodium L-glutamic acid N,N-diacetic acid

NMR : Nuclear Magnetic Resonance

PALS : Phase Analysis Light Scattering

PPM : Parts Per Million

SEM : Scanning Electron Microscope

SW : Synthetic Seawater

TDS : Total Dissolved Solids

UTMN : Uthmania Crude Oil

XRD : X-Ray Diffraction

XRF : X-Ray Fluorescence

ABSTRACT

Full Name : Amjed Mohammed Hassan Sheikh Mohammed

Thesis Title : Optimization of In-Situ Generated CO_2 Using Chelating Agents for EOR from Carbonate Reservoirs

Major Field : Petroleum Engineering

Date of Degree : November 2015

Carbon dioxide in miscible/immiscible flooding has been considered as one of the most effective techniques for enhancing oil recovery, since CO_2 decreases the oil viscosity and reaches the part of formations that many fluids cannot reach it. The main disadvantages of this technology is the availability of natural CO_2 sources, CO_2 transportation system, breakthrough of CO_2 into the producers, the corrosion of wells and field surface facilities, environmental and safety problems. To eliminate CO_2 negative impacts and to hermetic process control, a new method of in-situ generation of CO_2 was proposed.

The goal of this research is to investigate the application of an environmentally friendly and cost effective chelating agent as an enhance oil recovery fluid from limestone reservoir rock by in-situ carbon dioxide generation, and to study the impacts of chelating agent concentration on the optimization of the in-situ carbon dioxide generation. Core flooding experiments were conducted using Indiana limestone core samples under reservoir conditions using different concentrations of chelating agents at the tertiary mode after seawater flooding.

In an attempt to identify the mechanism leading to significant incremental oil recovery, comprehensive zeta potential measurements were performed to investigate the impact of chelating agent solutions on the rock surface charge which might lead to wettability

alteration. Based on the results of this study, it is found that using the chelating agent solutions prepared using synthetic Arabian Gulf seawater change the limestone surface charge to more negative zeta potential values leading to alteration of limestone rock wettability to a more water-wet condition. The presence of crude oil in the solution results in more negative values for the zeta potential, then improves the wettability alteration and therefore more oil recovery can be obtained.

Interfacial tension (IFT) was assessed between different concentration of chelating agent and crude oil, to examine the alteration of IFT due to introduction of the chelating agents. Interfacial tension for oil in deionized water (DIW), oil in seawater (SW), and oil in chelating agent solution showed that, chelating agent solutions can result in better oil recovery than DIW and SW due the lower IFT value, as low IFT means favorable flowing conditions; therefore more oil can be produced. Increasing the chelating agent concentration leads to lower IFT values.

Synthetic Arab-D formation brine with TDS of about 206,911 ppm was prepared to establish the initial water saturation. Synthetic Arabian Gulf seawater with a salinity of 57,285 ppm was prepared to displace crude oil. Dead crude oil (API = 30.77) from Uthmaniyah Arab-D crude oil was used in this study. The compatibility between chelating agents and seawater were investigated over wide range of pH values to determine the minimum pH without precipitations. XRD (X-ray diffraction) and XRF (X-Ray Fluorescence) analyses were performed using crushed Indiana limestone rock to identify the mineralogical and elemental composition of the core plugs.

During all core flooding experiments, the pH value of the produced effluent was changing in a small range and it stabilized at each phase which indicates that, the reactions between chelating agent solutions and the core samples reached the equilibrium state at each phase. Solution pH has significant effect on the oil recovery, the lowest pH is the better since more CO_2 can be produced, no carbon dioxide was observed during EDTA flooding with pH of 6, however in GLDA flooding, the reaction between the carbonate rock and GLDA solutions led to in situ CO_2 generation as it was observed in the effluent, and the amount of CO_2 increased with the GLDA concentration. The optimum concentration of EDTA and GLDA solutions to maximize the oil recovery without severe rock dissolution was the 3wt%, while the best sequential scenario for enhancing the oil recovery can be achieved by flooding with 3wt. % followed by 5wt% for both chelants GLDA and EDTA.

ملخص الرسالة

الاسم الكامل :أمجد محمد حسن شيخ محمد

عنوان الرسالة :تحسين الإنتاج الموضعي لغاز ثاني أكسيد الكربون عن طريق إستخدام العوامل المخلبية من أجل تعزيز إنتاج النفط من المكامن الكربونية

التخصص :هندسة البترول

تاريخ الدرجة العلمية :ديسمبر 2015

يعد إستخدام غاز ثاني أكسيد الكربون من أفضل الوسائل الفعالة لزيادة إنتاج النفط ، حيث يعمل الغاز على تقليل لزوجة النفط و يمكنه الوصول إلى أجزاء واسعة من الطبقات الصخرية. لكن تكمن عيوب هذه الوسيلة في التالي: توفر المصادر الطبيعية لغاز ثاني أكسيد الكروبون بعيدا عن حقول النفط، و وسائل نقل الغاز من مناطق الإنتاج الى حقول النفط ،و تأكل الانابيب و المنشأت النفطية التي يمر عليها الغاز و بعض المشاكل البيئية الأخرى. لتفادي كل هذه المشاكل و الحفاظ على الجوانب الإيجابية ، تم اقتراح طريقة جديدة هي الإنتاج الموضوعي لغاز ثاني أكسيد الكربون.

الهدف الأساسي من هذا البحث هو دراسة إستخدام العوامل المخلبية لزيادة إنتاج النفط من الصخور الجيرية عن طريق الإنتاج الموضعي لغاز ثاني أكسيد الكربون، و من ثم دارسة تأثير تركيز هذه المواد على تحسين إنتاج الغاز موضعيا و بالتالي زيادة إنتاج النفط. تم إجراء عدة تجارب لإزاحة النفط عن طريق مياة البحر و المواد المخلبية بإستخدام صخور جيرية تحت ظروف مماثلة للظروف المكمنية من حيث درجة الحرارة و الضغط.

بالإضافة إلى ذلك، تم إجراء قياسات مكثفة لجهد زيتا لبحث تاثيرات العوامل المخلبية وتراكيزها على الخصائص السطحية للصخور الجيرية. هذه القياسات اظهرت التالي: إن إستخدام العوامل المخلبية يمكن أن يؤدي الى تغير خصائص التبلل الصخري من زيتي الى مائي التبلل ما يزيد إنتاج النفط من المكامن الكربونية. اظهرت المقارنة بين استخدام المياه منزوعة الأيونات و مياه البحر المخففة و محاليل العوامل المخلبية أن إستخدام العوامل المخلبية يزيد من تغير التبلل الصخري من زيتي الى مائي التبلل بصورة أكثر من إستخدام مياه البحر المخففة عند نفس الظروف الأخرى. كما أن وجود النفط الخام يزيد القيم السالبة لجهد زيتا مما يؤشر إلى زيادة التغير إلى مائي البلل و بالتالي زيادة الإنتاج النفطي من هذه الصخور.

تم قياس التوتر السطحي بين النفط الخام و محاليل العوامل المخلبية باستخدام محاليل مختلفة التراكيز ذلك من أجل دراسة تغيرات التوتر السحطي الناتجة من إستخدام العوامل المخلبية. تم قياس التوتر السطحي للنفط الخام مع المياه منزوعة الايونات، و مع مياه البحر و مع محاليل العوامل المخلبية و التي اظهرت أن فعالية العوامل المخلبية في تقليل التوتر السطحي أفضل من المياه منزوعة الأيونات و مياه البحر مما يدل على أن العوامل المخلبية يمكن ان تزيد إنتاج النفط بصور أكثر من مياه البحر و المياه منزوعة الأيونات.

تم قياس الرقم الهايدروجيني للعينات المنتجة من كل تجارب إزاحة النفط بالغمر المائي، و وجد أن الرقم الهايدروجيني يتغير بشكل طفيف مما يدل على أن التفاعل بين المحاليل المحقونة (و التي تشمل مياه البحر و محاليل العوامل المخلبية بتراكيزها المختلفة) و الصخور الجيرية قد وصل إلى حالة الإستقرار و الإتزان في كل مراحل الحقن. لم يتم ملاحظة تكون لغاز ثاني أكسيد الكربون خلال عمليات الغمر باستخدام محاليل العامل المخلبي EDTA عند رقم الهايدروجيني 6، ولكن عند حقن الصخور الجيرية بإستخدام محاليل العامل المخلبي GLDA فإن التفاعل الكيميائي بين الصخور و العامل المخلبي أدى إلى إنتاج كميات كبيرة من غاز ثاني أكسيد الكروبون و إلتي ظهرت بصور واضحة في العينات المنتجة من هذه التجارب، كما أن زيادة تركيز العامل المخلبي أدي إلى زيادة كمية الغاز المنتج. من خلال هذه التجارب وجد أن أفضل تركيز لكل من العاملين المخلبيين هو 3% لأنه يؤدي إلى زيادة إنتاج النفط بصورة فعالة جدا من غير تكوين ثقوب شديدة في الطبقات الصخرية و من غير زيادة كبيرة في تكاليف الإنتاج. كما وجد أن أفضل حقن تسلسلي هو بإستخدام تركيز 3% يتبعه 5% لأنه يؤدي إلى زيادة الإنتاج بصورة إقتصادية.

CHAPTER 1

INTRODUCTION

The oil recovery processes have been classified into primary, secondary, and enhanced oil recovery (EOR) or tertiary processes. The primary production results from the use of energy naturally existing in the reservoir as the main source of displacement energy. Usually after primary production water flooding or gas injection are implemented as secondary recovery. After the secondary recovery become uneconomical EOR processes are used. However many reservoir production operations are not conducted in the specified order.

EOR processes is used to create a favourable conditions for oil recovery, these include reducing the interfacial tension, wettability alteration, oil swelling or oil viscosity reduction. In addition, the EOR processes supplement the natural energy in the reservoir.

Chemical enhanced oil recovery (EOR) includes processes in which chemicals are injected to improve oil recovery. Chemical methods are one of three categories of EOR, the others being thermal and miscible. A number of liquid chemicals are commonly used in chemical enhanced oil recovery, including polymers, surfactants, and hydrocarbons solvents.

1.1 Chemical Enhanced Oil Recovery Processes

The main purpose of the chemical processes is to reduce the interfacial tension between the displacing liquid and oil, so more oil can be recovered. The most chemicals used in oil industry are the polymers which are used to recover oil and to increase the water viscosity thereby decreasing the viscous fingering and allowing control on the mobility ratio, so it enhances the macroscopic sweep efficiency. Recently a combination of more than two types of injectants has shown significant promise (Green and willhite, 1998).

Using carbon dioxide in reservoir flooding is considered as one of the most effective techniques for enhancing oil recovery. However, CO_2 flooding process experience gravity override and viscous fingering which decrease the sweep efficiency. Therefore, many investigators were motivated to look for foam techniques, which involve the injection of CO_2 with solution of a CO_2-foaming agent (Chang and Grigg, 1999). The main disadvantages of this technology is the availability of natural CO_2 sources, corrosion of wells and field surface facilities environmental and safety problems, to eliminate CO_2 negative impact and to hermetic process control in-situ generation of CO_2 was proposed.

In this study chelating agent was investigated to optimize the in situ generation of carbon dioxide in carbonates which leads to decrease of the residual oil saturation and therefore improves the oil recovery, through altering the rock wettability and reducing the interfacial tension (IFT) between the crude oil and the injected fluids.

1.2 Objectives

The main objective of this study is to investigate the chelating agents (EDTA and GLDA) as an EOR chemical fluid to improve oil recovery through in-situ generation of carbon dioxide in carbonate reservoirs.

To achieve these objectives, core flooding tests using EDTA and GLDA after seawater flooding were performed at reservoir conditions. Different concentrations of EDTA and GLDA were tested in order to optimize the additional oil recovery. The specific objectives are:

1. To investigate the in-situ Carbon dioxide generation using chelating agents after seawater flooding.
2. To study the effect of chelating agent concentration on optimizing the in-situ carbon dioxide generation in carbonates.
3. To study the effect of in-situ carbon dioxide generation on increasing oil recovery.
4. To better understand the mechanism leading to incremental oil recovery using EDTA and GLDA in carbonate reservoirs.

1.3 Thesis Organization

The organization of this thesis is as follows:

Chapter 1: Presents an introduction to this research and summarizes the objectives of the study.

Chapter 2: Summarizes the literature review covering rock wettability classification, chelating agents and the chelation chemistry of these chemicals, and the previous methods used to generate CO_2 in-situ. Also this chapter presents a review of the formation damage due to precipitation in limestone formations and the permeability change during CO_2 injection into carbonate reservoirs.

Chapter 3: Presents experimental materials used in this study as well as the methodology followed to achieve the stated objectives. The experimental procedures of zeta potential, interfacial tension and core flooding are discussed in this chapter.

Chapter 4: This chapter presents all the results of different experiments conducted during this study with detailed analysis and discussion.

Chapter 5: Presents the conclusions and recommendations for future studies in this area of research. In addition, all measured data in the current study are tabulated in the Appendixes.

CHAPTER 2

LITERATURE REVIEW

2.1 Rock Wettability Concept

Rock wettability can be defined as the tendency of one fluid to spread on or adhere to a rock surface in the presence of other immiscible fluids, in reservoir engineering the fluids are oil, water or gas while the solid surface is the reservoir rocks (Craig, 1971). The rock wettability plays significant role in the estimation of the residual oil saturation and the ultimate oil recovery during the water flooding operations. The wettability of the rock can be indicated by using the contact angle technique and/or zeta-potential (ζ) measurements. For oil/water system, if the contact angle is ($0\text{-}75^{o}$) the rock is water wet, ($75\text{-}115^{o}$) intermediate, and ($115\text{-}180^{o}$) oil-wet (Anderson, 1986). Reservoir wettability can be altered from water wet to more oil wet by adsorption of polar compounds or deposition of organic materials from crude oil. This alteration will affect the relative permeabilities and oil-water capillary pressure therefore impact the water flooding process. The wettability alteration depends on the oil composition, the brine water chemistry and the type of mineral on rock surface (Alotaibi and Nasralla, 2011).

Figure 1 shows the fluids distributions in pore spaces, the smallest pores and narrow channels are occupied by the wetting phase while the largest pores are filled with non-wetting phase, in case of water-wet oil droplets remain in the center of the pores, if the

surface is oil-wet reverse condition holds, and for mixed-wet case water has been displaced by oil from some surfaces and some still some oil droplets in the center of water-wet part, even so all the cases have the similar oil and water saturations (Abdallah et al., 2007).

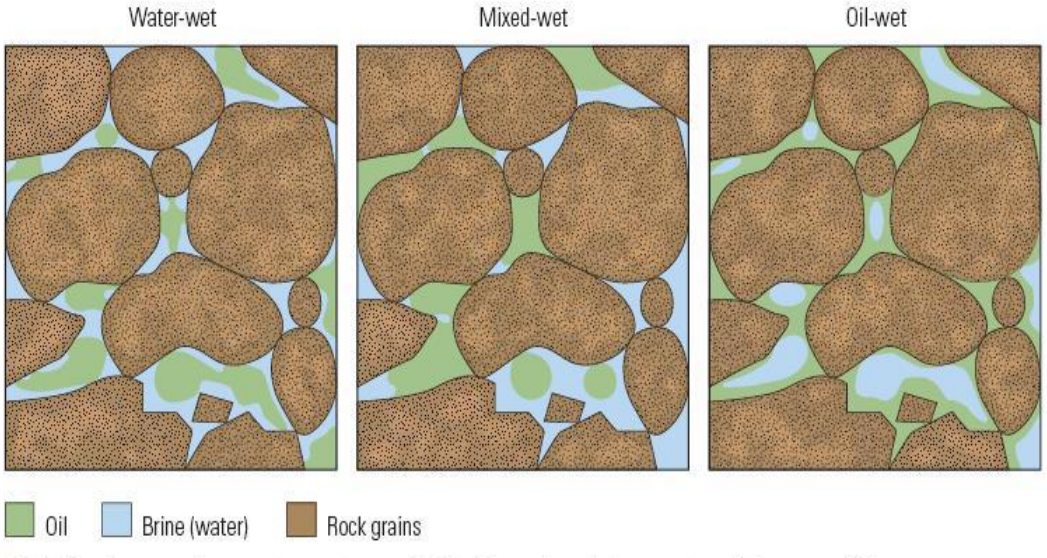

Figure 1: Fluids Distributions in Pores, Water-wet "Left", Mixed-wet "Middle" and Oil-wet "Right". After (Abdallah et al., 2007)

2.2 Zeta-Potential (ζ)

Zeta potential or Electrokinetic is a physical property which is exhibited by any particle in suspension. It can be used to optimize the formulations of emulsions and suspensions. The time needed to produce trial formulations can be reduced by utilizing the information given by the zeta potential measurements. It is also has a significant role in predicting long-term stability, (Zhang and Austad, 2006).

It usually refers to the electric potential at the outer limit of the boundary layer, often called shear plane of slipping plane whose location in the electric double layer is difficult to be defined precisely. This makes zeta potential an ambiguous measure of the potential

at the surface of the particle. The stability potential of the suspension can be evaluated using the magnitude of the zeta potential. If all the particles in the colloidal system have a low positive or negative zeta potential then there will be no force to prevent the particles coming together and flocculating. However, if the particles have large zeta potential values then there will be no tendency for the particles to come together and they will tend to repel each other (Hiemenz, 1977).

For carbonates, interactions between the rock surface and the potential determining ions (Ca_2^+, Mg_2^+ and SO_4^{2-}) result in wettability alteration. Zhang et al., (2007) demonstrated that, the potential determining ions present in seawater are able to influence the surface charges of the carbonate and alter the rock wettability to a more water-wet condition and help releasing more oil.

Rodriguez and Araujo (2006) reported that, in the aqueous media calcite minerals display complex behavior due to its solubility, which is governed by the chemical equilibrium and the electrical charge of the rock surface. Alotaibi et al., (2011) mentioned that, in high salinity solutions carbonate particles have positive charges. Also, other investigators found that calcite had positive charges in aqueous solutions (Yarar and Kitchener 1970; Siffert and Fimbel 1984). However, some researchers reported negative surface charges for calcite rock (Douglas and Walker 1950; Smani et al., 1975).

Douglas et al., (1950) used an electro-osmotic technique to evaluate the surface charge of pure Iceland Spar (which is crystallized form of calcium carbonate) against CO_2-water saturated solution, they found negative values for zeta potential, and they attributed these negative values to the severe solubility of the rock surface mainly the leaching of Ca^{2+}

ions for rock surface. Berlin and Khabakov (1961) stated that, the sign of zeta potential is dependent mostly on the excess availability of calcium or carbonate ions when the calcium carbonate was precipitated in the solutions. Ney et al., (1973) showed that, the calcium hydroxide ions can define the sign and the intensity of the electrical surface charge.

Somasundaran and Agar (1967) postulated the hydrolysis phenomena of the dissolved ions (especially Ca^{2+} and CO_3^{2-} ions) or of the rock surface can determine the behavior of the rock surface. Smani et al., (1975) reported that the hydrolysis can govern the surface charge of carbonate ions. Foxall et al., (1979) showed that, the potential determining ion of carbonate formations is the calcium.

Alotaibi et al., (2011) characterized the electrokinetics potential of limestone and dolomite suspensions to establish the reaction mechanisms at the rock/water interface. They used a phase analysis light scattering (PALS) technique to measure the electrokinetics force of carbonate particles in low and high saline brines over a wide range of ionic strength, pH, and temperature. They stated that, the zeta potential of the carbonate rock can be affected by; surfactant concentration, solution pH, and the ionic strength.

In addition, Alotaibi et al., (2011) concluded that, reducing the brine salinity can lead to more negative charges on limestone and dolomite surface by extending the thickness of the electrical-double-layer (EDL), surface charge of limestone rock is significantly affected by the concentration of calcium ions in the solution, and less negative values of zeta potential was obtained for limestone particles in high saline water. In summary, the

adjustment of rock surface charge from positive values to negative can alter the carbonate wettability from preferentially oil-wet to water-wet (Alotaibi et al., 2011).

2.3 Interfacial Tension (IFT)

Interfacial tension is a measurement of the cohesive force present at the fluids interface. In case of two immiscible liquids in contact with each other, the molecules at the surface of both of these liquids experience unbalanced forces of attraction. These unbalanced forces at the surface of separation between the two immiscible liquids (i.e., at the interface) give rise to interfacial tension. It can be defined in the same way as the surface tension.

Surface tension is an important factor in the phenomenon of capillarity. A very useful technique for measuring the interfacial tension is the spinning-drop method. It is especially suitable for measuring ultra-low interfacial tensions in presence of surfactant mixtures, which are used in micro-emulsions. Drop shape can also be analyzed to determine the interfacial tensions (Ghosh, 2009).

Alkaline flooding is an enhanced oil recovery (EOR) process in which alkali is injected during a flooding process to enhance the oil recovery by improving microscopic displacement efficiency. During the flooding, alkaline agents react with acidic components in the oil to form soap. This soap acts as a surfactant and reduces the interfacial tension (IFT) between the crude oil and the injected fluid into the reservoir. The soap also can change the rock wettability as well as help in reducing the adsorption of other chemicals in the injection fluid by the reservoir rock, (Hirasaki et al., 2011).

The disadvantage of alkaline flooding rises when the injected brine contains high concentrations of divalent cations (especially calcium and magnesium ions), so the increase in pH can result in severe scale formation. Furthermore, conventional scale inhibitors are typically ineffective at these elevated pH conditions. To avoid scale formation, consequent plugging, and other problems, water treatment methods such as water softening/desalination can be used.

Ultralow interfacial tension (IFT) values have been achieved using mixtures of petroleum sulfonate and alcohol (Hill et al., 1973; Foster 1973; Cayias et al., 1977). Also the effect of changing temperature, salinity, and oil composition on the interfacial tension were studied. Healy et al., (1976) demonstrated the relationship between the IFT and the behavior of micro-emulsion solutions.

Mahmoud et al., (2015) introduced a new chemical EOR method that uses chelating agents such as EDTA, HEDTA, and DTPA at high pH values. They studied the effect of chelating agents on surface and interfacial tension by measuring the interfacial tension at room temperature and atmospheric pressure using Du Nouy ring method in which a ring made of platinum was used. They concluded that, using chelating agents at high pH values reduced the IFT between the aqueous solution and crude oil, and increasing the chelating-agent concentration decreased the IFT.

2.4 Definition of Chelating Agent

Chelating agent is a chemical compound which forms a chelate with metal ions. There are many types of chelating agents, however; the common chelating agents used in petroleum industry are the aimnopolycarboxylic acid chelating agents. Fredd and Fogler

in 1997 were the first authors demonstrated the chelating agents as stimulating fluids, and they have shown that, chelating agent like EDTA does not induce asphalt precipitation and results in negligible corrosion; therefore it does not required chemical additives (Fredd and Fogler., 1997).

In some cases, fracture acidizing is undesirable to avoid shale break or maintain the natural boundaries to prevent gas or water production, matrix acidizing by using HCl at low injection rate will result in face dissolution or complete dissolution of formation rock near the well bore, but it consumes large volumes of acid to obtain small penetration. To avoid this problem, weak acids (like acetic and formic acid) and chemically retarded acids (such as micro-emulsion systems of external oil and HCl) have been used (Abrams et al., 1983). The retarded acid diffuses in the carbonate surface therefore the live acid can penetrate deeper in the rock. Aqueous HCl or/and nitrogen gas were used as foamed acids to prevent spending of the acid outside the primary dissolution channel, which promotes wormholes growing (Fogler et al., 1992).

Uses of HCl as stimulation acid faced by many problems, firstly, precipitation of asphaltic sludge from crude oil which causes severe formation damage; therefore, variety of additives (such as corrosion inhibitors ,anti-sludging agents and ion-reducing agents) have been used to prevent sludging problem, and to control the stimulation effectiveness compatible combination of additives are needed. Secondly, poor understanding of the chemistries complexity involved in the precipitation reactions. HCl is not effective at low pH values, because of asphaltene and corrosion problems, and face dissolution at low rate, researchers have looked for alternative stimulation fluids which overcome these problems. One of these alternative fluids is Ethylenediaminetetraacetic acid (EDTA)

which can be used to stimulate carbonate formations. EDTA is one of most effective chelating agents that can sequester the metal components of the carbonate matrix. The mechanism of dissolution differs from HCl because of the advantages of H^+ ions attack and chelation of metal ions at low pH (non-acidic conditions).

Second alternative fluid is HEDTA which is abbreviation for Hydroxyethylene-diaminetriacetic acid; this acid has been observed as an active solvent in limestone acidizing for different values of pH at high temperature up to 400 °F (Frenier et al., 2001). In addition, Hydroxyethyliminodiacetate (HEIDA) salt was also developed for use as oilfield stimulation fluids (Frenier et al., 2003). However; HEIDA is much more biodegradable than EDTA and HEDTA.

Glutamic acid diacetic acid tetrasodium salt (GLDA) is a new generation chelating agent. GLDA is marketed as Dissolvine® GL and both names will be interchangeably used. GLDA has been produced from sustainable and natural materials, to improve the chemical products and to reduce the cost effectively. It has high solubility over a wide pH range and readily biodegradable. Compared to NTA and EDTA, GLDA shows better performance in cleaning the hard surface. In addition, it is suitable in the personal care and cosmetic industries because it does not sensitize human skins or eyes which make it a far more effective chelating agent.

GLDA is a greener alternative to other commercially available chelating agents. GLDA has the smallest ecological footprint, and a significant portion of it comes from monosodium glutamate; an amino acid used as a food flavor enhancer and made from the

fermentation of sugar. Moreover, it shows good stain removing properties and has better biocidal boosting power.

GLDA forms more stable complexes with metal ions compared to other types of chelants. GLDA complexes hard water ions and retains its high chelating value at higher temperatures in comparison to other chelates. They are more significantly efficient because they have a stronger affinity for metals, and stable over a wider range of pH and temperatures. Studies show that Dissolvine® GL biodegraded can be classified as readily biodegradable, and is expected to have a low bioaccumulation potential, (AkzoNobel Functional Chemicals Product Stewardship). Table 1 and Figure 2 show different types of chelating agents and their structure (Szilágyi, 2007).

Table 1: Different types of chelating agents. After (Szilágyi, 2007).

EDTA	Ethylenediaminetetraacetate
HEDTA	Hydroxyethylethylenediaminetriacetate
EDDA	Ethylenediaminediacetate (generally N,N'-)
EDMA	Ethylenediaminemonoacetate
IMDA	Iminodiacetate
CDTA	Cyclohexanediaminetetraacetate
GLDA	L-glutamic acid-N,N-diaceticacid
DPTA	Diethylenetriaminepentaacetate
MIDA	Methyliminodiacetate
NTA	Nitrilotriacetate

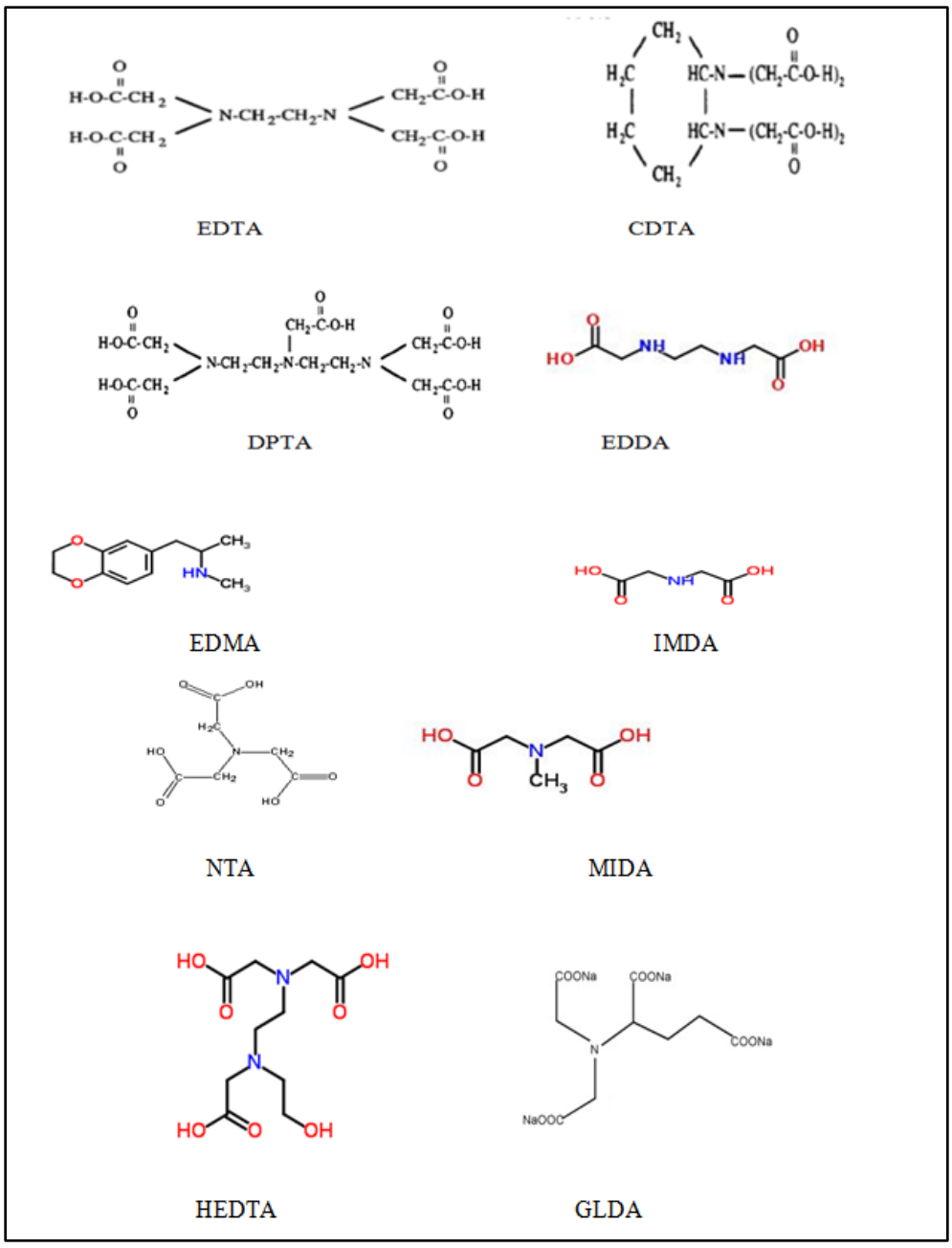

Figure 2: Structure of different types of chelating agents. After (Szilágyi, 2007; Mahmoud et al., 2010)

2.4.1 Chelation Chemistry

Chelating agents have been considered as organic molecules with negatively charges which able to form a stable ringed compositions or chelates by combining with metal ions

(M^{+n}). These chelates have superior stability, therefore they prevent the metal ions from reacting with other species, as a result of that, chelating agents have valuable applications such as water softening, titration of metal ions and inactivation of metal ions.

The ionic species distribution depends on the constants of equilibrium for the chemical reactions and the pH value of the solution. The equilibrium constant is the ratio of the chelated metal ion in equilibrium with the free metal ion and the chelating agent in solution, given by equation (2). When chelating agents react with calcium or magnesium they show high equilibrium constant (log K values above 8). Table 2 shows stability constant for CDTA, DTPA, and EDTA chelating agents. The ionic distribution for species such as CDTA, DTPA and EDTA obtained at room temperature are illustrated in Figure 3,(Fredd and Fogler., 1997).

$$\mathbf{M^{+n} + Y^{-4} \Leftrightarrow MY^{(n-4)}} \quad \ldots\ldots\ldots\ldots \quad (1)$$

$$\mathbf{K_{MY}} = \frac{[\mathbf{MY^{(n-4)}}]}{[\mathbf{M^{+n}}][\boldsymbol{Y^{-4}}]} \quad \ldots\ldots\ldots\ldots\ldots \quad (2)$$

Table 2: Stability constants for CDTA, DTPA, and EDTA chelates. After (Fredd and Fogler., 1997)

	Log K_{MY}		
Chelates / Metal Ion	CDTA	DTPA	EDTA
Calcium	12.3	10.34	10.59
Magnesium	11.34	8.92	8.69
Strontium	9.84	9.34	8.63
Barium	7.63	-	7.76

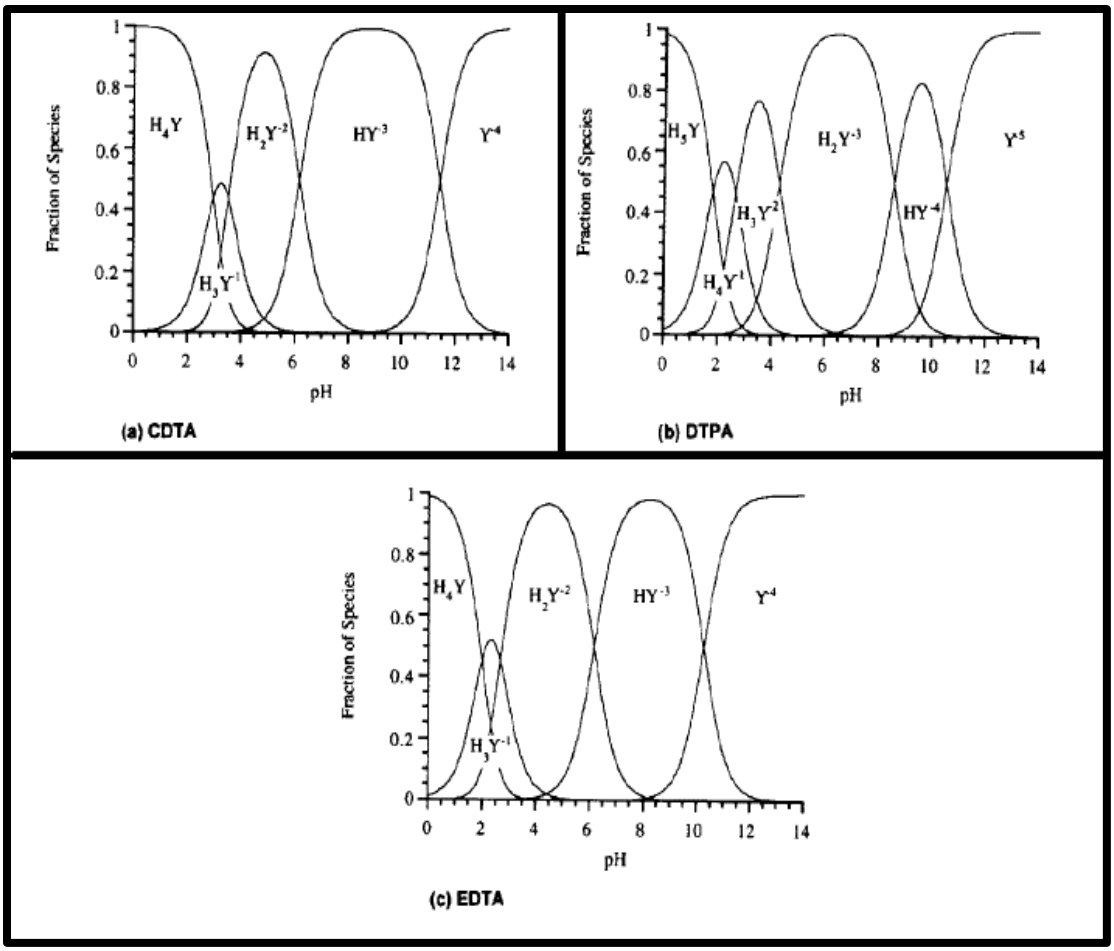

Figure 3: Distribution of ionic species of (a) CDTA, (b) DTPA, and (c) EDTA at room temperature. After (Fredd and Fogler., 1997)

In acidic medium calcite dissolved as follow:

$2H^+ + CaCO_3 \Leftrightarrow Ca^{+2} + H_2CO_3^*$ …… (3)

Where $H_2CO_3^*$ symbolizes $H_2CO_3 + CO_2$ (aq).It was found that, the calcite dissolution by HCl is limited at temperature above 0^oC. In neutral conditions, the calcite dissolution depends on many factors such as mass transport characteristic of the medium and the characteristics of the heterogeneous reactions at calcite surface. Under these environments three reactions are occurred simultaneously as follow:

$2H^+ + CaCO_3 \Leftrightarrow Ca^{+2} + H_2CO_3$ …….. (4)

$H_2CO_3^* + CaCO_3 \Leftrightarrow Ca^{+2} + 2HCO_3^-$ ……. (5)

$H_2O + CaCO_3 \Leftrightarrow Ca^{+2} + HCO^{3-} + OH^-$ …….. (6)

Present of chelating agents in the solution results in sequestering of the free calcium ions, which can be represented as:

$Ca^{+2} + Y^{-4} \Leftrightarrow CaY^{-2}$ …… (7)

EDTA has been used to remove the minerals from clay accumulations during carbonates dissolution in high pH conditions (10-12 pH), because this chelating agent prevents destroying clay species, (Fredd and Foglar, 1997). In addition EDTA has been utilized in removing the scale of calcium carbonate from sandstone formations and in dissolving dolomite ($CaMg(CO_3)_2$), anhydrite ($CaSO_4$), calcite ($CaCO_3$), magnesite ($MgCO_3$), apatite and gypsum ($CaSO_4 \cdot 2H_2O$).

2.5 In-Situ CO_2 Generation

Using carbon dioxide in miscible/immiscible flooding is considered as one of the most effective techniques for enhancing oil recovery, since CO_2 decreases the oil viscosity and reaches the part of formations that many fluids cannot reach it. However, the disadvantage is that CO_2 has very low density and viscosity when compared to the crude oil, consequently, CO_2 flooding process experience viscous fingering and gravity override decrease the sweep efficiency. Therefore, many investigators were motivated to look for foam processes, which involve the injection of CO_2 with solution of a CO_2-foaming agent (Chang and Grigg, 1999).

The main disadvantages of this technology is the availability of natural CO_2 sources, CO_2 transportation system, breakthrough of CO_2 into the producers, corrosion of wells and field surface facilities, environmental and safety problems. To eliminate CO_2 negative impact and to hermetic process control in-situ generation of CO_2 was proposed. The rest of this section summarises the major findings and results from experimental studies carried out to investigate the application of in-situ carbon dioxide generation.

2.5.1 Previous Methods of In-Situ CO_2 Generation

Gumersky et al. (2000) proposed a new technology to enhance oil recovery by in-situ CO_2 generation by using exothermic chemical reaction between low concentrated acid and gas forming water solution. They mentioned that the negative factors accompanied oil displacement by CO_2 can be eliminated by the new technology, these negative factors include corrosion of wells and oil field surface facilities, problems associated with transportation systems, expensive technology, the availability of CO_2 source and environmental impact. Surfactant is used to improve the visco-elastic of water solution; also it minimizes well and oil field equipment corrosion. Gas forming solution creates an additional resistance for the injected water which improves the water flooding efficiency.

However this technology preserves all positive factors of CO_2 flooding, which are increases of water mobility/viscosity when CO_2 dissolved in water, when CO_2 dissolved in oil it reduces oil viscosity, increases oil volume and decreases interfacial tension between oil and water. It was concluded that using of in-situ CO_2 generation technology improves the ultimate oil recovery by 3-5 % and increases the efficiency of water flooding by 20-30 % in comparison with conventional water flooding. At particular

thermobaric conditions major part of generated CO_2 solved in water which creates barrier in the water zones and increases the viscosity of water and the sweep efficiency, while the rest of CO_2 mixes in unlimited proportions of oil.

Laboratory studies displayed that, at certain pressure and temperature (super-critical condition) the gases, such as carbon dioxide, behave like liquids since the density of the compressed gas increases sharply till it reaches the liquid density, while the gas viscosity remains constant, as presented in Figure 4. Two functions can be carried out by carbon dioxide at super-critical condition; the first is decreasing the viscosity of oil and improving the displacement efficiency by the solvent. The second is that, CO_2 in gas form can enter to places where many solvents cannot enter to and increase the oil displacement.

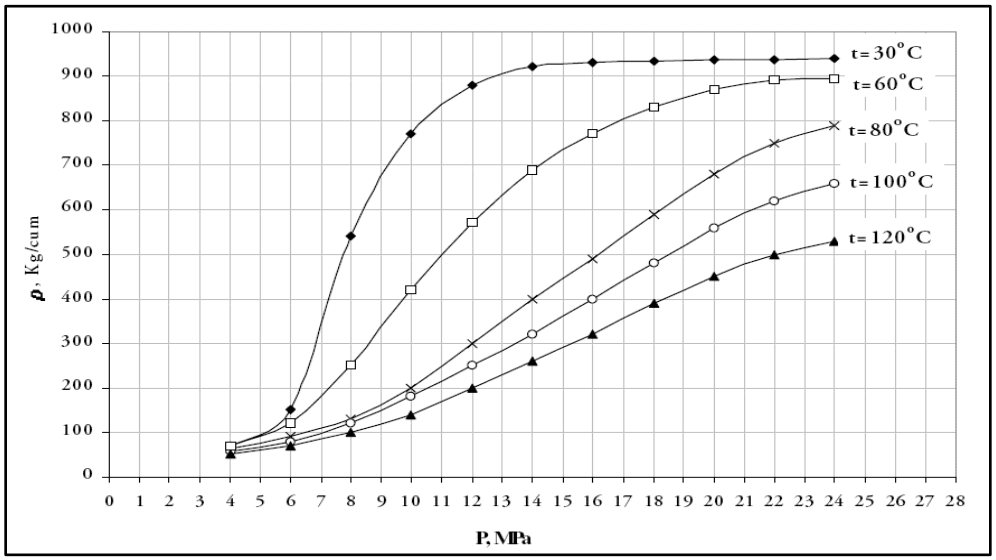

Figure 4: Carbon dioxide density at different temperature. After (Gumersky et al., 2000)

A physical model of two layers (quartz sand as 90% and 10% clay) had been used to compare between the displacement efficiency of the conventional water flooding and the

proposed technology, and it was found that, the new method resulted in additional displacement efficiency of 16 % comparing with displacement by water, when 0.1 PV of gas-forming solutions was used. To determine the thermobaric condition at which CO_2 can be generated Gumersky et al. (2000) conducted special test and their results are presented in Figure 5; the pressure profile consists of two stages. Due to the gas micronucleus forming the pressure increase and then stabilize in the first stage, and in the second stage the pressure decreases sharply when the formed gas micronucleus solved in the system. Figure 6 shows the temperature profile during the test. The new technology of carbon dioxide in-situ generation was conducted in field pilot test. It was found that the oil production from the tested wells started to increase by two times in average, whereas the water production was reduced.

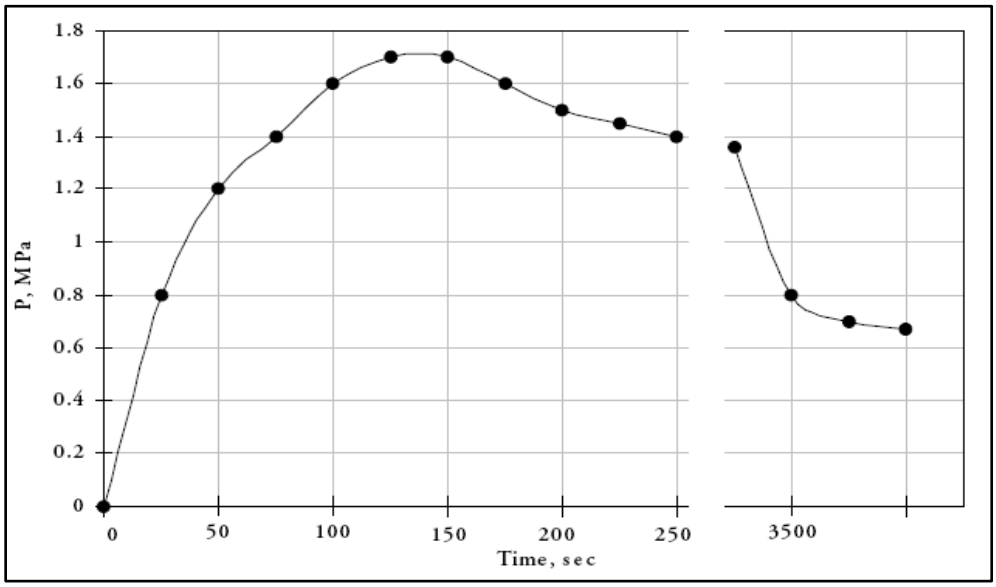

Figure 5: Changes of pressure during gas micronucleus and bubbles formation. After (Gumersky et al., 2000)

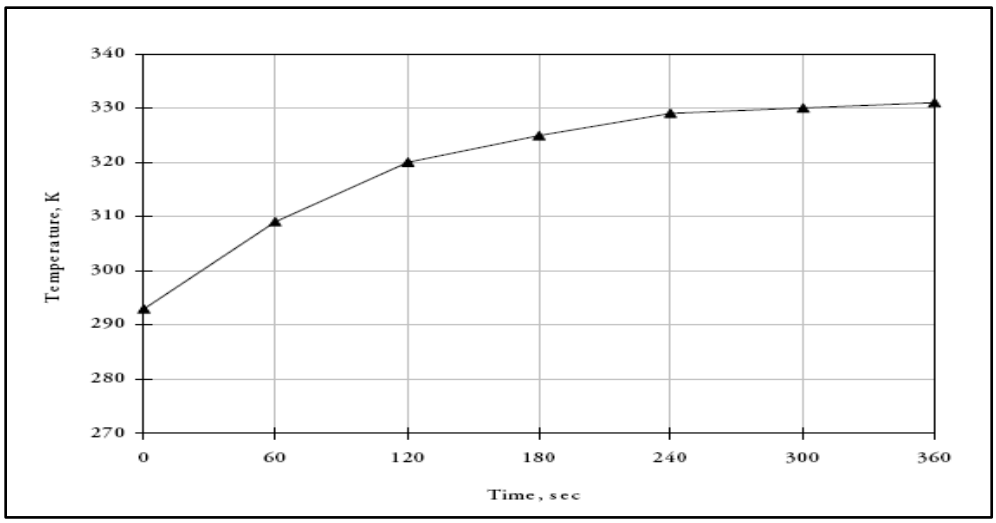

Figure 6: Temperature increase during gas micronucleus and bubble formation. After (Gumersky et al., 2000)

Ben Shiau et al. (2010) investigated the synthesis that can lead to in situ generation of carbon dioxide in order to improve the oil recovery. They generated a considerable amount of CO_2 from ammonium carbamate at 85^{o}C which can improve the oil recovery by about 10% compared to traditional chemical flooding, and they noted that, the oil properties (especially the viscosity and colour) are changing by the generated carbon dioxide.

In general, the most effective technologies to capture and separate CO_2 are using the chemical solvent methods, (Wolsky et al., 1986). In the high temperature reservoirs carbon dioxide can be generated from carbamate in surfactant-based system, which result in reducing the oil viscosity and therefore improves the oil relative permeability. Carbamates and bicarbonates can be formed by chemical reaction between CO_2 and solvents like aqueous amines (R_1R_2NH) as follow (Khatri et al., 2006):

$$2\ R_1R_2NH + CO_2 \longleftrightarrow R_1R_2NH_2^{+} + R_1R_2NCOO^{--}\ \text{(carbamate)} \ldots\ldots. (8)$$

$$R_1R_2NH + HO_2 + CO_2 \longleftrightarrow R_1R_2NH_2^{+} + HCO_3^{--} \text{ (bicarbonate)} \ldots\ldots (9)$$

From the reversible reaction, ammonia and carbon dioxide can be generated in high temperature conditions, and the CO_2 is less soluble in water than in oil which leads to significant reduction in oil viscosity. Also the swelling of clay mineral in the reservoir formation is decreased by ammonia and CO_2, which improves the reservoir permeability, (Altunina et al., 2006). This alternative method of in-situ generation CO_2 combined with steam flooding was used in Russia. In this case the oil production rate was increased by 40% on average and the water cut was significantly reduced.

Figure 7 shows the linear relationship between the amounts of CO_2 generated and the concentration of ammonium carbamate solution when 4M HCL and titrate method are used. The same relationship can be obtained at higher temperature (92^oC) as shown in Figure 8. In general, the carbon dioxide generated from the thermal method is less than 30 % in comparison to the acid titration method with temperature of 92^oC, Figure 9. Based on Khatri studies, ammonium carbamate can generate more CO_2 at higher temperature, greater than 100 ^oC, and no carbon dioxide was observed from both methods when methyl carbamate was used, (Khatri et al., 2006). Many combinations of chemical solvents were investigated to optimize the amount of generated CO_2. Figure 10 shows the comparison between polymer/surfactant and polymer/ carbamate/surfactant solvents when 0.1 and 0.3 PV were flooded. It can be clearly seen that, more oil was recovered when polymer/ carbamate/surfactant was used. Based on their results they concluded that, using of carbamate in surfactant system results in ultralow interfacial tension between water and oil which improves the oil recovery.

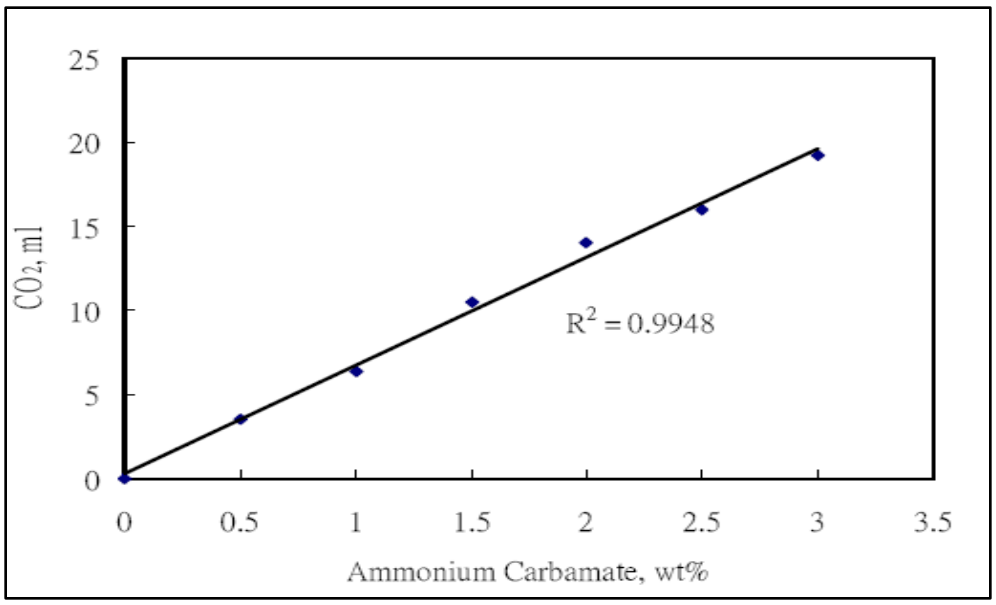

Figure 7: CO_2 measurement of ammonium carbamate using titration method. After (Shiau et al. 2010)

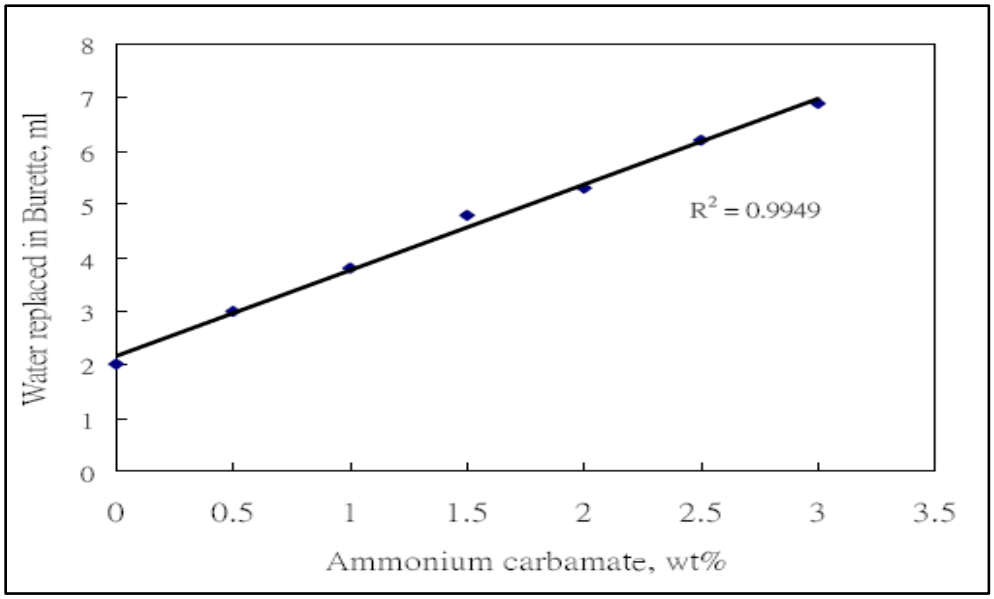

Figure 8: CO_2 measurement of ammonium carbamate using thermal method. After (Shiau et al. 2010)

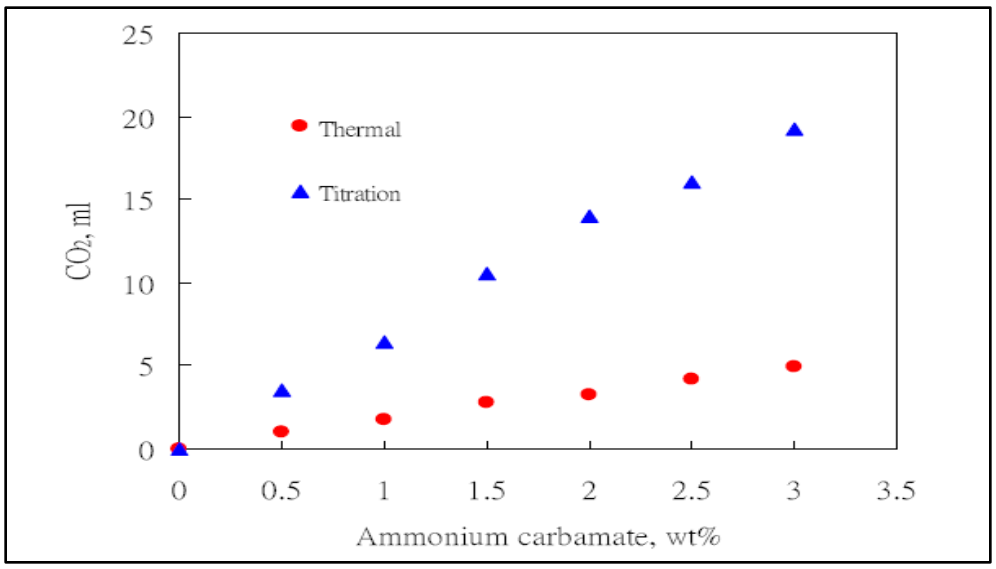

Figure 9: Comparison of CO_2 evolved from titration method and thermal method. After (Shiau et al. 2010)

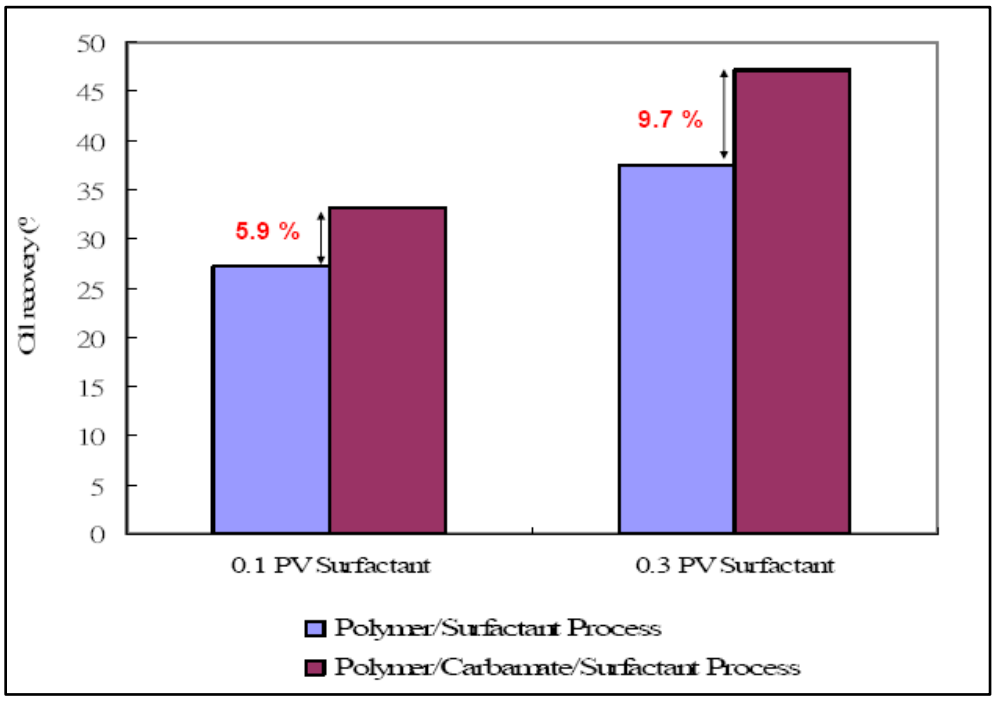

Figure 10: Comparison of polymer/surfactant and polymer/carbamate/surfactant/ processes with different amounts of surfactant flooding (polymer= 0.1 PV and carbamate= 0.5 PV). After (Shiau et al. 2010)

Xiaofei Jia et al. (2013) examined the application of In-situ carbon dioxide generation on SZ Chinese oilfield, which is characterized by high oil viscosity, severe heterogeneity, huge thickness and high permeability. Quick water breakthrough and high water cut were resulted from the severe heterogeneity and unfavourable mobility ratio, Figure 11. Based on lab experimental study, field pilot test of in-situ CO_2 generation was carried out in 2010, significant reduction of injection pressure and effective plugging of the channel between injection-production well were observed besides increasing the oil recovery. In this study, low concentrated acid (hydrochloric acid) was mixed with low concentrated surfactant (sodium carbonate) and polymer to generate CO_2 in high permeable layers through exothermic chemical reaction. When low concentrated acid interacts with polymer, a stable foam barrier will be formed to block layers with high permeability while penetrates into low permeable layers, and it shows visco-elastic properties and displaces oil from them. Surfactant was used to decrease the interfacial tension between the water and oil then reduce the residual oil. An additional oil recovery was achieved when CO_2 dissolved in oil. There are two systems of in-situ CO_2 generation, single-fluid system and double-fluid system. The salt solution with poor thermal stability is injected in single-fluid system, to degrade into CO_2 under the geothermal condition. However, in double-fluid system after injecting the salt solution, low concentrated active acid is used to generate CO_2 by exothermal reaction between the two agents. Figure 12 compares the two systems under the reservoir temperature.

Figure 11: Injecting water breakthrough at the producer. After (Xiaofei Jia et al. 2013)

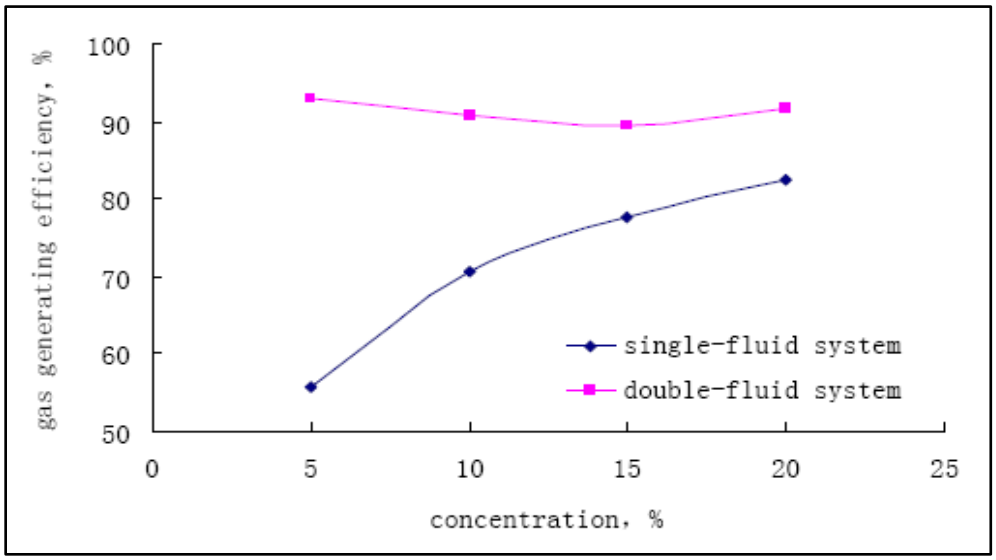

Figure 12: Gas generating efficiency test. After (Xiaofei Jia et al. 2013)

They found that single-fluid system is suitable for high temperature reservoirs, and the gas generation efficiency increases as the concentration of the main agent solution increases. Also they concluded that, double-fluid system requires more additives, like corrosion inhibitor and polymer, because the gas generation efficiency and the reaction speed are high. The crude oil expands as the carbon dioxide dissolve in it, the crude

expansion and the visbreaking results under reservoir condition are shown in Table 3. They used 2010 mPa.s crude oil viscosity at 60^{o}C, 20 % main agent concentration, and original experiment pressure is 10 MPa. They also carried out sand packed tube model to compare the oil recovery from in-situ carbon dioxide generation by both double-fluid system and single-fluid system, Figure 13.

Table 3: Results of the experiment of the expansion and visbreaking After (Xiaofei Jia et al., 2013)

Simulated oil (crude oil: Kerosene)	Increased pressure (MPa)	Increased volume (mL)	Expansion Rate, %	Visbreaking Rate, %
0:1	0.48	4	10.0	38.1
1:1	0.54	5	12.5	42.1
2:1	0.66	8	20.0	48.0
1:0	0.74	10	25.0	52.7

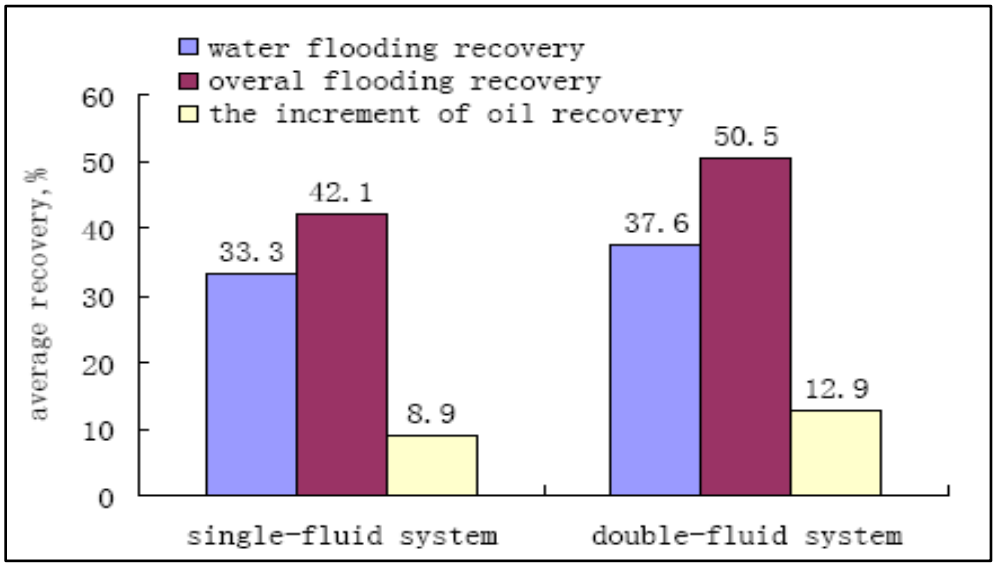

Figure 13: The increment of oil recovery with different injection system. After (Xiaofei Jia et al. 2013)

They concluded that, using in-situ carbon dioxide generation technology results in damage removal and better control of water flooding in strong heterogeneity reservoirs, and the higher oil in place and stronger vertical heterogeneity lead to better results. Also as temperature and system concentration increases the amount of gas generation and then the oil volume will increase.

Mahmoud et al. (2013) and Abdelgawad et al. (2014) investigated the application of In-situ carbon dioxide generation on Indiana limestone by using H_2Na_2EDTA (pH=4.5), H_3HEDTA (pH=2.5) and Na_4EDTA (pH= 12) chelating agents, no additives were used to protect against corrosion since the concentration of the chelating agent was 5 wt%. The experiment was conducted at 100^oC and 0.25 cc/min injection rate. 58% of the initial oil was recovered by seawater flooding i.e. 42% of the oil still inside the core. In addition, 81% of the residual oil (34% of the initial oil) was recovered using one pore volume of 5 wt% H_3HEDTA (pH=2.5), Figure 14. However, flooding operation with very low pH solutions will lead to bulk dissolutions and wormholes due to the interaction between the low pH fluid and the reservoir matrix, as results fine precipitations and formation damage will take a place, which can lead to increase the residual oil saturation and reduce the ultimate oil recovery. Figure 15 compares the oil recovery by H_2Na_2EDTA at pH=4.5 and Na_4EDTA at pH= 12, more than 90 % of the initial oil in place was recovered using the first acid. H_2Na_2EDTA is not powerful as H_3HEDTA in generating CO_2, therefore, more volume of H_2Na_2EDTA is required to recover additional oil equal to that recovered by H_3HEDTA. They concluded that, a proper selection of chelating agent type, PH value, and solvent concentration lead to maximize the oil recovery. Table 4 shows summary of the previous methods to generate carbon dioxide in-situ.

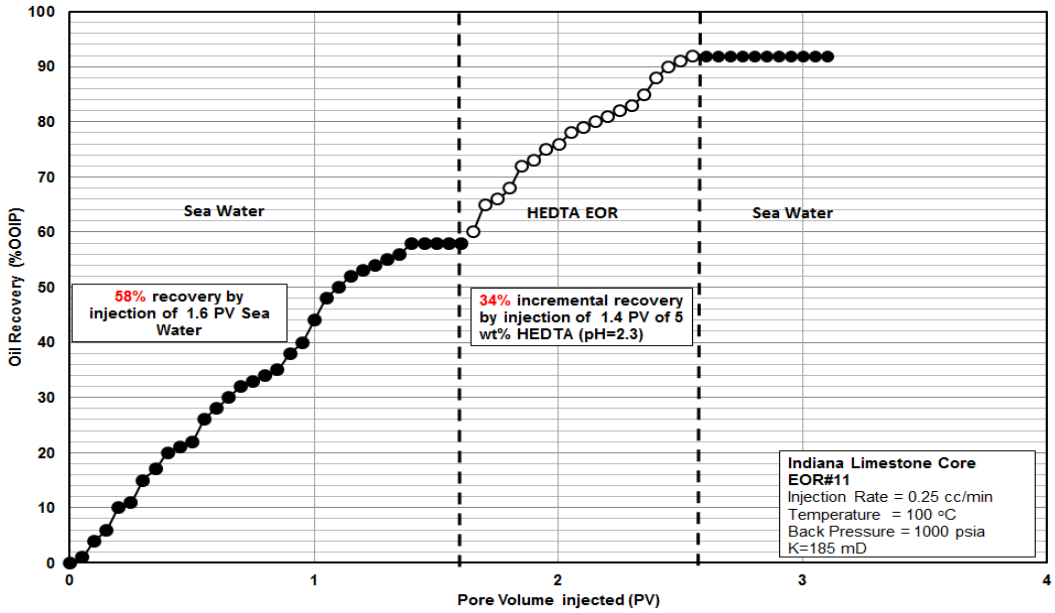

Figure 14: Oil recovery by the in-situ generation of CO_2 using H_3HEDTA, pH=2.5. After (Mahmoud et al., 2013)

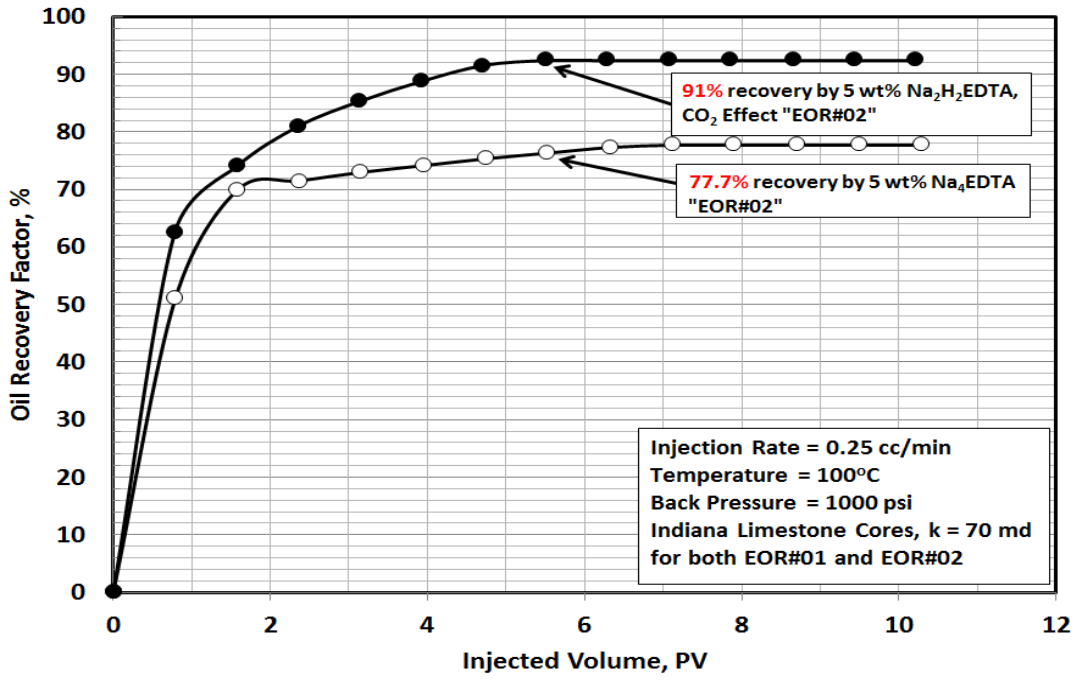

Figure 15: Oil recovery by in-situ generation of CO_2 using H_2Na_2EDTA (pH=4.5) and Na_4EDTA (pH= 12). After (Mahmoud et al., 2013)

Table 4: Summarization of previous methods to generate carbon dioxide in-situ. After ([a] Gumersky et al. 2000, [b] Ben Shiau et al. 2010, [c]Xiaofei Jia et al. 2013, [d] Mahmoud et al. 2013 and Abdelgawad et al. 2014)

Solvent/Chelating Agent type	[a] Sodium carbonate and hydrochloric Acid	[b] ammonium carbamate	[c] hydrochloric acid, sodium carbonate &polymer	[d] H_3HEDTA	[d] H_2Na_2EDTA	[d] Na_4EDTA
Concentration wt.%	-	0.51	20%	5	5	5
pH Value	-	-	-	2.5	4.5	12
Temperature ^oC	60	85	60	100	100	100
Formation Type	-	Berea sandstone	Sand packed tube	Indiana limestone	Indiana limestone	Indiana limestone
Pervious Water-flooding Recovery, %OOIP	-	37.3	37.6	58	58	58
Recovery by Chelating Agent, % OOIP	-	9.7	12.9	34	33	19.7
Recovery , %Residual Oil	-	16	21	81	79	47
Ultimate Recovery , OOIP	-	47	50.5	92	91	77.7
Year	2000	2010	2013	2013	2013	2013
Type of additives	corrosion inhibitor & polymer	corrosion inhibitor & polymer	corrosion inhibitor & polymer	no additives	no additives	no additives
comments	16% increase of displacement additionally to water flooding	0.3PV + deionized water + improve Kro	double fluid system	1.4 PV + seawater	seawater	seawater

2.5.2 The Chemicals used to Generate CO_2 In-Situ

1. **Sodium carbonate and hydrochloric Acid**

Sodium carbonate Na_2CO_3 (also named as soda ash), is one of a carbonic acid salts which can be dissolved in water. It is commonly found as crystals, or as white powder. In general, this salt has been used to neutralize the corrosive effects of high pH and chlorine, Hydrochloric acid (HCl) is a colourless, clear, and highly pungent solution. In addition, this acid is strong, highly corrosive and has many industrial uses. The chemical structure of Na_2CO_3 is shown in Figure 16.

At the first step, sodium bicarbonate ($NaHCO_3$) is generated from sodium carbonate hydrochloric acid as shown in the following reaction:

$Na_2CO_3 + HCl \rightarrow NaHCO_3 + NaCl$ …….. (10)

In the second phase, sodium bicarbonate reacts with hydrochloric acid to release the gas of carbon dioxide

$NaHCO_3 + HCl \rightarrow NaCl + H_2O + CO_2$ ……. (11)

The balanced overall chemical reaction can be shown as the following equation:

$Na_2CO_3 + 2\ HCl \rightarrow 2\ NaCl + H_2O + CO_2$……. (12)

2. **Ammonium carbamate**

Ammonium carbamate can be produced when ammonia reacts with carbamic acid. This salt can be characterized as white solid, slightly volatile at room temperature, and extremely soluble in alcohol and water. The chemical structure of the Ammonium carbamate is shown in Figure 16.

This salt is not stable at high temperature and may return to ammonia and carbon dioxide as follows

$NH_2CO_2NH_4 \rightarrow 2NH_3 + CO_2$ ……..…. (13)

3. **EDTA (H_3HEDTA, H_2Na_2EDTA & Na_4EDTA)**

EDTA is abbretivation for Ethylenediaminetetraacetic acid. It has been used to dissolve limescale, as it is composed of six-toothed (or hexadentate), i.e. it is able to "sequester" metal ions like Fe^{3+} or Ca^{2+}. After being bound by EDTA, these ions will lose their ability to react with other components in the solution. EDTA has been generated as different salts, such as $CaNa_2$EDTA (calcium disodium EDTA) or H_2Na_2EDTA (disodium EDTA).

The structures of chelating agents are typically represented by H_nY where the n hydrogen's are those of the carboxylic acid group. Aminopolycarboxylic acids reach the fully ionized state by losing protons step by step as shown by equation (14) through equation (17) for EDTA or CDTA (Fredd and Fogler., 1997)

$H_4Y \rightleftharpoons H_3Y^- + H^+$ ……..…. (14)

$H_3Y^- \rightleftharpoons H_2Y^{-2} + H^+$ ……. (15)

$H_2Y^{-2} \rightleftharpoons HY^{-3} + H^+$ ……..…. (16)

$HY^{-3} \rightleftharpoons Y^{-4} + H^+$ ……..…. (17)

In the first stage, H_3HEDTA reacts with calcium carbonate to produce Ca_2HEDTA and carbonic acid as shown below:

$H_3HEDTA + 2CaCO_3 \longrightarrow Ca_2EDTA + 2H_2CO_3$ …….. (18)

Carbonic acid is a weak acid that dissociates as.

$H_2CO_3 \rightleftharpoons H_2O + CO_2$ ……. (19)

4. **Citric acid**

Citric acid is an organic acid characterized by $C_6H_8O_7$formula. Citric acid is relatively non-toxic, non-corrosive, non-flammable and is biodegradable (weak acid). This acid has been found as white crystalline powder at room temperature. It can be generated as monohydrate or anhydrous (water-free) forms. Citric acid is an excellent chelating agent, however, it was only used as a stimulation fluid and no one used it before to generate carbon dioxide. During the 1950s, the citric acid was replaced by EDTA which is more efficient in stimulation operations. Citric acid (H_3AOH) ionizes in water stepwise, (Al-Khaldi et al. 2005, 2007,2010).

$H_3AOH \Leftrightarrow H_2AOH^- + H^+$,..... (20)

$H_2AOH \Leftrightarrow HAOH^{2-} + H^+$,..... (21)

$HAOH^{2-} \Leftrightarrow AOH^{3-} + H^+$,..... (22)

$AOH^{3-} \Leftrightarrow AOH^{4-} + H^+$,..... (23)

Al-Khaldi et al reported that, at pH range of 1.8 - 5, citric acid can react with calcite as follows

$2H^+ + CaCO_3 \Leftrightarrow Ca^{2+} + H_2O + CO_2\uparrow$, pH = 1.8 – 5, ... (24)

$H_2AOH^- + Ca^{2+} \Leftrightarrow CaH_2AOH^+$, pH = 1.8 – 5, ... (25)

$Ca^{2+} + 2(CaH_2AOH^+)\ (aq) \Leftrightarrow Ca_3(AOH)_2(s)\downarrow + 4H^+$ ..... (26)

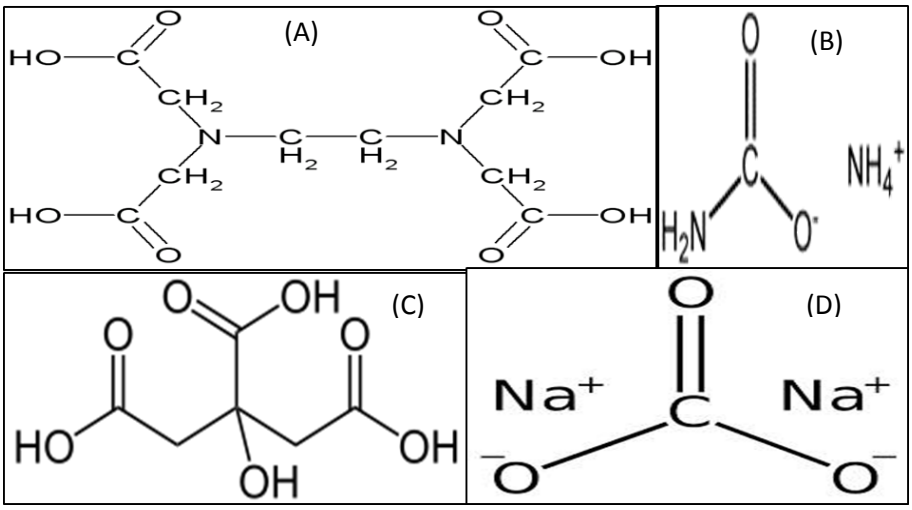

Figure 16: The chemical structure of (A) EDTA, (B) Ammonium carbamate, (C) the citric acid, and (D) Sodium carbonate, From Wikipedia.

2.6 Formation damage due to Precipitation in carbonate Reservoirs

Scale deposition is a common issue in producing oil or gas, which end up with permeability reduction in the area around the wellbore. The reservoir pressure has been maintained by water injection, the incompatibility between the formation water and the injected water leads to inorganic scale precipitations in the surface facilities, flow lines, production tubing and the reservoir formations. However, the most severe and most expensive problem is the precipitations inside the reservoir, (Mahmoud et al., 2013).

Several factors may cause scale formation, the concentration of the solution is the prime factor, especially when the solution becomes super-saturated with minerals (i.e. concentration of minerals exceeds the solution solubility). Others factors include, pressure, temperature, pH value and the partial pressures. (Abu-Khamsin and Ahmad,

2005) devised sound and simple methodology for determining the rate of reaction for scale precipitation in Berea sandstone based on laboratory studies.

Barite ($BaSO_4$), celestite ($SrSO_4$) and anhydrite ($CaSO_4$) are the typical sulfate scales arise when sea water is injected into aquifers/reservoirs. Sulfate precipitation can significantly reduce the formation permeability and therefore the hydrocarbon mobility, (Mahmoud et al., 2013).

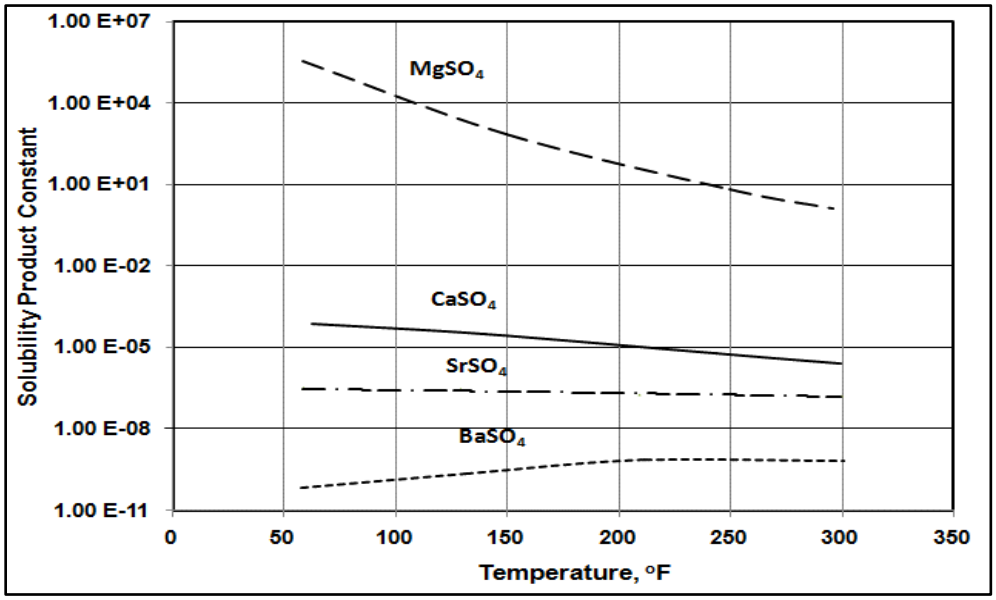

Figure 17: Sulfate Solubility Product Constant. After (Mahmoud et al., 2013)

Figure 17 compares the solubility constant for different sulfate as a function of temperature, strontium sulfate ($SrSO_4$) scale has become a growing concern in oil production systems and it is observed in several wells around the world, since it has very low solubility compared to calcium sulfate, also most of the field scale contains strontium. Figure 18 shows the solubility of strontium sulfate as function of temperature.

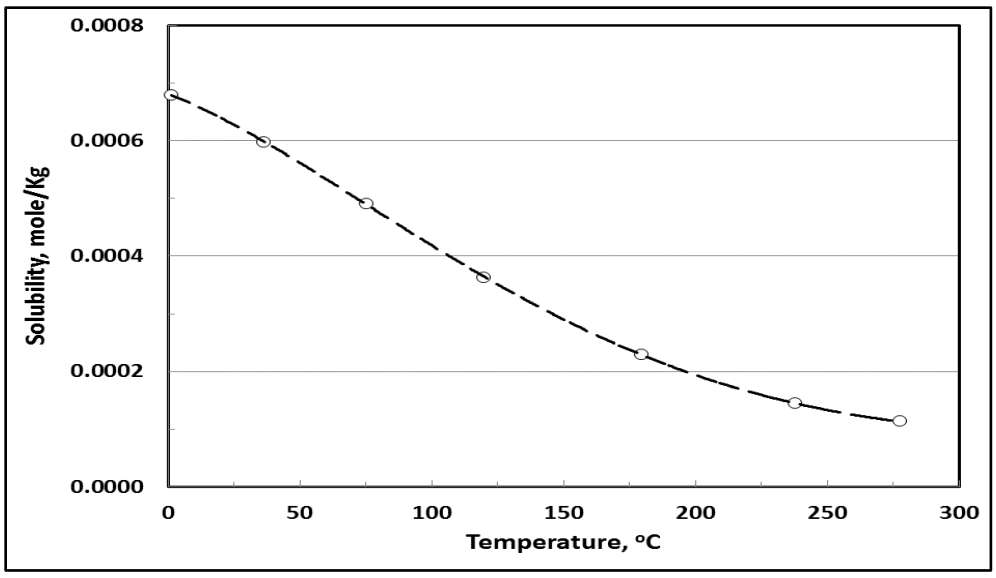

Figure 18: Solubility of Strontium Sulfate as function of Temperature. After (Mahmoud et al., 2013)

Different Chelating agents have been used to prevent the precipitation of calcium sulfate scale. Mahmoud et al. (2013) used EDTA, HEDTA and HEIDA with 1, 5, and 10 wt% concentration at pH=11 to investigate the effectiveness of chelating agents as precipitation inhibitors. High salinity sea water was used for preparing the chelating agent solutions. Berea sandstone and Indiana limestone core samples were used in the core flood experiments; formation brine (connate water) was used to saturate the cores. They found that, EDTA at high concentration (10 wt. %) is the best chelating agent for damage preventing and permeability enhancement in Indiana limestone, Figure 20. Moreover, EDTA with different concentrations was used in Berea sandstone to improve the formation permeability. Figure 21 shows the performance of EDTA in Indiana limestone and Berea sandstone cores. It can be seen from this figure that, the performance of EDTA in Indiana limestone is much better than in Berea sandstone (Mahmoud and Abdelgawad, 2013).

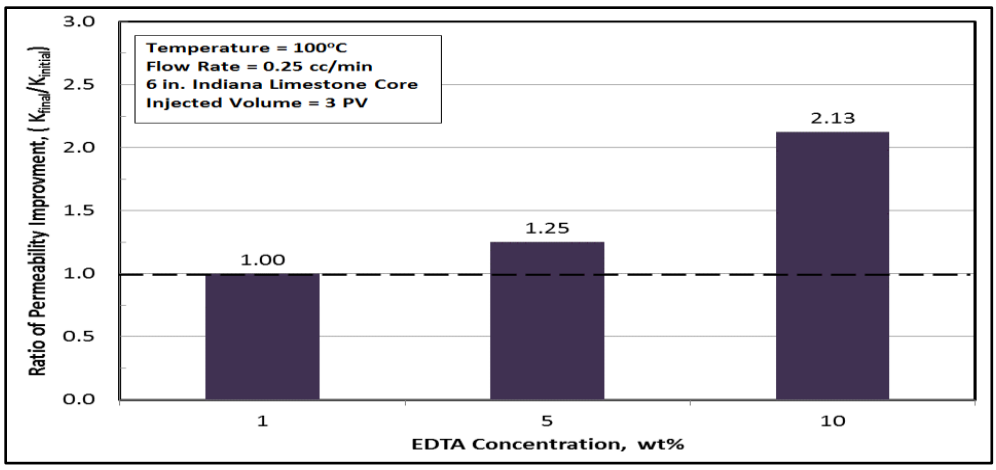

Figure 19: Improvement in permeability of Indiana Limestone cores using different concentration of EDTA at pH=11. After (Mahmoud et al., 2013)

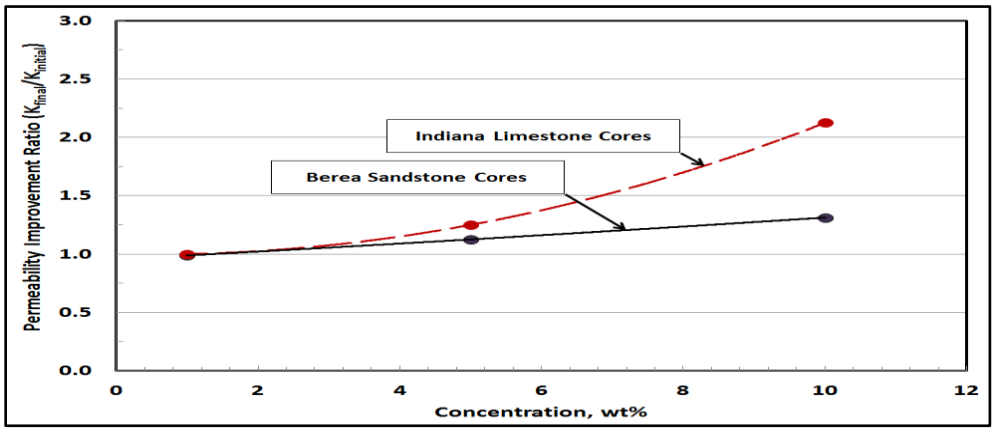

Figure 20: Improvement in permeability using different concentration of EDTA at pH=11 in Berea Sandstone and Indiana Limestone cores. After (Mahmoud et al., 2013)

The pH value has a significant effect on the compatibility between chelating agent and sea water. Based on Mahmoud et al. (2013) experiments, when de-ionized or fresh water is used with EDTA no precipitation was observed for pH values above 4.36. However, using EDTA with sea water at low pH values leads to noticeable precipitation. Therefore, pH values should be greater than 7 to achieve compatibility between chelating agent and sea water to prevent precipitation.

2.7 Permeability Change during CO_2 injection in Carbonate Reservoirs

During CO_2 injection, formation permeability may be changed negatively due to precipitation of calcium carbonate, CaCO3, or positively due to dissolution of carbonate rock (Mohamed et al., 2010). They investigated the back pressure effects on the core porosity and permeability during CO_2 injection, and found that when CO_2 gas injected instead of supercritical CO_2 (i.e. when the back pressure decreases) lead to permeability and porosity enhancement, as shown in Figure 22.

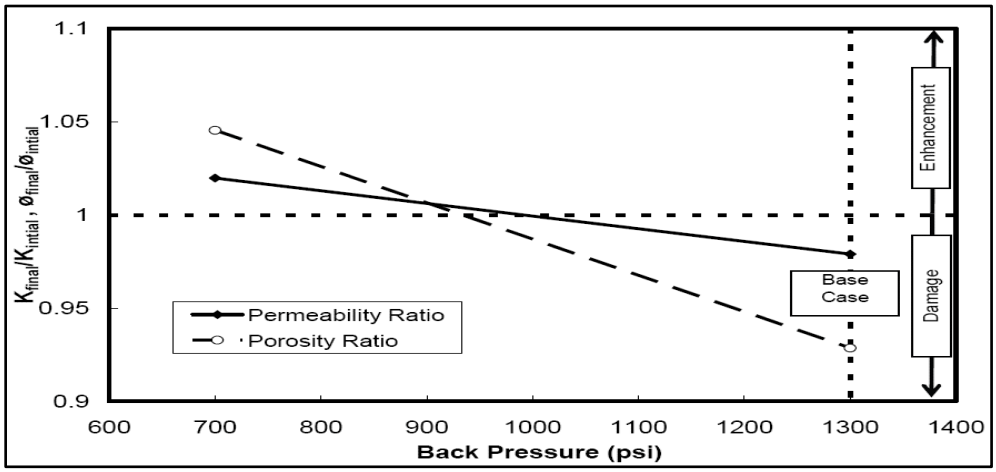

Figure 21: Effect of back pressure on the permeability and porosity after CO_2 injection. After (Mahmoud et al., 2010)

In addition, they studied the effect of CO_2 to water volumetric ratio on core permeability and porosity. Figure 23 shows that as the ratio of CO_2 becomes greater than 2 more permeability enhancement is observed which means less precipitation and then less formation damage. In contrast the core porosity decreases as more CO_2 injected.

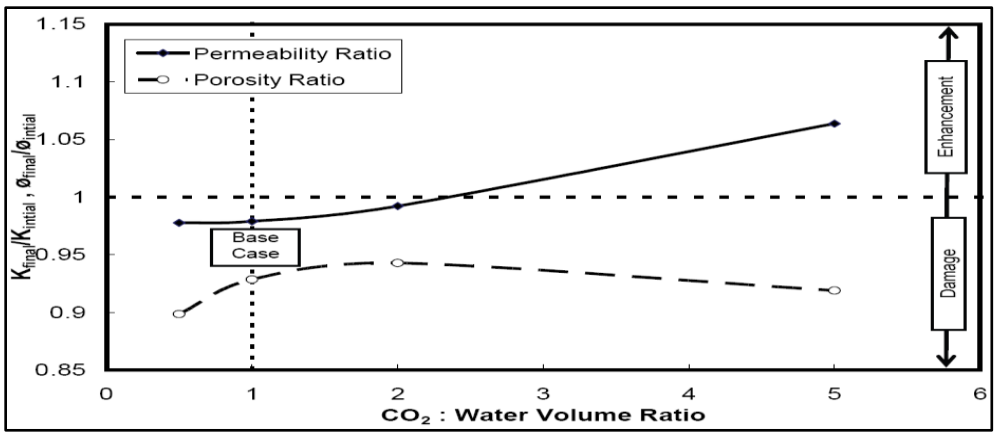

Figure 22: Effect of volumetric ratio on the permeability and porosity after CO_2 injection. After (Mahmoud et al., 2010)

Based on the literature review it can be summarized that, major research on in-situ generation of carbon dioxide was conducted to enhance the oil recovery by only CO_2 flooding without considering the other mechanisms such as wettability alteration or IFT reduction and rock integrity. The maximum incremental oil recovery of 34% OOIP was achieved using in-situ CO_2 generation by injecting EDTA with pH of 2.5 (Abdelgawad et al., 2014), however in oil industry, it is not recommended to flood the reservoir formations with very low pH solutions to avoid bulk dissolutions and wormholes. Therefore, further investigation and evaluation to identify the best conditions for this type of applications is presented in this research.

CHAPTER 3

MATERIALS AND METHODOLOGY

3.1 Experimental Materials

3.1.1 Brine

All brines used in this study were synthetically prepared from analytical grade salts and de-ionized (DIW) water. The ultra-pure DIW water utilized was produced with a Millipore Milli-Q lab water system, and it had a conductivity of 0.055 μS.cm-1 (resistivity of 18.2 MΩ.cm) at 25°C. Synthetic Arab-D formation brine with TDS of about 206,911 ppm was prepared to establish the initial water saturation. Synthetic Arabian Gulf seawater with a salinity of 57,285 ppm was prepared to displace crude oil. The detailed composition of brine solutions are summarized in Table 5. The viscosity and density of seawater were measured as a function of temperature as shown in Figures 23 and 24 respectively.

Table 5: Composition of formation and seawater brines. After (Lindlof and Stoffor 1983, and Jabbar et al., 2013)

Ions	Formation brine (ppm)	Seawater (ppm)
Sodium	62,000	18,043
Calcium	23,314	652
Magnesium	1,268	2,159
Sulfate	250	4,450
Chlor	120,000	31,808
Bicarbonate	79	173
TDS	206,911	57,285

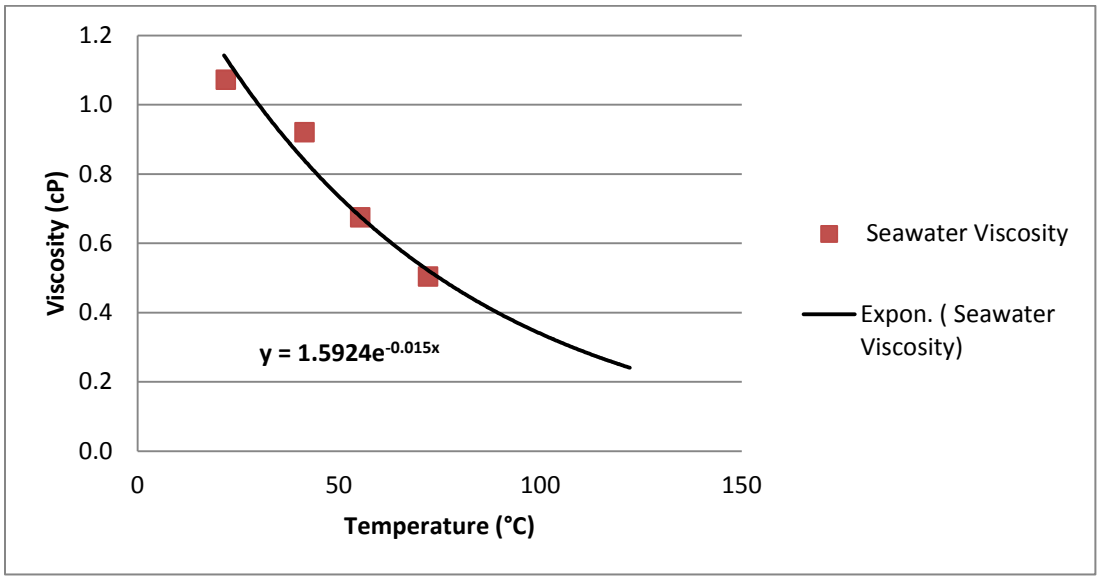

Figure 23: Viscosity of seawater as a function of temperature at atmospheric condition.

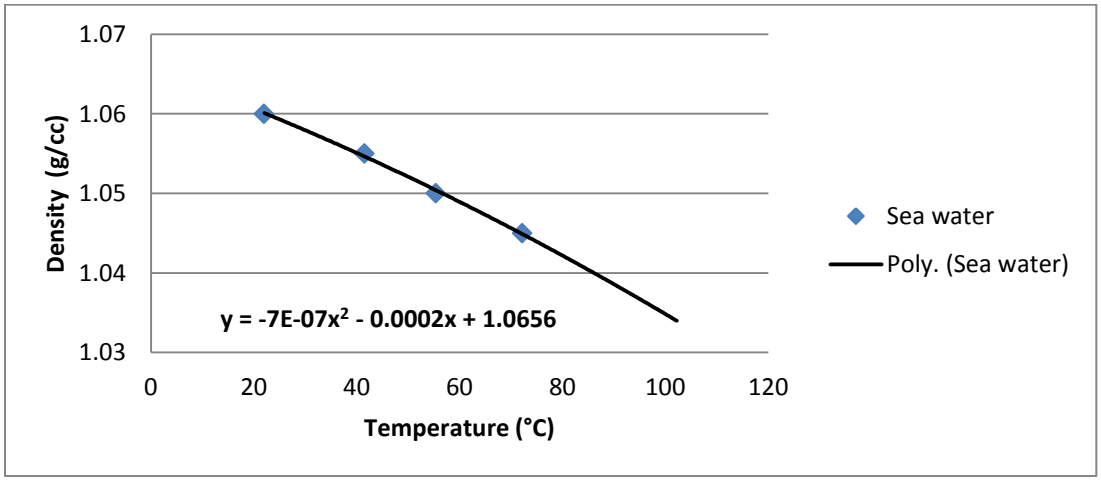

Figure 24: Density of seawater as a function of temperature at atmospheric condition.

3.1.2 Crude Oil

Dead crude oil (API = 30.77) from Uthmaniyah Arab-D crude oil was used in this study, typical oil composition is shown in Table 6. The oil viscosity and density over wide range of temperature were measured as shown in Figures 25 and 26 respectively, and then extrapolated to the reservoir temperature of 100 °C.

Table 6: Composition and properties of Uthmaniyah crude oil

Component	Moles	Moles %
C5	0.00216	1.23
C6	0.007434	4.23
C7	0.018767	10.67
C8	0.027806	15.81
C9	0.025519	14.51
C10	0.025371	14.43
C11	0.019607	11.15
C12+	0.049211	27.98
Density (at 27 ^{o}C)	0.872	
Viscosity (at 27 ^{o}C)	13.06	

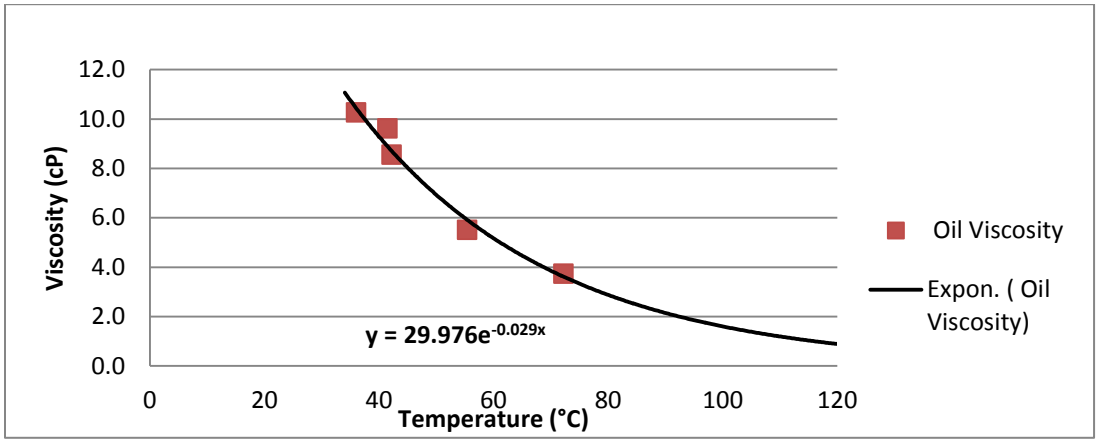

Figure 25: Viscosity of UTMN dead oil as a function of temperature at atmospheric condition.

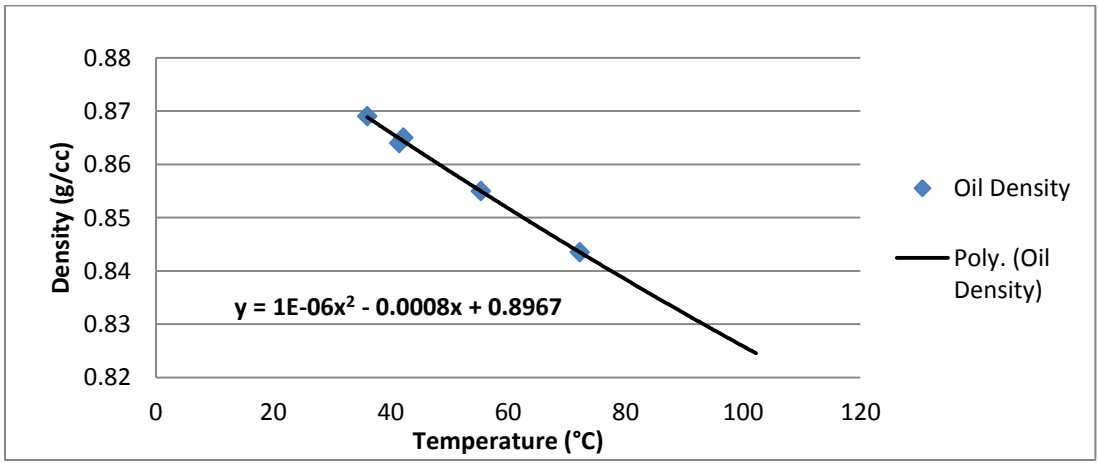

Figure 26: Density of UTMN dead oil as a function of temperature at atmospheric condition.

3.1.3 Chelating Agents

In the current study, Ethylenediaminetetraacetic acid, di-sodium salt (Na_2EDTA) and L-glutamic acid N,N-diacetic acid, di-sodium salt (Na_2GLDA) chelating agents with different concentrations (3wt%, 5wt%, 7wt% and 10wt %) at moderate and low pH were examined as potential chemical flooding fluid for in situ CO_2 generation. The viscosity and density of chelating agents were measured over wide range of temperature and then extrapolated to reservoir temperature of 100°C. The compatibility between the chelating agents and the seawater was first investigated to obtain the minimum pH value without participation.

3.1.4 Compatibility between Chelating Agents and Seawater

Twelve solutions were prepared from EDTA and GLDA using seawater to investigate the compatibility between chelating agents and seawater over wide range of pH values at room temperature. Hydrochloric (HCl) acid and sodium hydroxide (NaOH) were used to adjust the pH. Table 7 and Figures 27, 28 and 29 show the effect of pH on the compatibility of EDTA and seawater, white precipitate was observed for pH less than 5.5, the precipitation increases as the pH value decreases and as the EDTA concentration increases. The highest precipitation was observed at 10 wt. % and pH of 3, increasing the pH value to 7 made the EDTA compatible with seawater and no precipitation was observed. In addition, 5 times diluted seawater was used to prepare EDTA solutions and the same trend was observed, precipitation occurred for all pH values less than 5. These observations show that, EDTA cannot be used with seawater or diluted seawater at low pH values less than 5.

GLDA chelating agent was also investigated at low pH values. GLDA with a concentration of 5wt.% was prepared in seawater at pH= 2.5, 2.9, 3 and 4, and no participation was observed for all samples as shown in Figure 30. GLDA reacts with carbonate formation and generates CO_2 during flooding process and improves the formation permeability.

Table 7: Summary of compatibility tests between EDTA and Seawater

EDTA wt.%	Aqueous Solution	pH	Remarks
5 %	Seawater	7	No precipitation was observed
5 %	Seawater	4	precipitation was observed
5 %	Seawater	2	precipitation was observed
10 %	Seawater	3	precipitation was observed
5 %	5 times diluted seawater	4	precipitation was observed
5 %	5 times diluted seawater	2	precipitation was observed

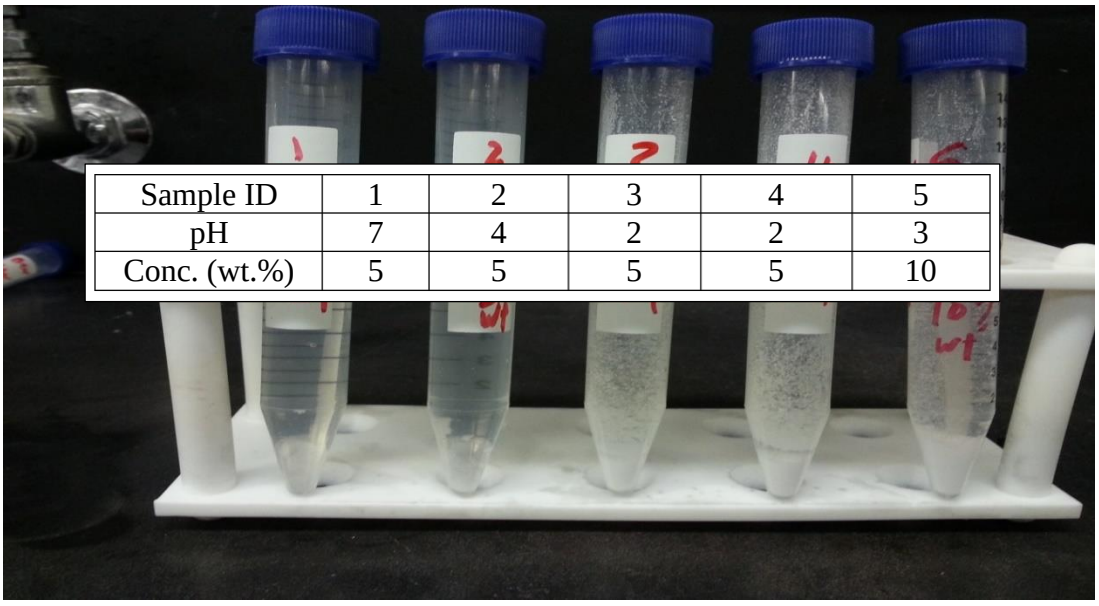

Figure 27: Effect of pH on EDTA/seawater solution compatibility at 23 °C, different EDTA concentrations at pH= 2, 4, and 7.

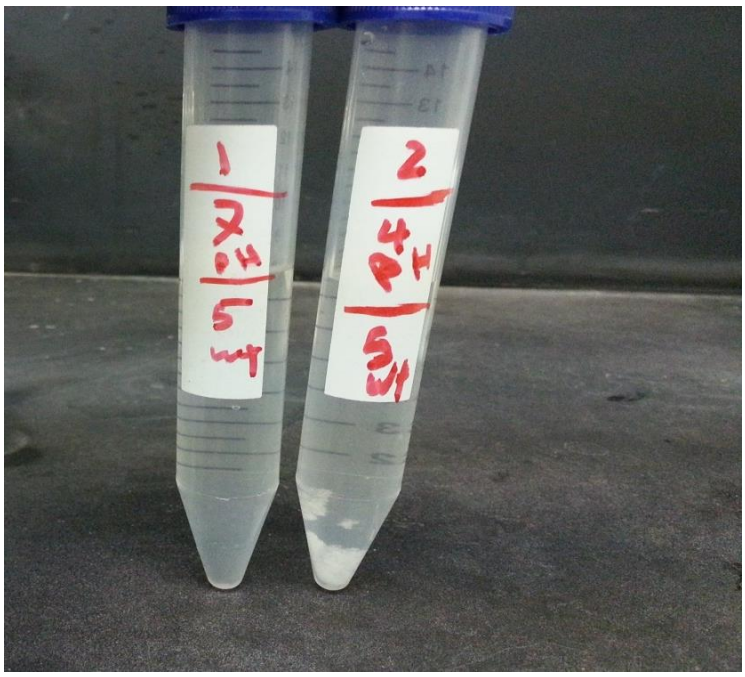

Figure 28: 5 wt. % EDTA in seawater for pH= 7 and 4, at 23°C, no precipitation was observed at pH of 7, while small precipitation was observed at pH=4.

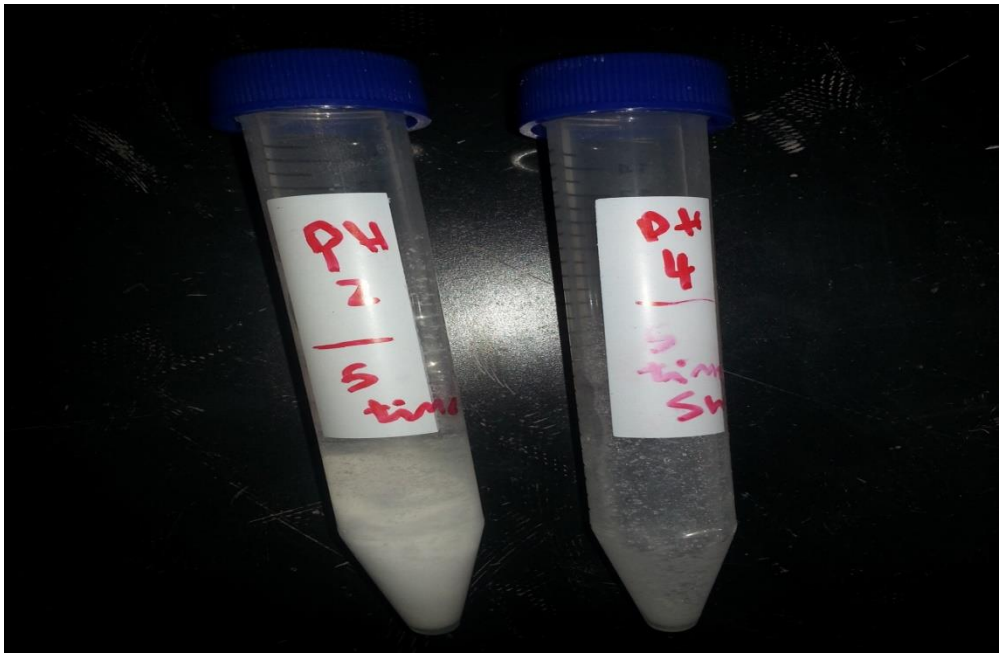

Figure 29: 5 wt. % EDTA in 5 time diluted seawater at pH= 2 and 4, at 23°C, significant participation was observed immediately during the preparation.

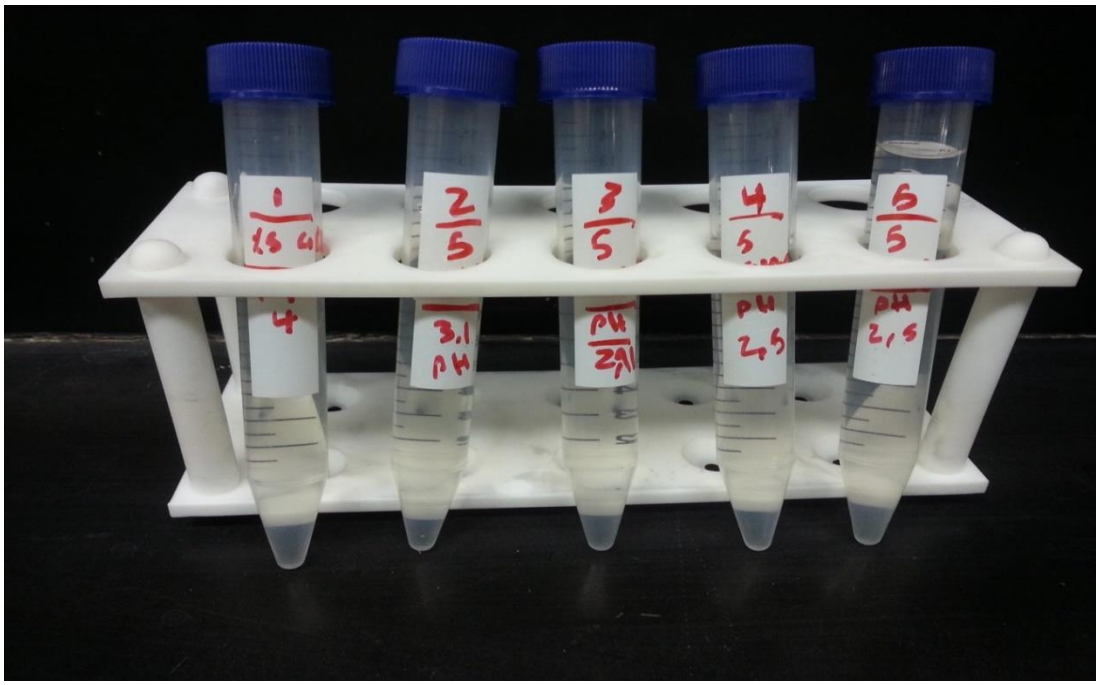

Figure 30: 5wt% GLDA in seawater at pH= 2.5, 2.9, 3 and 4 at 23°C, no participation was observed for all samples.

In addition, the stability of GLDA at high temperature was investigated, and no participation was observed at temperature of 85 °C for 1 day, Figure 31. It can be concluded that GLDA is compatible with seawater over wide range of pH values and at high temperature conditions. Khatere et al. (2013) reported that, GLDA is a stable chelate at 350°F compared to other chelates and it starts to degrade at temperature greater than 350°F. Also, the thermal stability of this chelating agent enhances significantly as pH increases.

Figure 31: 5 and 7wt% GLDA in SW at pH= 4, after heating at 85 °C for 1 day, no precipitation was observed.

3.1.5 Core plugs

Indiana limestone core plugs were used in all core flooding experiments. Core dimensions are 1.5" diameter and 2" length. CT scan (X-ray computed tomography) and SEM (scanning electron microscope) were used to determine the pore geometry by producing tomographic images for the core samples, as shown in Figure 32, 33, and 34. Figure 32 illustrates the SEM results, no clay particles were observed in those images, this result does not necessarily means that there are no clay minerals in core samples, however, XRD results shows small percentages of Illite (<3 wt%).

Figures 33 shows the CT scan results of the first core sample before core flooding experiments, this core sample can be considered as heterogeneous rock since it contains considerable pores in the lower part more than upper part of the sample, However, second

core can be classified as homogenous sample because it has uniform pores distribution as illustrated in Figures 34, which was confirmed lately by the permeability measurements.

In addition, XRD (X-ray diffraction) and XRF (X-Ray Fluorescence) analyses were performed using crushed Indiana limestone rock to identify the mineralogical and elemental composition of the core plugs; Figure 35 illustrates the XRD analysis for the Indiana Limestone, and Table 8 lists the quantitative results from XRD analysis, the samples showed very high amount of calcite (~97% $CaCO_3$) while small percentages of quartz low and Illite (<3 wt%) were detected. The elemental composition from XRF analysis is provided in Table 9.

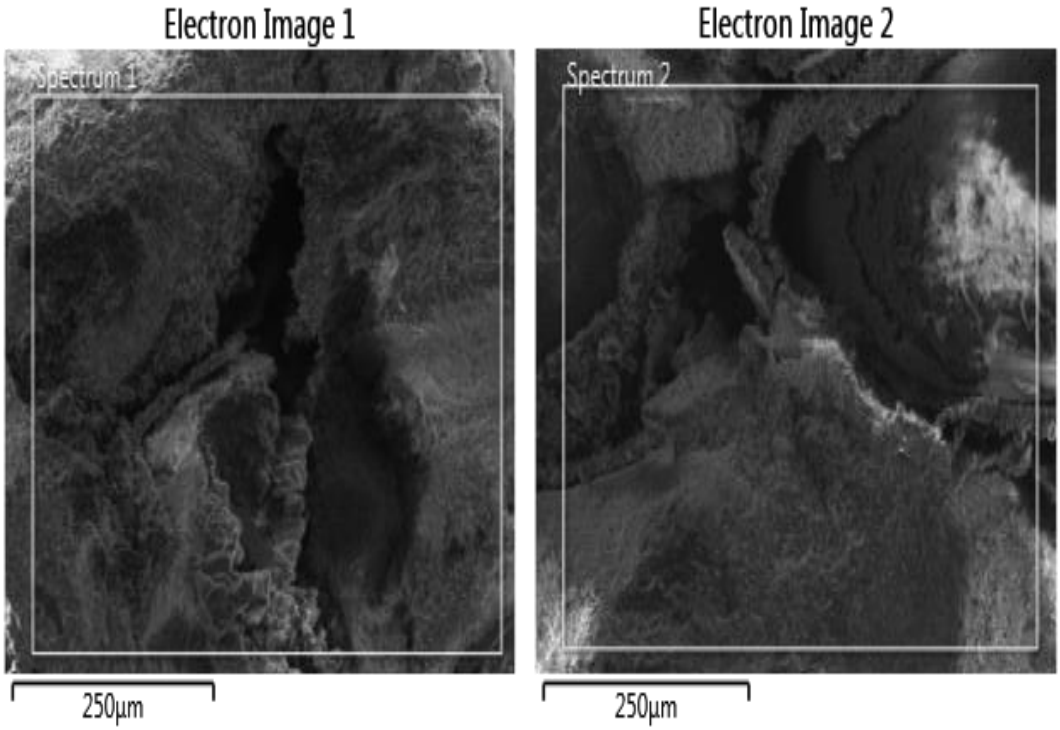

Figure 32: SEM images for Indiana Limestone at different locations.

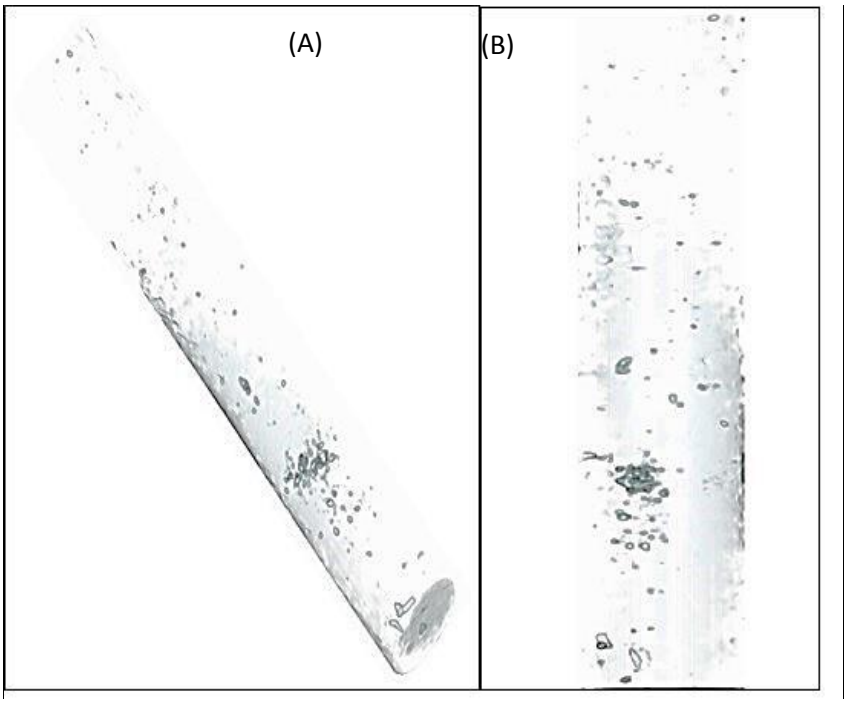

Figure 33: CT scan before flooding for the first core sample (A) 3D view, (B) Right side view.

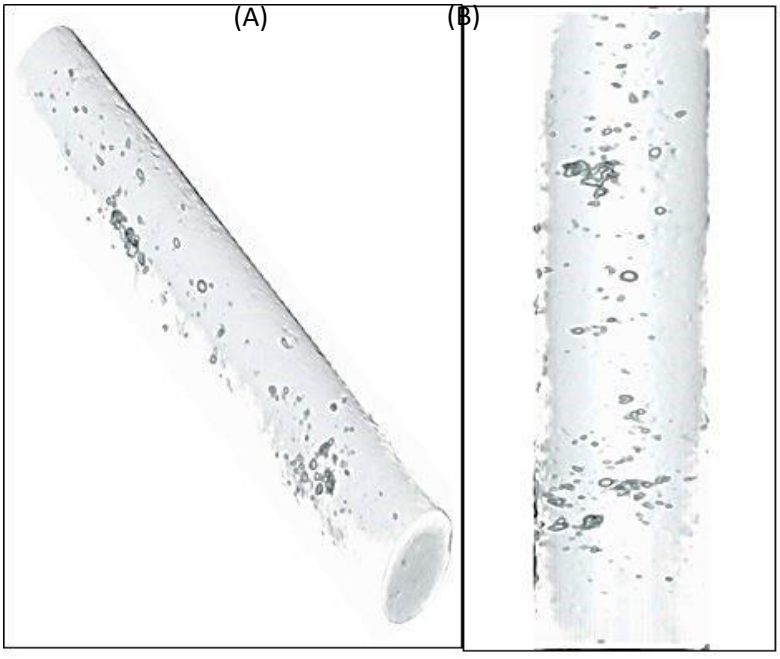

Figure 34: CT scan before flooding for the second core sample (A) 3D view, (B) Right side view.

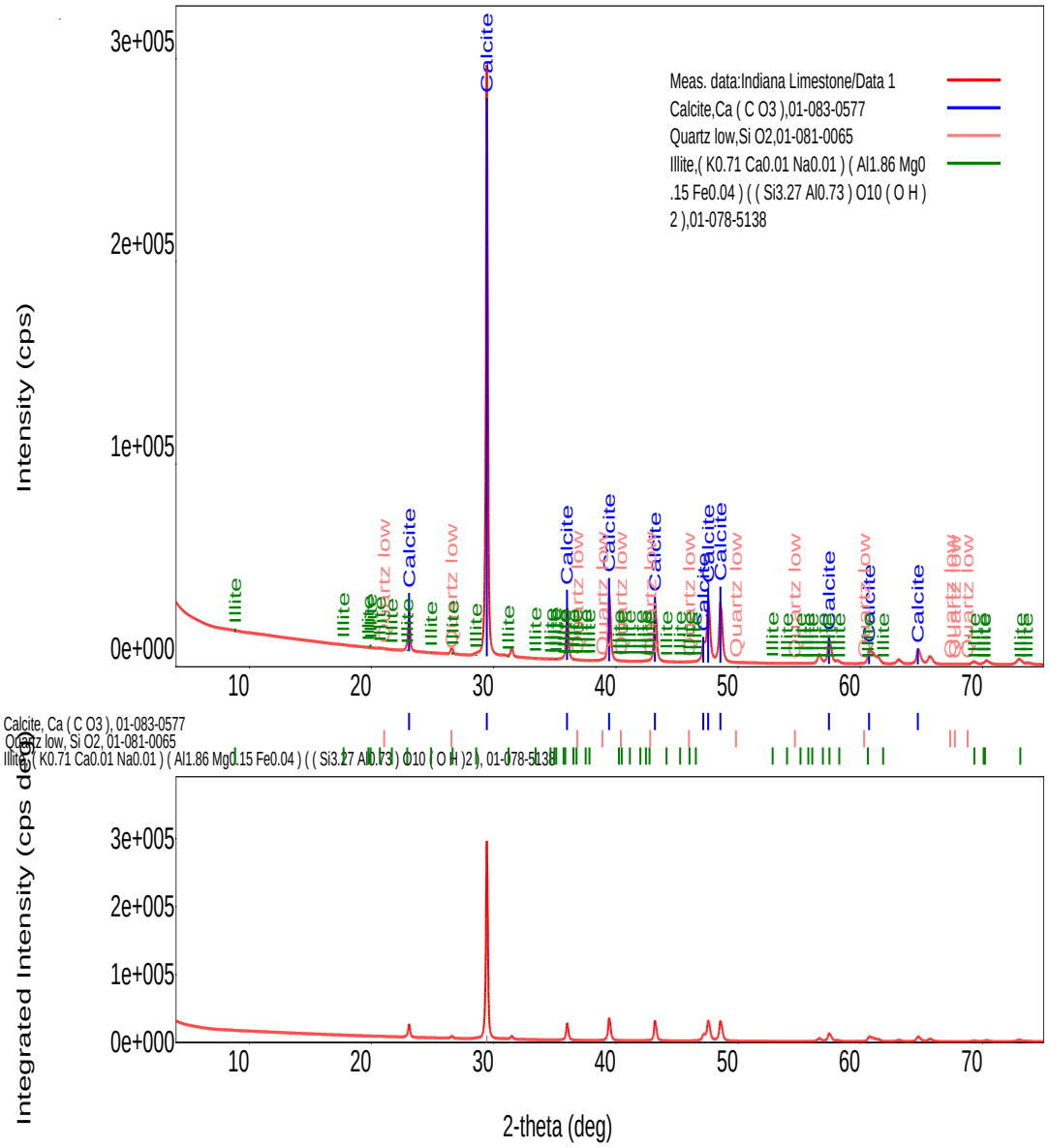

Figure 35: XRD analysis for the Indiana Limestone.

Table 8: Quantitative results from XRD analysis

Phase Name	Calcite	Quartz low	Illite
Content (%)	97(3)	0.158(3)	2.61(15)

Table 9: Elemental Composition of Indiana Limestone from XRF Analysis

Component	Result (wt.%)
CaO	96.678
MgO	1.1243
SiO_2	0.7948
Fe_2O_3	0.4113
Al_2O_3	0.3602
SO_3	0.1732
K_2O	0.1501
Cl	0.0998
P_2O_5	0.0746
SrO	0.067
Na_2O	0.0667
Sum	**100.00**

3.1.6 The mechanism of in-situ CO_2 generation in carbonate formation

Limestone composes largely of calcium carbonate. Carbon dioxide can be generated when chelating agent reacts with the calcium carbonate ($CaCO_3$). In the first stage, H_3HEDTA reacts with calcium carbonate to produce Ca_2HEDTA and Carbonic acid, Since Carbonic acid is a weak acid, it dissociates to produce carbon dioxide and water, Al-Khaldi et. al, 2007 and 2010. The amount of CO_2 depends mostly on the concentration of the chelating agent and the solution pH. The generated CO_2 increases as the concentration of chelating agent increases and as the pH decreases. A simple test was performed to observe the reaction between chelating agent and carbonate, calcite crystals were immersed in EDTA and GLDA solutions individually, and both solutions have concentrations of 5wt. % and pH of 4. Figure 36 and 37 show crystal of Calcite in EDTA and GLDA, respectively. Both solutions reacted with the Calcite crystal and generated CO_2; However, GLDA solution produced CO_2 more than EDTA, which indicates that GLDA is more powerful than EDTA since same conditions (concentration and pH) were used. Solutions with different pH values were used to investigate the possibility of CO_2

generation, CO_2 was observed using camera only for solutions with pH less than 7 (acidic condition).

Based on this study it can be concluded that, CO_2 cannot be generated in base solutions (pH greater than 7). In addition, increasing the temperature may lead to accelerating the chemical reaction; therefore, more CO_2 will be generated at higher temperature. The chemical reaction between EDTA and $CaCO_3$ can be summarized as follows, (Alkhaldi et al., 2005,2007 and 2010):

$H_4EDTA + 2\ CaCO_3 \longrightarrow Ca_2EDTA + 2H2CO_3$

$2H_2CO_3 \rightleftharpoons 2H_2O + 2CO_2$

So, 1 mole of EDTA can react with 2 moles of $CaCO_3$ and produce 2 moles of CO_2, the amount of CO_2 generated from 500 ml of 10wt% EDTA can be determined as follow:

1. Molarity of EDTA (10% wt.) =

$$\frac{w * 1000}{mw * v} = \frac{10 * 1000}{384.2 * 100} = 0.26\ \text{mole/L}$$

2. No. of moles of 500 ml EDTA =

$$\frac{m * v}{1000} = \frac{0.26 * 500}{1000} = 0.13\ \text{mole}$$

3. No. of CO_2 moles = 2 * No. of EDTA moles = 0.26 mole

4. mass of CO_2 = No. of mole * mw

   = 0.26*44.01 = 11.45 gm.

5. Volume of CO_2 at room condition = $\frac{w}{\rho} = \frac{11.45}{1.96*10^{-3}} = 5.844$ L

6. The CO_2 density at 100 ^{0}C and 1500 psi is 0.198 gm./ml

7. Volume of CO_2 at 100°C and 1500 psi = 57.83 ml, which is the maximum volume that could be produced from the reaction of limestone with 500 ml of 10wt% EDTA at pH less than 7.

Where:

w = the concentration of EDTA reacts with carbonate in wt.%,

v = volume of EDTA reacts with carbonate in ml,

mw = the molar weight of EDTA in mole per gram,

m = the molarity of EDTA solution in mole/L,

ρ = density of CO2 at room condition, $1.96 * 10^{-3} gm/ml$

Figure 36: Calcite crystal in 5wt% EDTA at pH= 4.

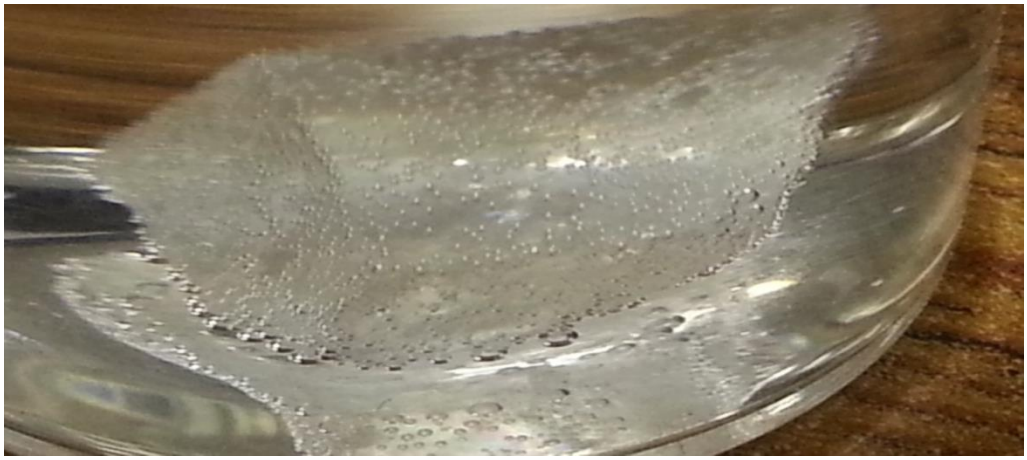

Figure 37: Calcite crystal in 5wt% GLDA at pH= 4.

3.2 Zeta Potential Measurements Procedure

In order to study the effects of rock mineralogy and chelating agent solutions on the rock wettability condition; ZetaPALS (Phase Analysis Light Scattering) instrument was used to measure zeta potential for solid/brine and oil/brine interfaces before and after using the chelating agents to investigate the changes in the surface charges resulting from the surface dissolution of the rock leading to alteration of the rock wettability to more water wet condition. The apparatus uses He–Ne laser as a light source, and it calculates the zeta potential value from measuring the electrophoretic mobility of charged colloidal suspensions. The measurement procedure is summarized as follow:

1. The limestone powders were prepared by taking small sections of the core plugs and crushing them using ROCKLAB crushing machine which produced very fine powder of 5 μm.
2. To obtain the zeta-potential at rock/brine interface; mixtures of rock/brine with different concentrations of Na_4EDTA (0%, 1%, 5% and 10%) were used; suspensions were prepared by mixing 0.125 gm. of powder particles of limestone with 25ml of aqueous solution. For investigating the effect of the presence of oil on zeta-potential, 0.5wt% of Uthmania crude oil was added to those suspensions
3. Then the solutions were placed into a multi-wrist shaker at room temperature (25^oC) for 48 hours, after removed from the shaker the samples kept for 30 minutes to allow all the large particles to settle down, glass syringe was used to separate the upper part of the sample and filter through 5 μm filter.
4. Finally, ZetaPALS zeta potential analyzer, manufactured by Brookhaven Instruments Cooperation was used for zeta potential measurements

3.3 Interfacial Tension (IFT) Measurement Procedures

To examine the change in the IFT due to the chelating agents, first the interfacial tension was measured between crude oil and deionized water (DIW), then between crude oil and seawater (SW). Thereafter, the interfacial tension was assessed between different concentration of chelating agent (GLDA) and crude oil.

Theta Optical Tensiometer instrument was used to carry out the interfacial tension measurements between Uthmaniyah Arab-D crude oil and the chelating agent fluid systems. The instrument was calibrated using the calibration ball and its magnetic field, thereafter; the interfacial tension was measured between deionized water and air to validate the instrument, IFT varies in a small range with an average of 72 mN/m, then the error limit of 3.47% was obtained.

The interfacial tension measurement was conducted by introducing the chelating agent solution (Heavy Phase) into the measuring cuvette before it was placed onto the sample stage, the syringe was filled with UTMN crude oil (light phase), then a hooked needle was inserted into the heavy phase, a drop with appropriate size (5-6 µL) was pushed up from the tip of the hook into the middle of the heavy phase. The temperature was adjusted to the required level and after that the live analysis mode was activated to measure the interfacial tension using pendant drop and flip Y option.

3.4 Petrophysical Analysis and Core Flooding Procedures

Core plugs of 1.5 in. in diameter and 2 inches in length were cut from Indiana limestone. The average porosity and the permeability of the core samples are 17 % and 120 mD,

respectively. Formation brine was used to saturate the samples using the saturator system, the cores were saturated under vacuum for 3 hours then the saturated samples were kept in a high pressure cell at 2500 psi overnight. The porosity of cores was determined using the saturation method.

The absolute permeability was measured utilizing permeability measurement system (Liquid Permeameter) and formation brine at different flow rates. The irreducible water saturation (S_{wi}) was established using the rock centrifuge (ACES-100). The samples were de-saturated using air at 5000 RPM and room temperature for 24 hours, the initial water saturation was calculated by measuring the weight before and after the centrifuging. After that, the core plugs were aged in filtered oil at 100 ^{0}C and 2500 psi for two weeks. Table 10 lists the core properties used in core flooding tests.

Table 10: Indiana Limestone core data

Core No.	Length (cm)	Diameter (cm)	Dry wt. (gm.)	Bulk vol. (cc)	Saturated wt. (gm.)	PV (cc)	Porosity (%)	Perm. (mD)	Swi (%)	OOIP (cc)
1.1	5.24	3.8	130.3	59.4	139.8	8.3	13.9	32	25.4	6.2
1.2	4.88	3.8	117.1	55.3	127.6	9.2	16.6	121.7	22.8	7.1
1.3	4.89	3.8	119.1	55.2	130.4	9.8	17.8	242.7	22.8	7.6
1.4	4.91	3.8	118.9	55.5	130.1	9.7	17.6	267.2	22.3	7.6
2.1	4.89	3.8	119.9	55.5	129.1	8.0	14.5	42.2	28.4	5.7
3.2	4.82	3.8	117.6	54.6	125.6	7.0	12.9	41.9	31.5	4.8
2.4	4.89	3.8	118.9	55.6	127.5	7.4	13.4	34.6	31.2	5.1
3.1	5.05	3.8	123.0	57.3	132.6	8.4	14.6	62.6	27.8	6.1

3.4.1 Core Flooding System

The core flooding experiments were conducted at reservoir conditions with overburden pressure of 2500 psia, pore pressure of 1500 psia and the reservoir temperature is 100°C,

the core flooding system comprises of oven, stainless steel core holder, fluid accumulators, pressure transducers, pressure diaphragm, back pressure regulator (BPR), confining pressure pump and fractional collector, Figure 38. An external Isco pump was used to inject the overburden fluid (distilled water) into the annulus between the core holder and the sleeve (i.e. to obtain a 2500 psia overburden pressure), while pore pressure was maintained by the back pressure regulator at the core outlet

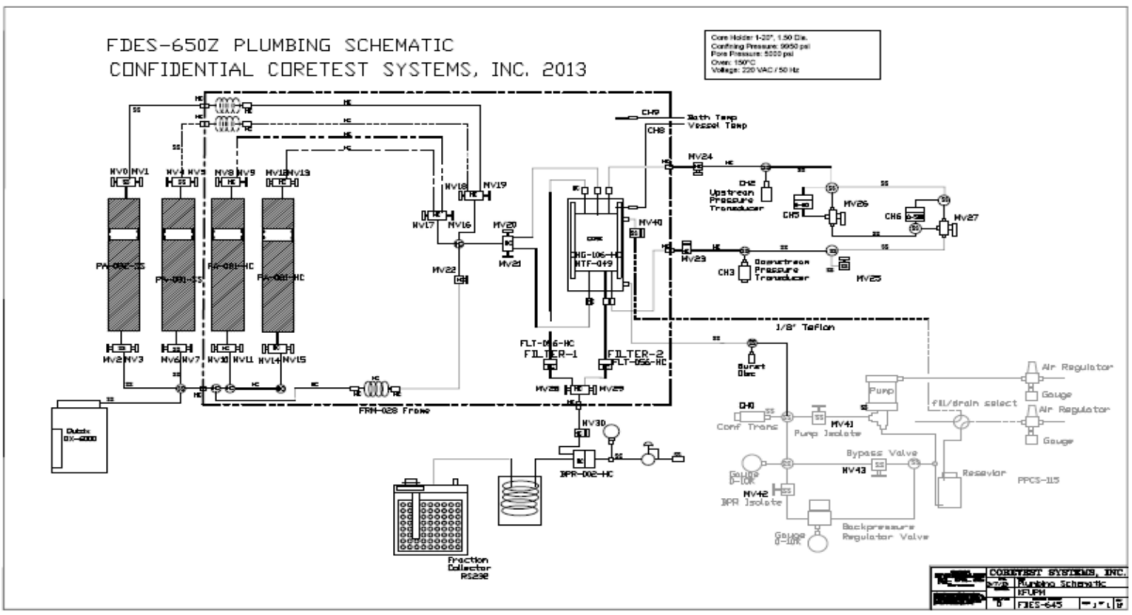

Figure 38: Core flooding schematic (FDES-650Z).

3.4.2 Experimental Procedure

The core flooding experiments were conducted on the prepared limestone plugs at reservoir conditions as follow:

- First, the system was cleaned using Kerosene and distilled water to remove any corrosion products and previous chemicals, then air was used to displace those fluids.

- All accumulators were filled with the injected fluids which are filtered crude oil, sea water and chelating agent with different concentrations.
- The composite cores consist of two core plugs, at residual water saturation, were placed into a rubber sleeve and loaded into the core holder.
- Overburden pressure of 2500 psia was applied by filling the core holder with distilled water using the external pump. The pore pressure was raised up to 1500 psia using the back pressure regulator.
- The system was heated for 8 hours to a temperature of 100°C using the oven. After that, the composite cores were flushed with several pore volumes using the filtered crude oil till the pressure stabilized and then the effective oil permeability was measured using different flow rates.
- The core flooding test was performed by first injecting the sea water at 0.5 cc/min till no more oil recovery, during this phase, the pressure drop across the sample and effluent were recorded as a function of time and injected volume.
- The next phase, chelating agent solutions was used to flood the samples till no more oil production, different concentration of GLDA and Na_4EDTA (3, 5, 7wt%) with pH of 4 and 7 were injected at 0.5 cc/min, the effluent was collected and the pressure drop was recorded as a function of time and injected volume.

CHAPTER 4

RESULTS AND DISCUSSION

4.1 Zeta-Potential Measurements

The main objective of this part is to study the changes in the surface charges resulting from surface dissolution of the rock which may lead to alteration of the rock wettability to more water wet condition.

Brookhaven ZetaPALS instrument was used to measure the zeta potential of the limestone particles in the formulated brines. Suspensions of limestone in different solutions were prepared by mixing 0.125 g of powder particles of limestone with 25ml of aqueous solution for 24 hours on a multi-wrist shaker at room temperature. Conditioned mixtures were filtered by 5 μm syringe filter to produce the final suspensions for the zeta potential measurement. Hydrochloric acid (HCl) and sodium hydroxide (NaOH) were used to adjust the pH of the solution. This instrument measures the electrophoretic mobility of the suspension; and then determines the zeta potential using Smoluchowski Model. To achieve good reproducibility, at least 4 measurements of a single run each of 100 cycles were made, after all runs, only the most stable range of motilities was considered, then zeta potential values which have motilities within this range were selected, while all zeta potential values out of this range were excluded, and an average value of zeta potential was selected. In addition the particles size was measured for all

samples (refer to Appendix F), it is extremely important to conduct a particle sizing measurement before measuring zeta potential to ensure that the measurements will be within the machine's specifications, especially in term of the particle size. Also particle sizing measurement will give some valuable information about the suspension, such as particles size distribution and polydispersity.

The following chart (Figure 39) illustrates the experiment that has been performed to measure the zeta potential.

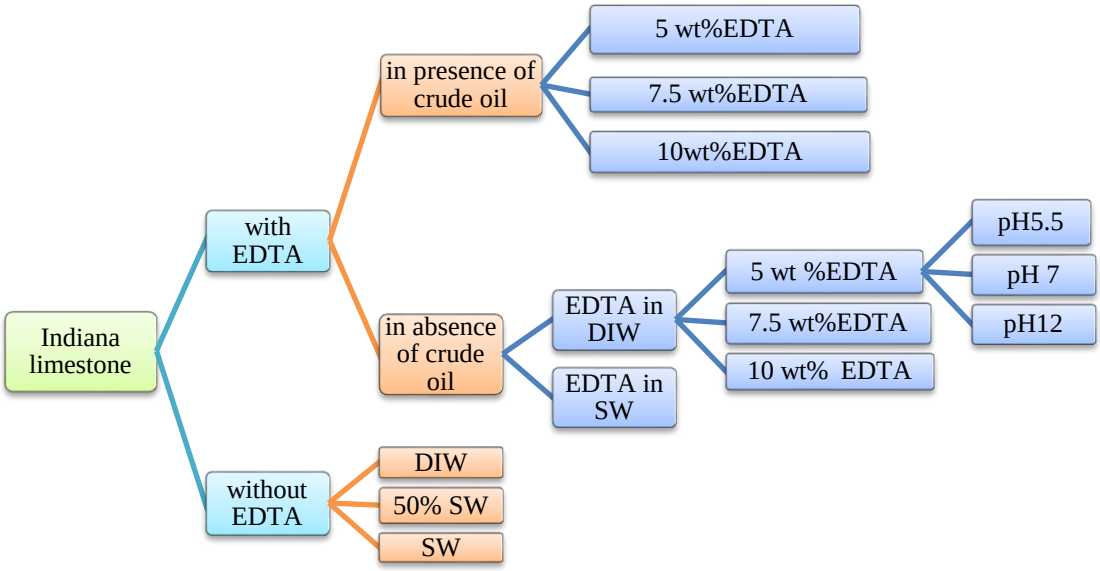

Figure 39: Flow chart of zeta-potential experiments.

4.1.1 Results and Discussion:

1. Effect of Low Salinity water at pH 7 in the absence of EDTA

Carbonate rock has been reported as positively charged particles (Alotaibi et al., 2011), seawater contains significant amount of positive ions, which prevents any ions leaching from the carbonates, and results in positive zeta values (i.e. Carbonate particles carry

positive charges in high-salinity brines). While in deionized water calcium ions leach from the rock surface and lead to negative surface charge. Twice diluted seawater (50%SW) shows intermediate behavior, Figure 40. Since the oil droplets demonstrate negative zeta values for intermediate and high pH (Alotaibi et al., 2011), therefore, as the negative value of zeta potential increases the repulsion force between the carbonate rock and oil particles will increase, so the rock is altered toward water-wet. As a conclusion, surface-charge adjustment from positive to negative can alter the wettability of carbonate rock surface from preferentially oil-wet to water-wet leading to a decrease in the residual oil saturation.

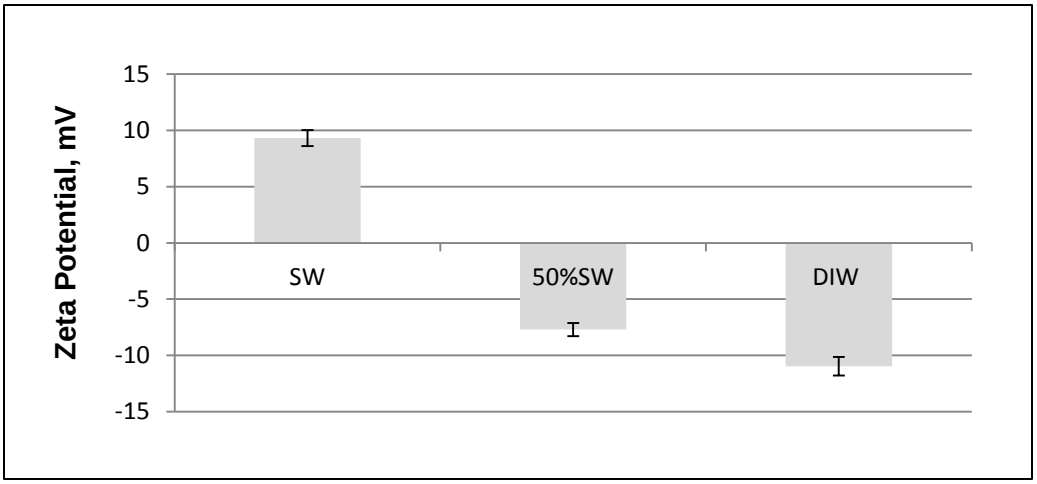

Figure 40: Effect of Low Salinity water at pH 7, without EDTA.

2. Effect of using EDTA in DIW at pH 7 for different EDTA concentrations

Figure 41 presents the measured zeta potential for limestone particles in different EDTA solutions. The EDTA solutions were prepared using DIW and the zeta potential was measured at 23°C and pH of 7. It can be seen from this figure that all EDTA concentrations produced negative zeta potential, and as the EDTA concentration

increases, the zeta potential was more negative. To avoid the high salinity difficulties and to achieve understandable and unambiguous trend, deionized water was used to prepare the EDTA solutions to obtain the general trend of zeta potential with respect to pH, however in the petroleum industry, seawater has been used for diluting the chemical solutions to reduce the total cost. Negative surface charges were obtained for all EDTA solution, which can be attributed to chelation of the cations from the surface lattice (especially the calcium and magnesium ions), and consequently reduce the concentration of these ions in the surface lattice (Ca^{2+} and Mg^{2+}). Higher EDTA concentration leads to an increase of the chelation force and results in a decrease of the concentration of cations, leading to more negative zeta values.

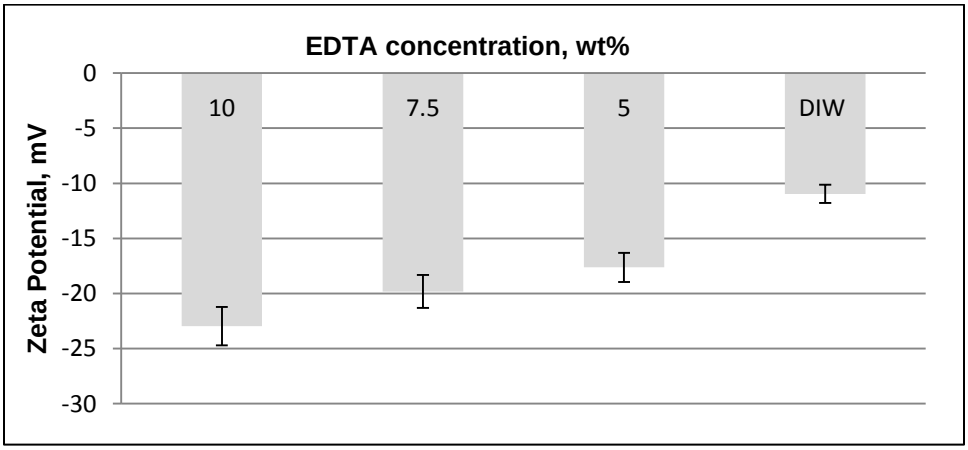

Figure 41: Effect of using EDTA in DIW at pH= 7, for 5, 7.5 and 10wt% of EDTA.

3. Effect of EDTA in SW at pH 7 for different EDTA concentrations

As mentioned earlier, seawater was used to prepare low concentrated solutions of chelating agents. Again EDTA shows negative values of zeta potential for all concentrations, the negative value increases with increasing EDTA concentrations. All measurements were conducted at the same pH value (pH= 7), as shown in Figure 42.

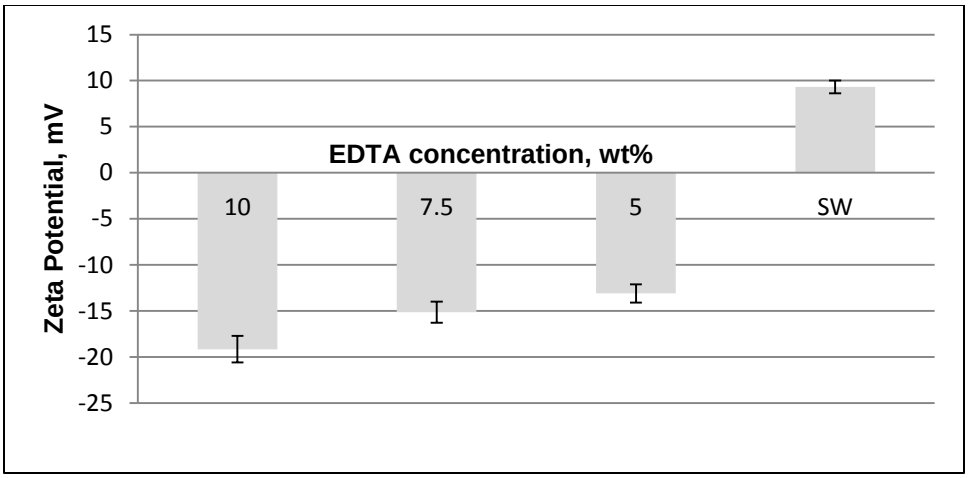

Figure 42: Effect of using EDTA in SW at pH 7, for 0, 5, 7.5 and 10wt% of EDTA.

4. EDTA Dilution in DIW and SW, for different concentrations at pH= 7

Figure 43 compares the zeta potential for preparing EDTA in DIW and SW. Negative values were observed for all concentration in both DIW and SW, however, the presence of cations in seawater affect the chelation force of EDTA and lead to less negative values. More concentration means more chelation force (in both DIW and SW) and then more negative values for the surface charges.

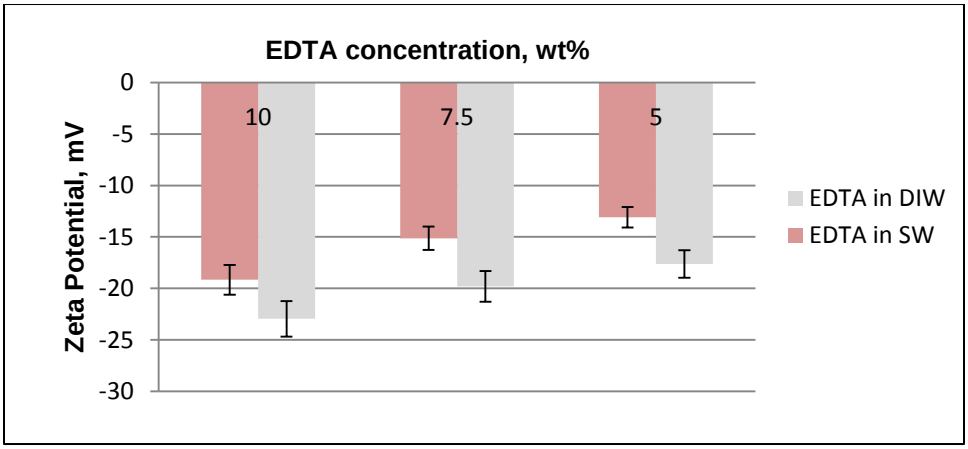

Figure 43: Dilution of EDTA in DIW and SW, for different concentrations at pH= 7.

5. Effect of the solution pH, EDTA in SW at different EDTA concentrations

Different trends have been reported in the literature, so more considerations have been devoted to the zeta potential and pH relationship, DIW was utilized to realize the general trend then SW was used to observe or investigate the effect of pH on the surface charge, Figure 44. In general, the high pH results in excess concentration of negative species, especially bicarbonate (HCO_3^-) and carbonate (CO_3^{2-}), while more positive species calcium ions (Ca_2^+, $CaHCO_3^+$, and $CaOH^+$) are present at low pH. As a result, the negative value of zeta potential increases with increasing solution pH, since more (OH^-) ions can be introduced to the solution at high pH.

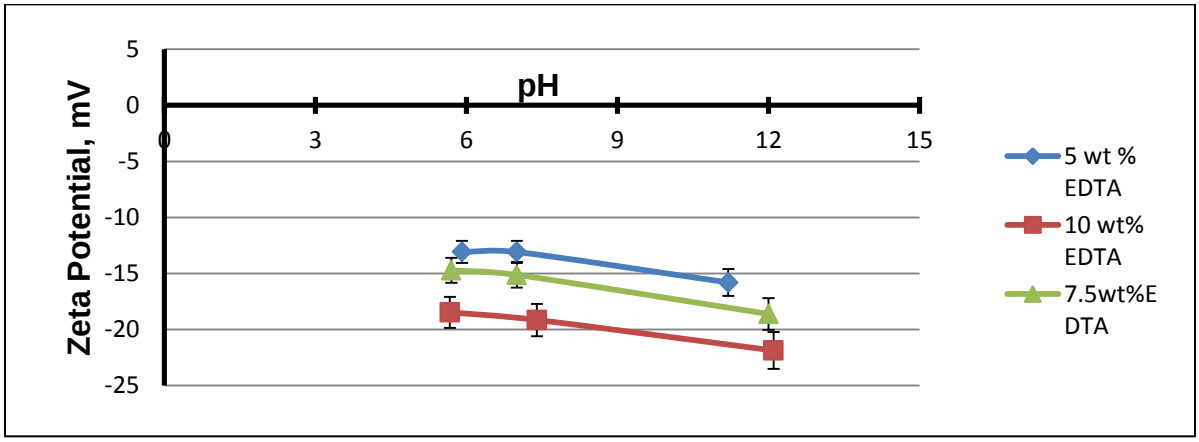

Figure 44: Effect of the solution pH on zeta potential, EDTA in SW at different concentrations.

6. EDTA Dilution in DIW and SW, for different pH at 10 wt. % EDTA

Figure 45 shows the effect of pH and the dilution in SW/DIW; highest negative value was obtained at12 pH for EDTA in DIW, while EDTA in SW provides a little bit smaller negative zeta value at the same pH. Decreasing the solution pH leads to decreasing the

absolute value of the zeta potential in all cases. It should also be noted that, the difference between EDTA in SW and EDTA in DIW decreases as pH decreases.

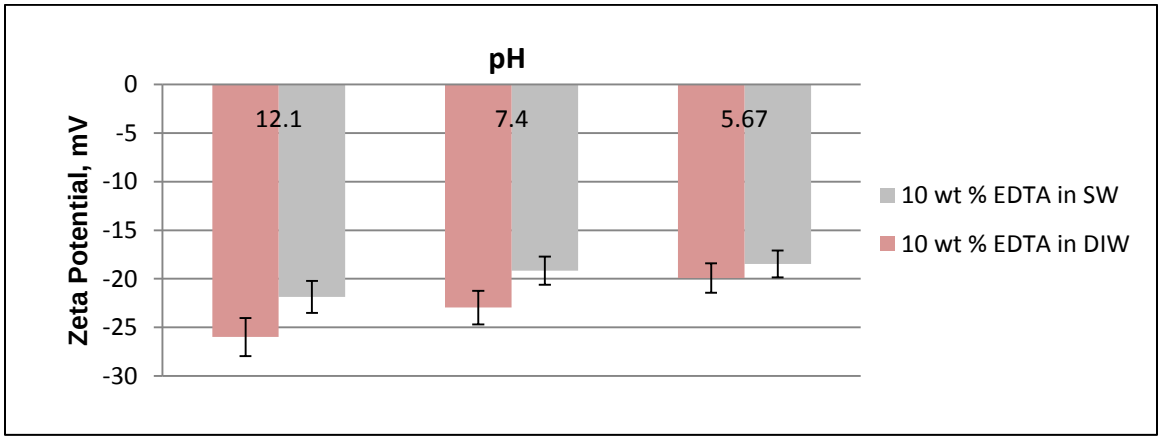

Figure 45: Effect of the solution pH and EDTA dilution in SW/DIW on zeta potential, 10wt% EDTA at different pH values.

7. Effect of crude oil, EDTA diluted in SW at different EDTA concentrations, pH = 12.

Crude oil contains carboxylic group which have negative surface charges, therefore, oil droplets demonstrate negative zeta values in saline solutions. The presence of crude oil in the reservoirs for millions of years can lead to adsorption of negatively charged polar components of the crude oil onto the rock surface; which results in more negative values for the zeta potential. As a result, the presence of crude oil will lead to increasing the negative values of the zeta potential for all EDTA concentrations, this increment increases with increasing the EDTA concentrations, maximum increment of 6 mV was obtained at 10wt%, as illustrated in Figure 46. This result is in agreement with the study performed by Kassim et al., 2012. In conclusion, the presence of oil can lead to more negative zeta values, which can be interpreted as that, both the limestone and crude oil

particles have negative surface charge in SW. Therefore, there will be a repulsion force between carbonate rock and crude oil and the rock tend to be more water-wet.

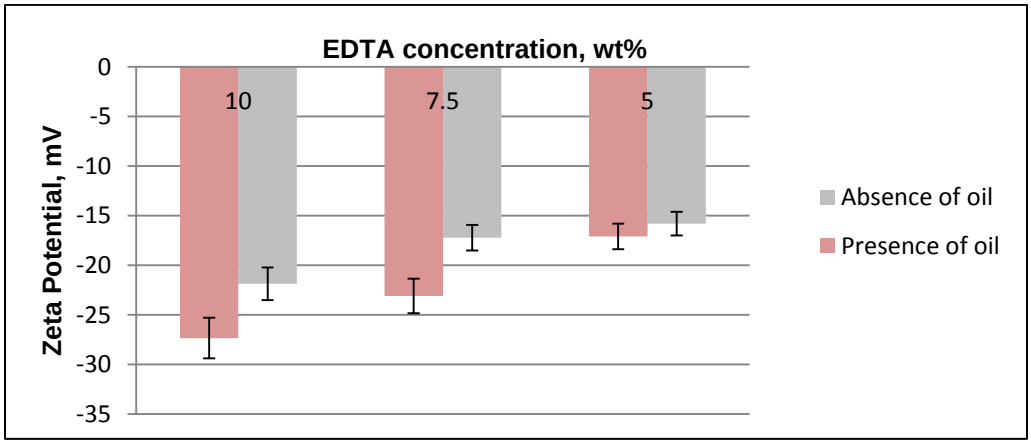

Figure 46: Effect of EDTA concentration diluted in SW at 23°C and pH=12, in the presence of crude oil

4.1.2 Summary

The above results show that, chelating agent (such as EDTA) can alter the rock wettability to more water-wet leading to an increase in the ultimate oil recovery from carbonate reservoirs through wettability alteration mechanism. This is in agreement with Hiorth et al. (2010) and Zahid et al. (2012) for the case of low salinity injection. Moreover, the comparison between deionized water, low salinity water and EDTA/seawater solution shows that, more wettability alteration can be obtained with minimum cost by using EDTA/seawater solutions instead of low salinity water. In addition, the presence of crude oil in the solution will result in more negative values for the zeta potential, indicating better wettability alteration toward more water-wet and therefore enhance the oil recovery.

4.2 Interfacial Tension (IFT) Measurements

Optical Tensiometer instrument was used to conduct the measurements at room and high temperatures; the instrument calculates the volume of the drop based on the image calibration. The interfacial tension measurement was conducted with a hooked needle with the denser liquid (Heavy phase) in a cuvette around it. A drop with appropriate size (5-6 µL) was pushed up from the tip of the hook and measurement was done using pendant drop option, Flip Y was selected from the recipe sheet since live analysis was used. Appendix B shows the transient interfacial tension data, IFT vs. Time for 5wt% GLDA.

Figure 47 shows the measured interfacial tension for oil in different solutions at temperature of 23°C. The lowest IFT (20.97 mN/m) was obtained when 5wt. % GLDA/ SW solution at pH=4 was used, while using SW produced the highest IFT value (31.75 mN/m). In general, low IFT means favorable flowing conditions; therefore more oil can be produced. So, it is expected that 5wt. % GLDA/SW solution will result in better oil recovery than DIW and SW due the lower IFT value.

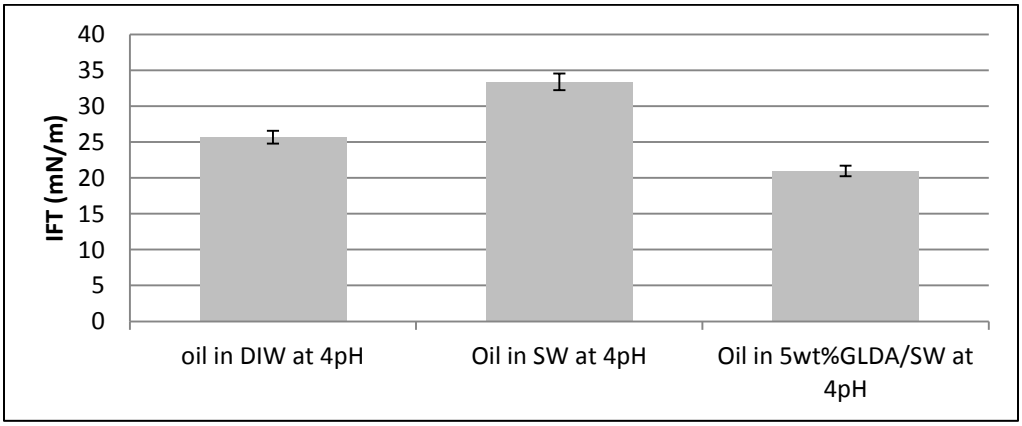

Figure 47: Interfacial Tension for oil in DIW, Oil in SW, and Oil in 5 wt. % GLDA, at temperature of 23°C.

The effect of temperature on the IFT reduction was investigated; the IFT was measured at different temperatures then extrapolated to the reservoir temperature. All measurements were conducted at normal pressure of 14.7 psi, since all the fluids used in this study are incompressible. Figure 48 shows the interfacial tension for oil in DIW, in SW, and in 5wt. % GLDA, at temperature of 100°C.

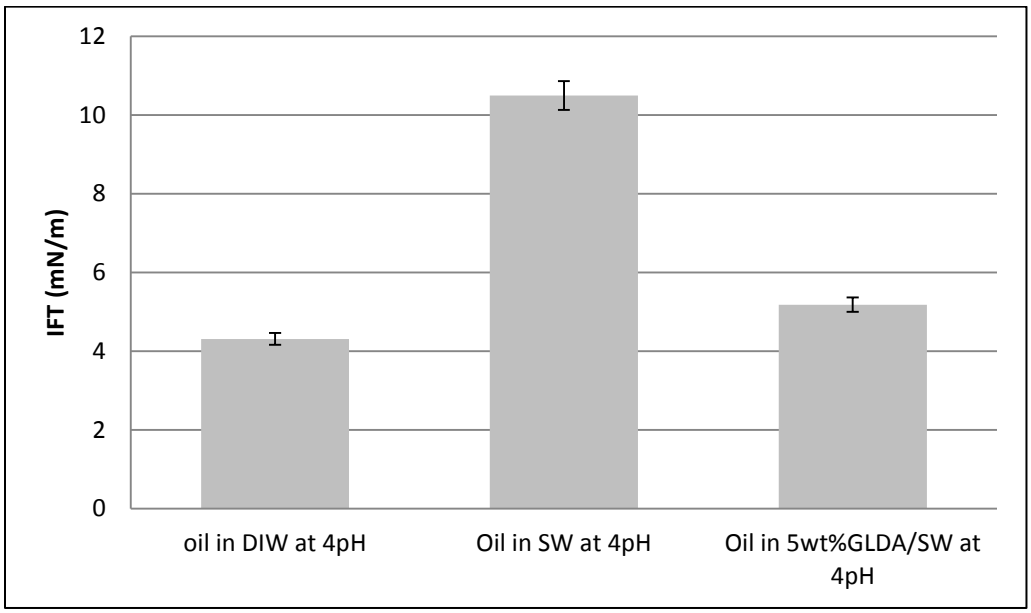

Figure 48: Interfacial Tension for oil in DIW, Oil in SW, and Oil in 5wt.% GLDA, at temperature of 100°C.

Figure 49 shows the interfacial tension for oil in different concentrations of GLDA prepared in seawater (pH = 4), at temperature of 100°C. The increase in the GLDA concentration from 3wt% to 7wt% will reduce the IFT values from 7.34 to 4 mN/m.

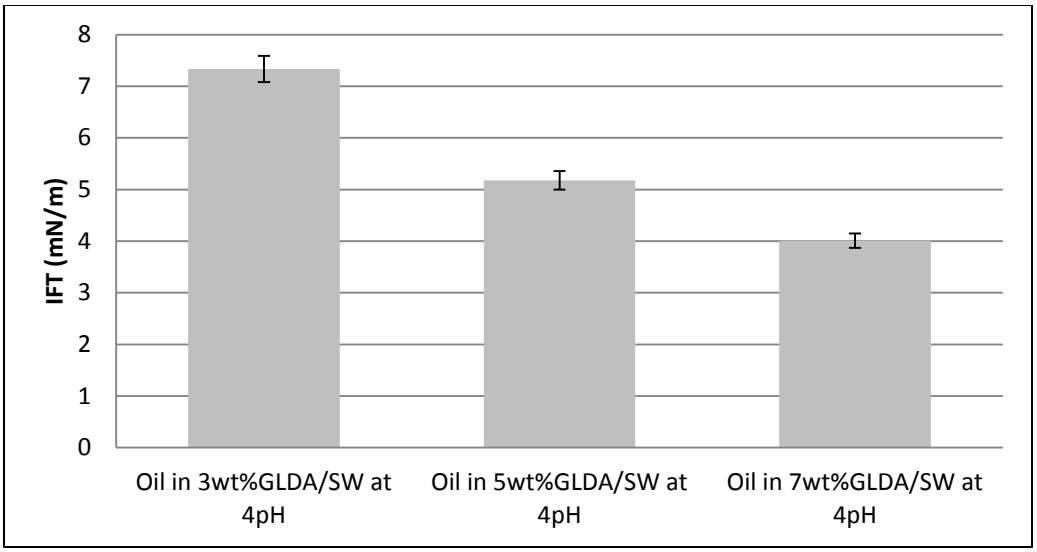

Figure 49: Interfacial Tension for oil in different concentrations of GLDA, at temperature of 100°C.

4.3 Core Flooding Experiments

4.3.1 Experiment No.1: Seawater flooding Followed by (3, 5 & 7wt. %) EDTA Solutions

Table 11 lists the properties of core plugs and core composite used in the first experiment. During this experiment, sequential flooding was used for oil recovery by injecting the seawater first, then EDTA /seawater solution (with pH= 6) at 3, 5, and 7wt% respectively; finally the seawater was injected again to recover any more oil.

4.3.2 Experiment No.2: Seawater flooding Followed by (3, 5 & 7wt. %) GLDA Solutions

The experiment was conducted using sequential flooding of seawater and different concentrations of GLDA. No additives were used such as corrosion inhibitors.

GLDA/seawater (with pH= 3.9) of 3, 5, and 7wt% were used as the EOR fluid system. Finally the composite core was flooded with seawater (with pH= 7.7) to see if additional oil recovery can be obtained. The properties of core plugs and core composite used in this experiment are listed in Table 12.

4.3.3 Experiment No.3: Seawater flooding Followed by (5, 7 & 10wt. %) GLDA Solutions

In the third experiment, GLDA with concentrations of 5, 7 and 10wt. % were injected sequentially after seawater flooding; seawater was used to prepare the GLDA solution without any additives. Table 13 lists the properties of core plugs and core composite used in this experiment. The pH of GLDA solutions were adjusted to 3.9 in order to increase the amount of in-situ generated CO_2, significant amount of CO_2 was observed inside the effluent at fractional collector. At last stage of the experiment seawater was injected again to sweep more oil.

4.3.4 Experiment No.4: Seawater flooding Followed by (5, 7 & 10wt %) EDTA Solutions

In the last core flooding experiment, different concentrations of EDTA (5, 7, and 10wt. %) with pH = 6 were injected sequentially after seawater flooding, finally the cores were flooded with seawater to get more oil recovery. The properties of core plugs and core composite used in this experiment are listed in Table 14. No significant amount of CO_2 was observed at the fractional collector, seawater was used to prepare EDTA solution and no additives were utilized.

4.4 Results Core Flooding Experiments

4.4.1 Experiment 1

Figure 50 shows oil recovery, pressure drop and pH profiles as a function of pore volume injected. It can be seen from this figure that, 48.5% of the OOIP was recovered after injecting 4 PV of seawater followed by 13.9% incremental OOIP after injecting additional 4.6 PV of 3wt% EDTA solution followed by 2% and 0.5% incremental OOIP after injecting additional 1.6 PV and 2.4 PV of 5wt% and 7wt% EDTA solutions respectively, while final seawater flooding increased the oil recovery by only 0.7% OOIP.

The effluent was collected using fractional collector at constant time intervals for analysis. The oil was recovered through different mechanisms, normal displacement or sweeping which achieved by both seawater and the chelating agent, wettability alteration and IFT reduction which achieved mainly during flooding with chelating agent and minor effect from final flooding with seawater, as discussed in IFT section, however significant impact on wettability alteration might be obtained if smart/low saline water used instead of seawater.

Slight changes in the pressure drop was observed during the flooding which implies that, there is no damage due to reaction between chelating agent and the formation, However, the permeability measurement and CT scan (after flooding) provided more information about the pore geometry and permeability improvement.

pH was changing in small range during the flooding and it stabilized at each phase which indicates that, the reactions reached the equilibrium. The pH changed from 7.7 to 7.8 during seawater flooding which means no reaction was occurred, while it increased from 6 to 8.75 during EDTA injection and that is because the reaction between the carbonate and EDTA solution. In addition, no carbon dioxide was observed during this experiment because carbon dioxide can be generated only in acidic solutions (pH less than 7).

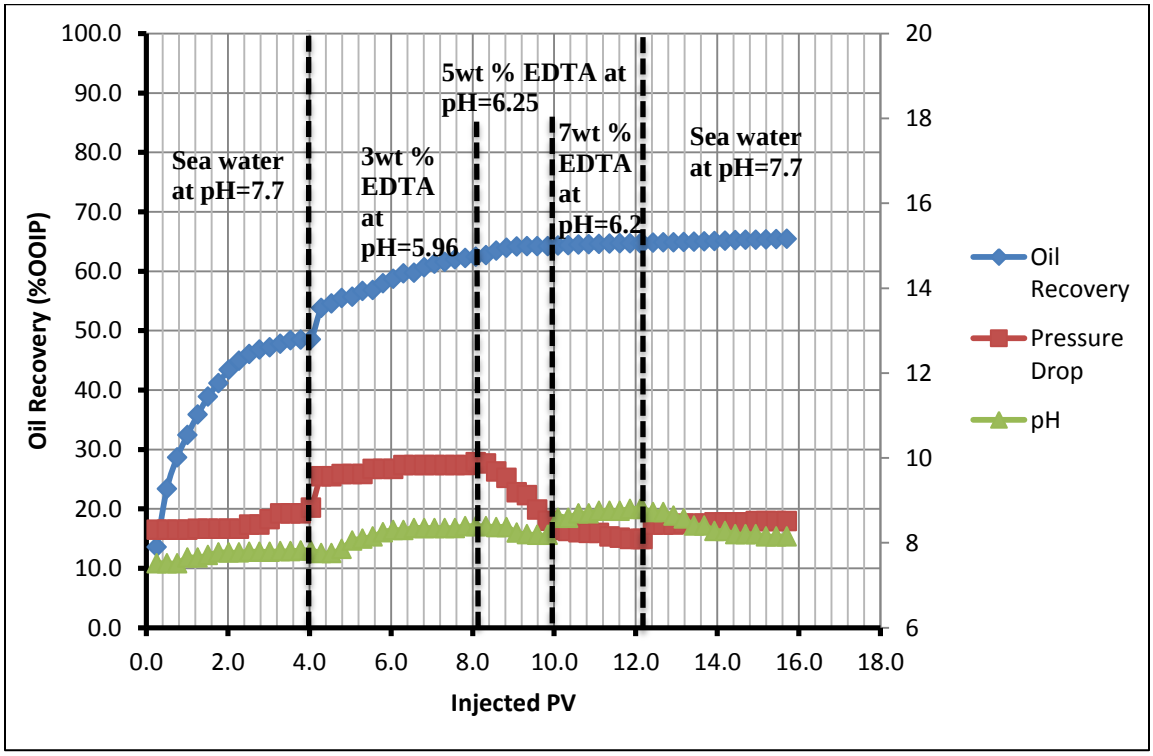

Figure 50: Oil recovery by seawater (pH=7.7) followed by 3wt%, then 5wt% and 7wt% of EDTA at pH =6.

Table 11: The properties of core samples used in the first core flooding test

Core No.	Length (cm)	Diameter (cm)	Dry wt (gm)	Bulk vol. (cc)	Saturated wt. (gm)	PV (cc)	Poro. (%)	Abs. Perm. (mD)	S_{wi} (%)	OOIP (cc)
1.1	5.3	3.8	130.4	59.4	139.9	8.3	13.9	32	25.4	6.2
1.2	4.9	3.8	117.1	55.4	127.6	9.2	16. 6	121.7	22.8	7.1
Composite										
1.1+1.2	10.1	3.8	247.4	114.7	267.5	17.5	15.3	62.4	24.1	13.3

4.4.2 Experiment 2

Figure 51 presents oil recovery, pressure drop and pH as a function of pore volume injected. It can be noticed from this figure that, 54% of the OOIP was recovered after injecting 7 PV of seawater followed by 16% OOIP after injecting 4 PV of 3wt% GLDA solution followed by 9% and 3.5% OOIP after injecting 2.8 PV and 3 PV of 5wt% and 7wt% GLDA solutions respectively, while second seawater flooding increased the oil recovery by 1% OOIP.

Fractional collector was used to collect the effluent at constant time intervals. Chelating agents enhance the oil recovery through different mechanisms; Normal oil displacement/sweep, IFT reduction, wettability alteration, permeability improvement and CO_2 flooding. In this experiment, the pH value and GLDA concentration were selected to ensure that, CO_2 can be generated inside the core. In addition, constant and small flow rate was applied in order to give sufficient time to achieve the stability/equilibrium state between the chelating agents and core samples (limestone), which can lead to maximize the CO_2 generation.

Pressure drop was changing within small range during the flooding which indicates that, the reaction between chelating agent and the carbonate did not produce any damages. However, the analysis of core after flooding by using CT scan and permeability measurement provided the effect of reaction on the core properties.

Slight change in pH was observed during the flooding, and it stabilized at each phase which implies that, an equilibrium state was reached. The pH changed from 7.7 to 7.8 during seawater flooding which means no reaction was occurred, while it increased from

3.9 to 6.3 during GLDA injection and that is because the reaction between the carbonate and GLDA solution. This reaction led to CO_2 generation as it was observed in the effluent, and the amount of CO_2 was increasing with the GLDA concentration.

The ultimate recovery in this experiment was 83.76% while it was 65.5% in the previous experiment which indicates that GLDA is more powerful than EDTA since same concentrations were used, also pH value has significant effect on the oil recovery, the lowest pH is the better since more CO_2 can be produced, however small concentrations should be used to avoid severe rock dissolutions.

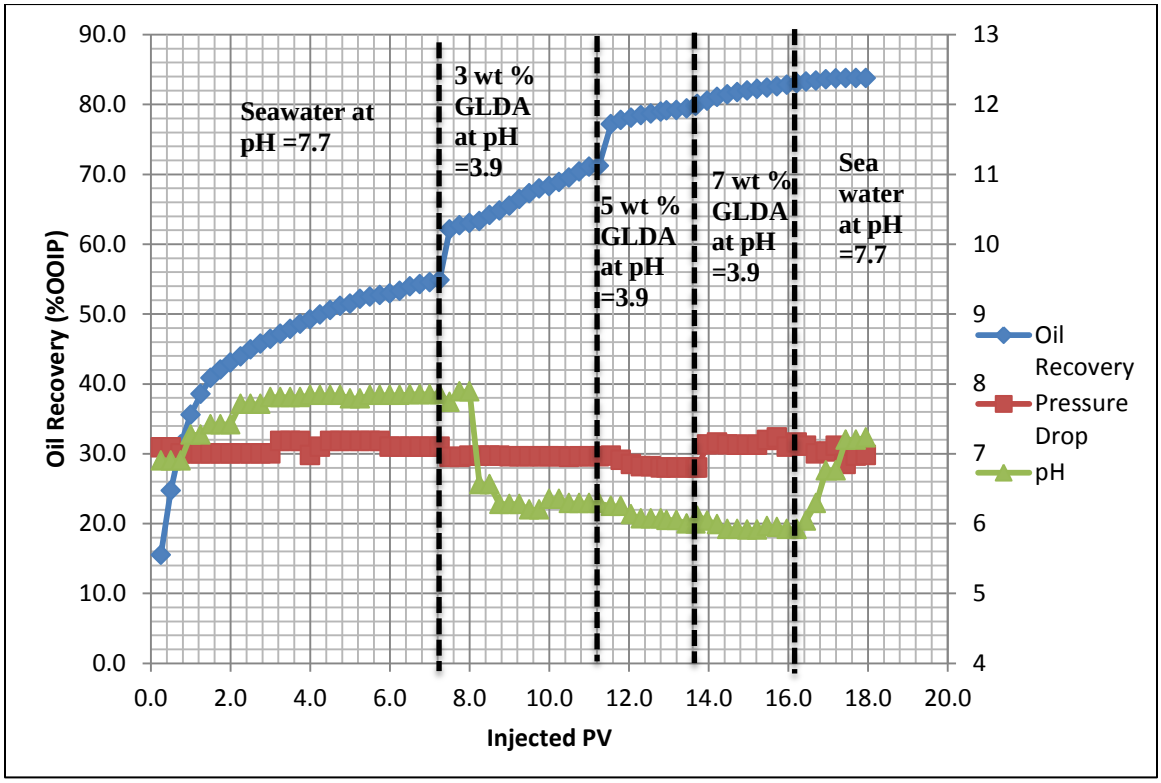

Figure 51: Oil recovery by seawater followed by 3wt% , then 5wt% and 7wt% of GLDA at pH =3.9.

Table 12: Properties of the core samples used in the second core flooding test

Core No.	Length (cm)	Diameter (cm)	Dry wt (gm)	Bulk vol. (cc)	Saturated wt. (gm)	PV (cc)	Poro. (%)	Abs. Perm. (mD)	S_{wi} (%)	OOIP (cc)
1.3	4.9	3.8	119.1	55.2	130.4	9.8	17.8	242.7	22.8	7.6
1.4	4.9	3.8	118.9	55.5	130.1	9.8	17.6	267.2	22.3	7.6
Composite										
1.3+1.4	9.8	3.8	237.9	110.7	260.5	19.6	17.7	254.6	22.6	15.2

4.4.3 Experiment 3

Figure 52 shows oil recovery, pressure drop and pH as a function of pore volume injected. It can be realized from this figure that, the ultimate recovery was 85.32% OOIP which distributed as following: 52.7% OOIP was recovered after injecting 10 PV of seawater, 5 PV of 5wt% GLDA gave 23.69% OOIP, 5 PV of 7wt% GLDA recovered 8.93% OOIP, and no oil was recovered from both 10wt% GLDA and second seawater.

In conclusion, it is recommended to use GLDA with concentrations less than 10wt% because no more oil was recovered with 10wt% GLDA, and significant precipitation was observed in the effluent which indicates that, severe rock dissolutions was occurred during core flooding. Moreover the CT scan results show that, channels/wormholes have been created inside the core samples which may lead to bypass more oil; then increase the residual oil saturation and reduce the ultimate oil recovery.

The pressure drop varies in small range (between 6.5 and 4.9), the maximum pressure drop was observed in the first stage of core flooding and then going down as chelating agent injected, minimum pressure drop was obtained during the injection of 10wt%

GLDA which implies that considerable rock dissolution was taken place and that was confirmed by CT scan.

The pH changed from 7.7 to 7.8 during seawater flooding which means no reaction was occurred, while it increased from 3.9 to 6.2 during GLDA injection and that is because the reaction between the carbonate rock and GLDA solutions.

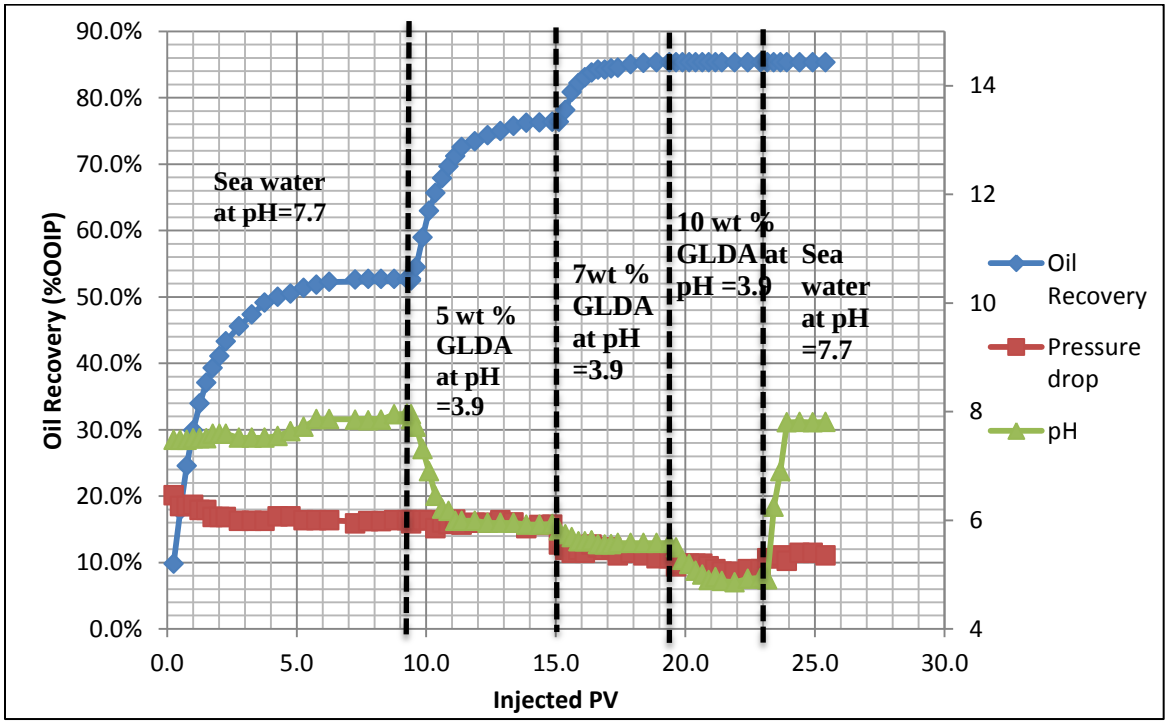

Figure 52: Oil recovery by seawater followed by 5wt% , then 7wt% and 10wt% of GLDA at pH =3.9.

Table 13: Properties of the core samples used in the third core flooding test

Core No.	Length (cm)	Diameter (cm)	Dry wt. (gm)	Bulk vol. (cc)	Saturated wt. (gm)	PV (cc)	Poro. (%)	Abs. Perm. (mD)	S_{wi} (%)	OOIP (cc)
2.4	4.9	3.8	118.9	55.5	127.5	7.5	13.4	34.6	31.2	5.1
3.1	5.1	3.8	123.0	57.3	132.6	8.4	14.6	62.6	27.8	6.1
Composite										
3.1+2.4	9.9	3.8	241.9	112.7	260.1	15.8	14.1	46.6	29.5	11.2

4.4.4 Experiment 4

Figure 53 shows oil recovery, pressure drop and pH profiles as a function of pore volume injected. It can be seen from this figure that, The ultimate recovery is 73.01% OOIP which distributed as following: 46.3% OOIP was recovered after injecting 10 PV of seawater, 5 PV of 5wt% EDTA gave 20.53% OOIP, 6 PV of 7wt% EDTA recovered 3.76% OOIP, 2.33% OOIP was recovered after injecting 4.5 PV of 10wt% EDTA, and final seawater flooding enhanced oil recovery by 0.095% OOIP.

The pressure drop changes slightly (between 6.71 and 5.2), seawater flooding showed the maximum pressure drop, then pressure drop decreases as EDTA solutions were injected till reached minimum values during the second seawater injection, from the pressure drop profile it can be concluded that, rock dissolution was occurred which was confirmed lately by CT scan.

The pH values changed from 7.7 to 7.9 during seawater flooding, while it stabilized at 8.9 during 5wt% EDTA flooding, then it increased a little bit more to reach 9.2 during 10wt% EDTA injection, thereafter, the pH drops till reached 8.2 during second seawater flooding.

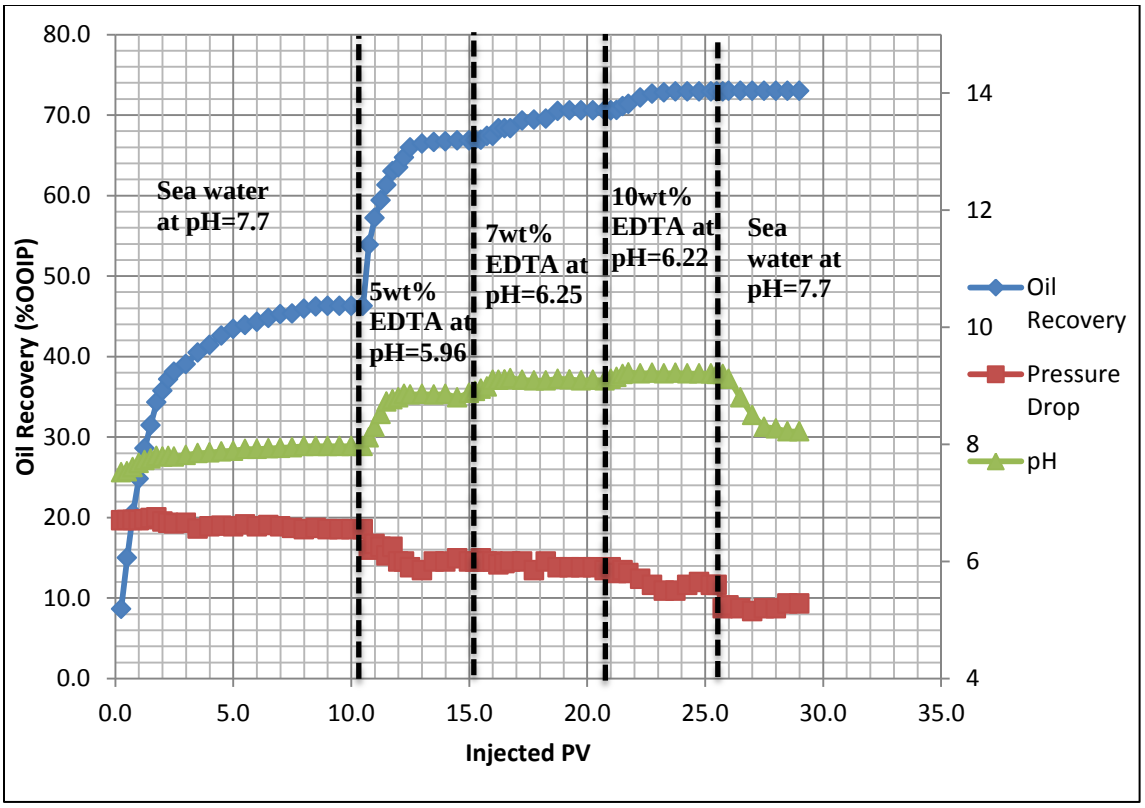

Figure 53: Oil recovery by seawater followed by 5wt%, then 7wt% and 10wt% of EDTA at pH =6.

Table 14: Properties of the core samples used in the fourth core flooding test

Core No.	Length (cm)	Diameter (cm)	Dry wt. (gm)	Bulk vol. (cc)	Saturated wt. (gm)	PV (cc)	Poro. (%)	Abs. Perm. (mD)	S_{wi} (%)	OOIP (cc)
2.1	4.9	3.8	119.9	55.5	129.1	8.0	14.5	42.2	28.4	5.7
3.2	4.8	3.8	117.6	54.6	125.6	7.0	12.9	41.9	31.5	4.8
Composite										
2.1+3.2	9.7	3.8	237.5	110.1	254.7	15.0	13.7	42.0	29.9	10.5

Figure 54 compares the oil recovery from the EDTA flooding (first experiment) and the GLDA flooding (second experiment); oil recovery was plotted against normalized injected PV. It can be clearly seen that, injection of GLDA can produce more oil than EDTA flooding when the same concentrations are used. Ultimate recovery of 83.76%

OOIP was achieved during the second core flooding, while EDTA flooding provides 65.5% OOIP as ultimate oil recovery. It can be concluded that, the solution pH and the chelating agent type have significant impact on the oil recovery; the lowest pH is the better since low pH condition leads to more CO_2 generation which may result in additional oil recovery through miscible/immiscible flooding. Compare to EDTA, GLDA performs better when it comes to enhance the oil recovery, because GLDA form more stable complexes with metal ions compared to other types of chelating agents and chelate more ions from the rock surface. However, chelating agent with small concentrations should be used to avoid severe rock dissolutions.

Figure 55 compares the oil recovery from seawater followed by 5wt. % , then 7wt. % and 10wt. % of GLDA (Experiment no. 3) and from seawater followed by 3wt. % , then 5wt% and 7wt. % of GLDA (Experiment no. 2). The ultimate oil recoveries are 83.76% and 85.3% OOIP in the second and third core flooding which indicates that, increasing the chelate concentration up to 10wt. % don't improve the oil production significantly. Therefore, it's recommended to use GLDA with concentrations less than 10wt% to avoid severe rock dissolutions and to optimize the oil recovery.

Figure 56 compares the oil production from seawater followed by 5wt. %, then 7wt. % and 10wt. % of GLDA (Experiment no. 3) and from seawater followed by 5wt%, then 7wt. % and 10wt. % of EDTA (Experiment no. 4). In both experiments, increase of the chelating agent concentration resulted in enhancing the oil recovery for each phase, and this recovery increment can be attributed to two mechanisms; wettability alteration and IFT reduction. As discussed earlier, more chelate concentration leads to increase the chelation force and then improve the wettability conditions to expel more oil. Also, the

increase of the chelating agent concentration creates favorable flowing conditions; therefore more oil can be produced. Table 15 presents a summary of the injected pore volumes, the incremental oil recovery and the ultimate oil recovery for all core flooding experiments.

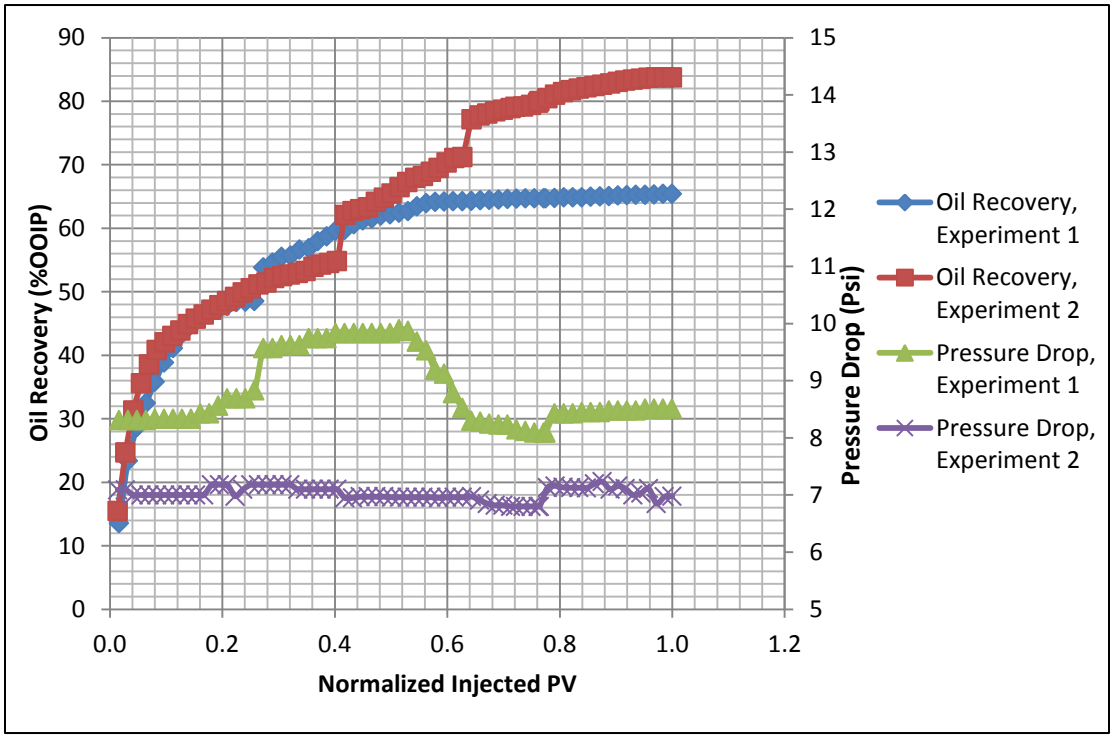

Figure 54: Comparison between the oil recovered and pressure drop from EDTA flooding (Experiment no. 1) and GLDA flooding (Experiment no. 2).

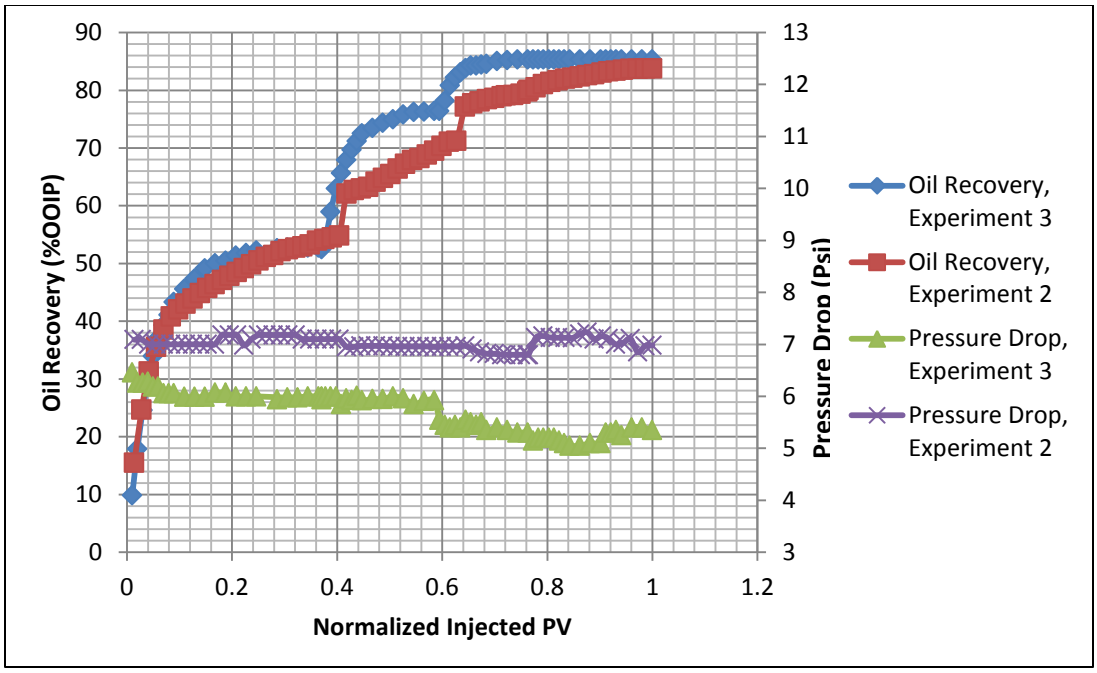

Figure 55: Comparison between the oil recovered and pressure drop from seawater followed by 5wt%, then 7wt% and 10wt% of GLDA (Experiment no. 3) and from seawater followed by 3wt%, then 5wt% and 7wt% of GLDA (Experiment no. 2).

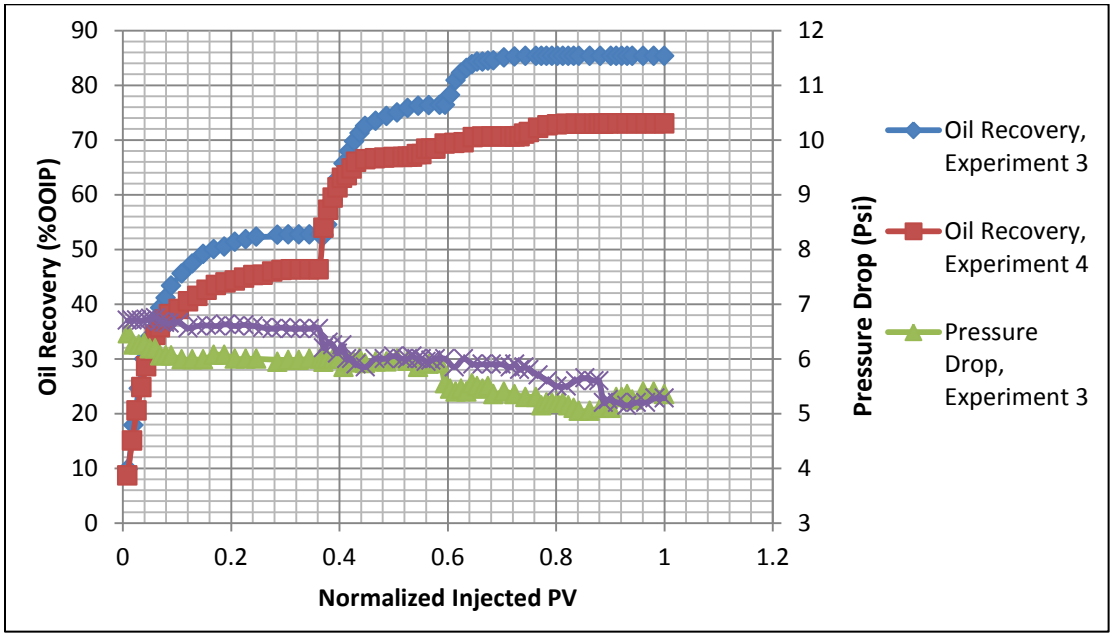

Figure 56: Comparison between the oil recovered and pressure drop from seawater followed by 5wt%, then 7wt% and 10wt% of GLDA (Experiment no. 3) and from seawater followed by 5wt%, then 7wt% and 10wt% of EDTA (Experiment no. 4).

Table 15: Summary of the injected pore volumes, the incremental oil recovery and the ultimate oil recovery for all core flooding experiments.

	Experiment 1 (EDTA)		Experiment 2 (GLDA)		Experiment 3 (GLDA)		Experiment 4 (EDTA)	
injected Fluid	Inj. PV	incremental Recovery (%OOIP)	Inj. PV	incremental Recovery (%OOIP)	Inj. PV	incremental Recovery (%OOIP)	Inj. PV	incremental Recovery (%OOIP)
SW	4	48.5	7.3	54.9	9.4	52.7	10.5	46.3
3wt%	4.4	14.2	4.5	16.4	--	--	--	--
5wt%	1.6	1.6	2.4	8.8	5	23.7	5	20.5
7wt%	2.5	0.5	3	2.9	4	8.9	5.5	3.8
10wt%	--	--	--	--	4	0	4.5	2.3
FSW	3	0.7	2	0.7	3	0	4	0.1
sub-total	8.5	16.2	9.9	28.2	13	32.6	15	26.6
Total	15.5	65.4	19.2	83.8	25.4	85.3	29.5	73.0

Based on the core flooding results it can be seen that, flooding with GLDA is better than EDTA flooding since it can recover more additional oil. However, to provide the optimum scenario in terms of chelating agent concentration, a comparison study was performed as follow; the effective injected PV (which is the injected PV till no more oil recovery), the required amount of chelating agent, and the incremental recovery were determined for each concentration. GLDA of 39wt. % and EDTA of 30wt. % were used to prepare the different concentrations of chelating agent solutions. Table 16 summarizes the comparison study where six scenarios are proposed, the required amount of chelating agent was determined based on the effective volume of the injected fluid. The ratio of oil recovery to the required chelating agent (the percentage of OOIP produced by 1 gm. of the chelating agent) was calculated to pick out the optimum scenario. From this study it can be concluded that, chelating agent with concentration of 3wt. % can be considered as the optimum scenario for both EDTA and GLDA flooding, since it provides the

maximum ratio of oil recovery to required amount of chelating agent, 1gram of EDTA enhances the recovery by 2.135% of OOIP, while a gram of GLDA increases the oil production by 2.715% of OOIP. Moreover, flooding with 3wt. % followed by 5wt. % GLDA shows the most economical scenario for enhancing the oil recovery, injecting of 5wt% followed by 7wt% GLDA provides the highest incremental oil recovery.

Table 16: Summarization of the comparison study

Scenarios	EDTA solutions		GLDA solutions		Oil recovery to required chelating agent ratio	
In term of wt.%	Required chelating agent (gm.)	Oil recovery (OOIP %)	Required chelating agent (gm.)	Oil recovery (OOIP %)	EDTA	GLDA
3	6.627	14.15	6.0299	16.3700	2.135	2.715
5	10.026	20.529	10.1470	23.6900	2.048	2.335
3+5	11.569	15.699	12.0613	25.1770	1.357	2.087
5+7	24.890	24.284	16.9666	32.6200	0.976	1.923
3+5+7	19.680	16.175	20.8582	28.1750	0.822	1.351
5+7+10	37.422	26.613	30.3607	32.6200	0.711	1.074

4.4 Characterization of Core Samples after Core Flooding Experiments

After core flooding experiments, core samples were cleaned to remove hydrocarbons and salts then oven was used to dry the samples, CT scan was performed to characterize the pore geometry after core flooding. Appendix E shows the CT scan results before and after core flooding. Thereafter, core saturation system was used to saturate core samples with formation brine at 2500 psi for 12 Hours; finally the absolute permeability was estimated using the formation brine at different flow rates. Table 17 lists the core

permeabilities before and after core flooding, and Figure 57 shows the permeability enhancement for core samples after core flooding.

Table 17: Permeabilites of the core samples before and after core flooding

Core Sample	Abs. Perm-Before Core Flooding (Ki)	Flooding Fluid	Abs. Perm-After Core Flooding (Kf)	Perm. Change (Kf/Ki)	Note
1.1	32.0	EDTA(3,5,7 wt.%)	63.03	1.970	Inlet
1.2	121.7	EDTA(3,5,7 wt.%)	265.33	2.180	Outlet
1.3	242.7	GLDA(3,5,7 wt.%)	3515.81	14.489	Inlet
1.4	267.2	GLDA(3,5,7 wt.%)	364.76	1.365	Outlet
2.1	42.2	EDTA(5,7,10 wt.%)	1222.02	28.992	inlet
3.2	41.9	EDTA(5,7,10 wt.%)	1093.86	26.125	Outlet
3.1	62.6	GLDA(5,7,10 wt.%)	5730.29	91.553	inlet
2.4	34.6	GLDA(5,7,10 wt.%)	1454.57	42.015	Outlet

It can be concluded that, GLDA gives more permeability improvement than EDTA with same concentrations sequences, and as the concentration increases the permeability enhancement increases, also more permeability increment was obtained closer to the core inlet. Significant pressure drop was observed during the third and fourth experiments which indicates severe rock dissolutions was occurred, CT scan results show that, channels/wormholes have been created inside the core samples after flooding with 10wt% of EDTA or GLDA. In addition, no core plugging or damage was occurred since all samples show permeability improvement after flooding experiments.

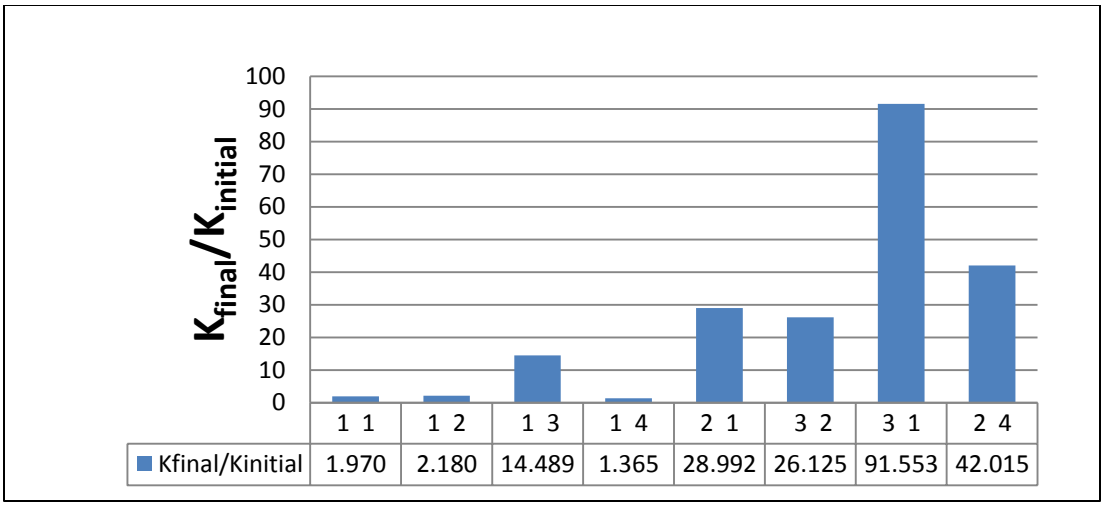

Figure 57: Permeability Enhancement for core samples after core flooding experiments.

4.4 Elemental Analysis of Produced Effluent from Core Flooding Experiments

The produced effluents were analyzed using inductively coupled plasma optical emission spectrometry (ICP-OES), which is a type of mass spectrometry capable to detect metals and several non-metals at concentrations as low as one part in 10^{15}. The machine utilizes inductively coupled plasma to ionize the sample and then uses mass spectrometer to separate and quantify those ions. Figure 58 and 59 show the Ca^{+2}concentration in the produced effluents with the change of both oil recovery and pH values for the first core flooding experiment. In this experiment seawater was injected followed by 3wt%, then 5wt% and 7wt% of EDTA. Ca^{+2} concentration increases when chelating agent was injected which can be attributed to that, chelating agents dissolve the rock sample and enhance the calcium leaching from the rock surface. Significant increase in the Ca^{+2} concentrations was observed during 7wt% EDTA flooding which indicates that, considerable rock dissolutions was taken a place.

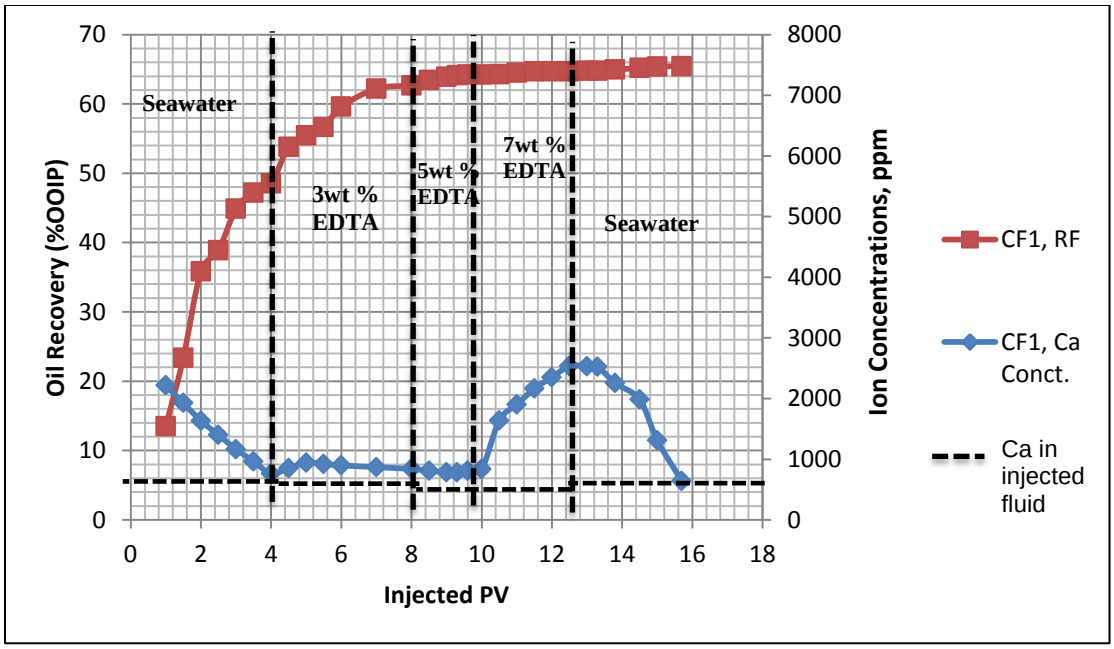

Figure 58: Oil Recovery and Ca^{+2} Concentration in the Produced Effluents from injection of Seawater (pH=7.7) followed by 3wt%, then 5wt% and 7wt% of EDTA at pH =6, Experiment 1.

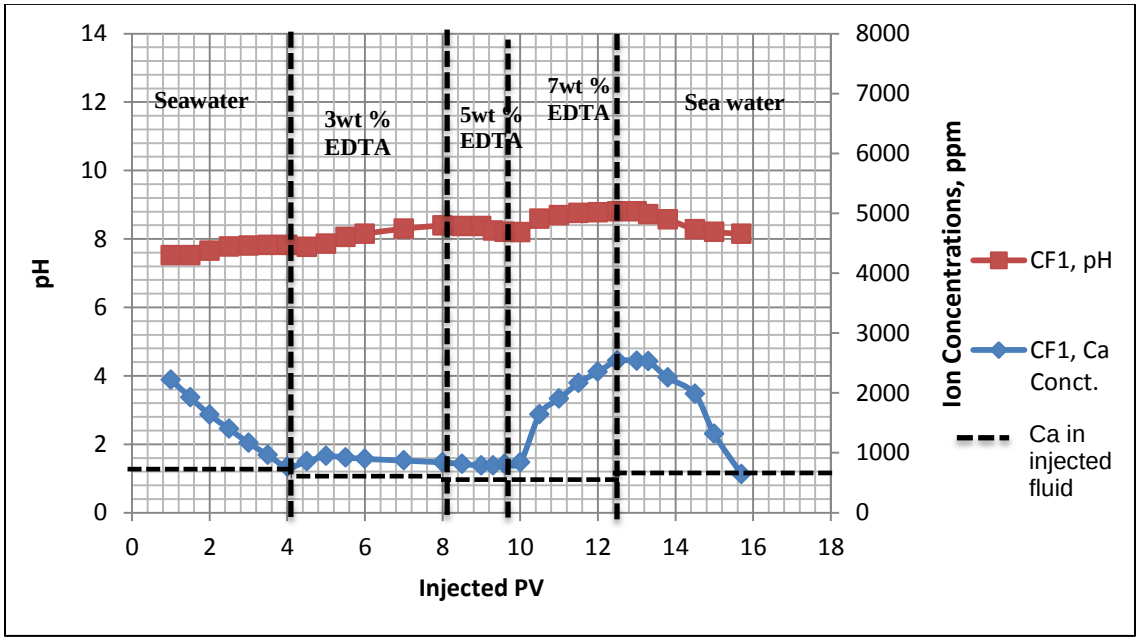

Figure 59: pH distribution and Ca^{+2} Concentration in the Produced Effluents from injection of Seawater (pH=7.7) followed by 3wt%, then 5wt% and 7wt% of EDTA at pH =6, Experiment 1.

Figures 60 and 61 show the profile of $Mg^{+2}$and Na^{+} concentrations during the first core flooding experiment with change of oil recovery. XRD and XRF results show that, the core samples contain small concentration of magnesium and sodium, therefore, Mg^{+2} and Na^{+} are coming only from the injected solutions. Mg^{+2} concentration decreases as chelating agents injected, since seawater has more concentration of Mg^{+2} than the chelating agent solutions, also this decrease may be due to replacement of calcium ions by adsorbed magnesium on the rock surface. However, sodium ions increase during the injection of chelating agent solution, and this is because the chelating agents used in this study are sodium based.

In addition, no potassium and manganese ions were detected in the solutions, because none of them were injected within seawater or chelating agent solutions. Besides that, the formation brine does not contain these ions and very small amount of potassium was presented in core samples as potassium oxide (K_2O). Moreover, ICP results showed some CO_3^{-2} ions in the effluents which confirmed that few amount of carbon dioxide was generated during this experiment, refer to Appendix D.

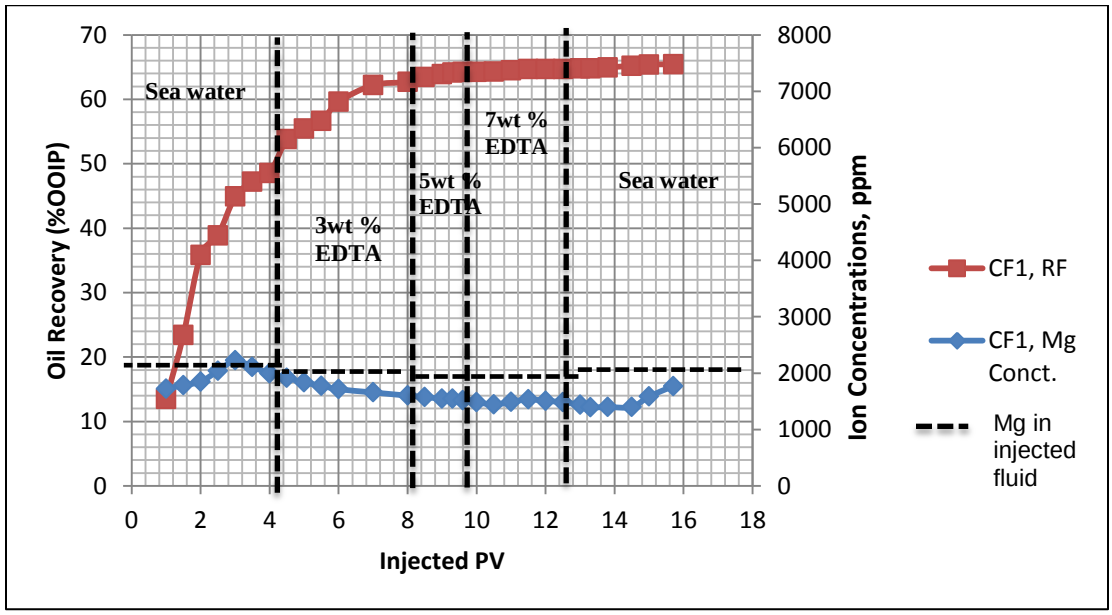

Figure 60: Oil Recovery and Mg^{+2} Concentration in the Produced Effluents from injection of Seawater (pH=7.7) followed by 3wt%, then 5wt% and 7wt% of EDTA at pH =6, Experiment 1.

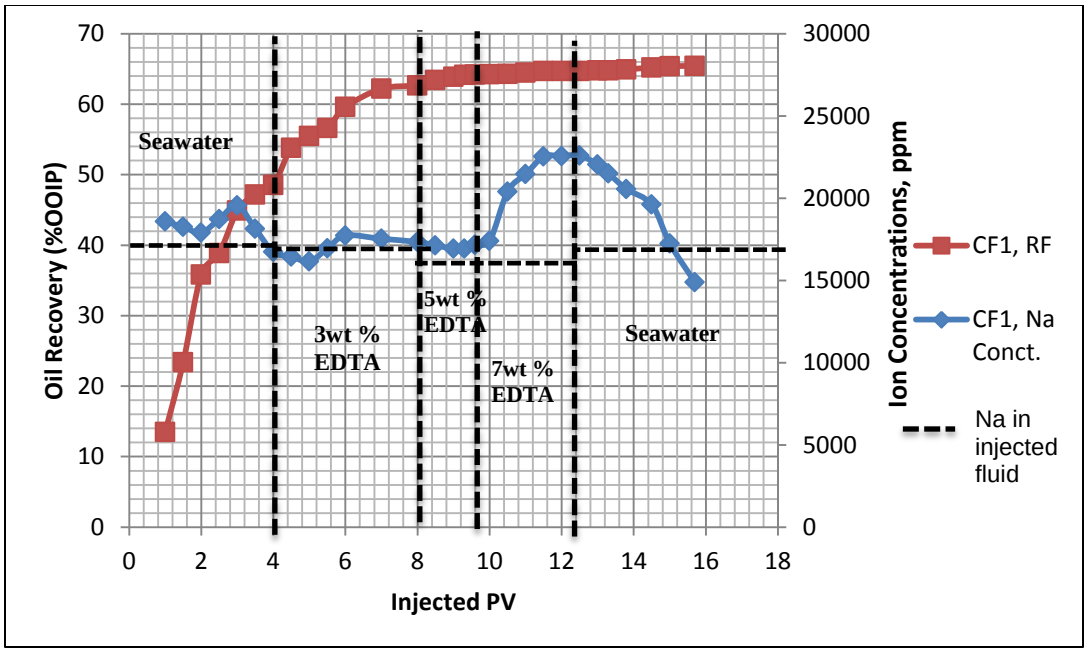

Figure 61: Oil Recovery and Na^{+} Concentration in the Produced Effluents from injection of Seawater (pH=7.7) followed by 3wt%, then 5wt% and 7wt% of EDTA at pH =6, Experiment 1.

Figures 62 to 65 show the profile of Ca^{+2}, $Mg^{+2}$and Na^{+} concentrations during the second core flooding experiment with change of both oil recovery and pH. In this experiment, seawater with 7.7 pH was injected followed by 3wt%, then 5wt% and 7wt% of GLDA at pH =4. It can be seen from those figures that, more Ca^{+2} concentrations were achieved in the effluents which proves that, GLDA is more powerful than EDTA in chelating the metal ions from the rock surface, since same concentrations were used. Same profiles were achieved for both Mg and Na ions, and that is because Mg^{+2} and Na^{+} are coming mainly from the injected solutions not from the rock sample. In addition, no carbonate ions were detected in the produced effluent which can be attributed to that, all carbonic acid was converted into carbon dioxide, refer to Appendix D.

In both experiments, the Ca^{+2} and Na^{+} concentrations in the produced effluent started with values higher than those in the injected seawater concentration; due to the mixing of the Ca^{+2} and Na^{+} from the formation brine which has higher amount of both Ca^{+2} and Na^{+} than the injected fluids. However, mixing of seawater and formation brine results in lower values of Mg^{+2}concentration than those in the injected fluid, therefore,

Mg^{+2}concentration started with lower values then increased toward their concentrations in the seawater.

It can be concluded that, flooding with GLDA shows higher concentrations of calcium ions than EDTA flooding with same concentrations sequences, which indicates GLDA can lead to more rock dissolution than EDTA, therefore it can result in better oil recovery than EDTA. As the chelating agent concentration increases the rock dissolution increases then more oil can be produced. Injecting chelating agents (both GLDA and EDTA) lead to decrease magnesium concentrations in the produced effluent which can be attributed to that, magnesium ions replaced the calcium ions on the rock surface.

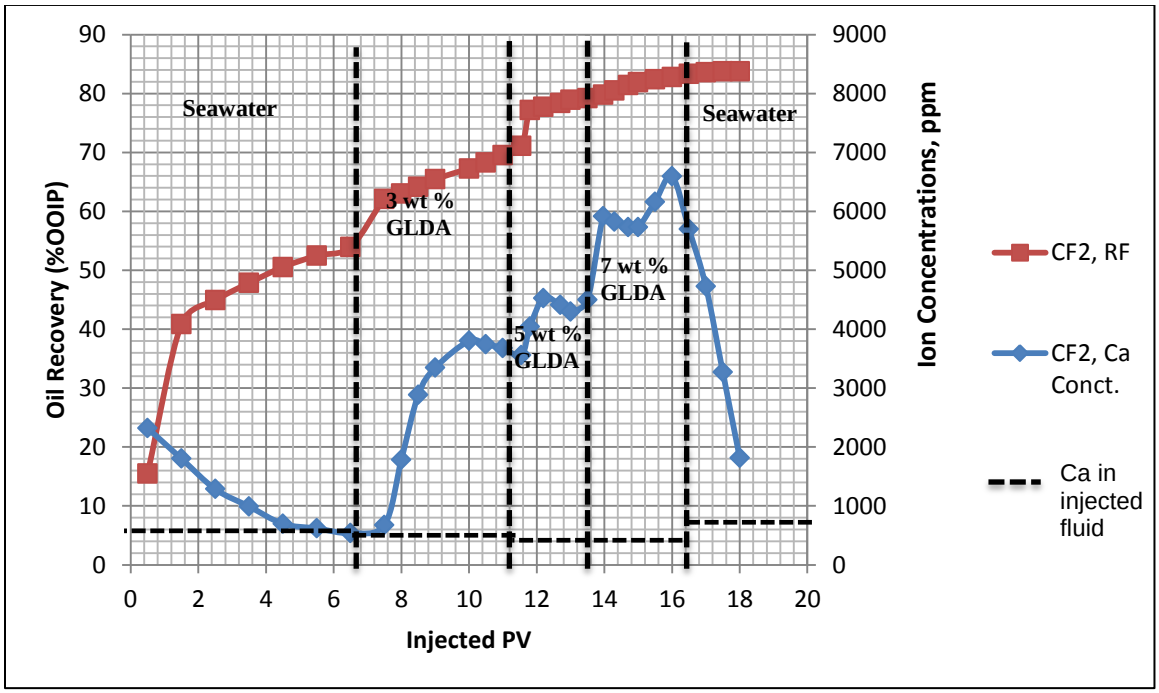

Figure 62: Oil Recovery and Ca^{+2} Concentration in the Produced Effluents from injection of Seawater (pH=7.7) followed by 3wt%, then 5wt% and 7wt% of GLDA at pH =4, Experiment 2.

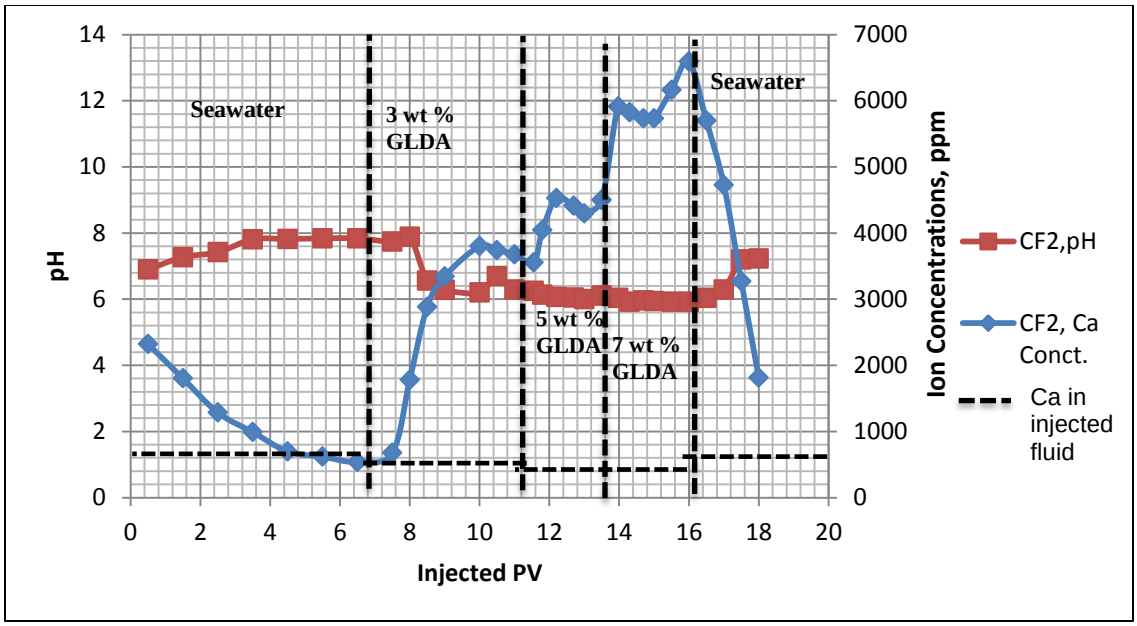

Figure 63: pH distribution and Ca^{+2} Concentration in the Produced Effluents from injection of Seawater (pH=7.7) followed by 3wt%, then 5wt% and 7wt% of GLDA at pH =4, Experiment 2.

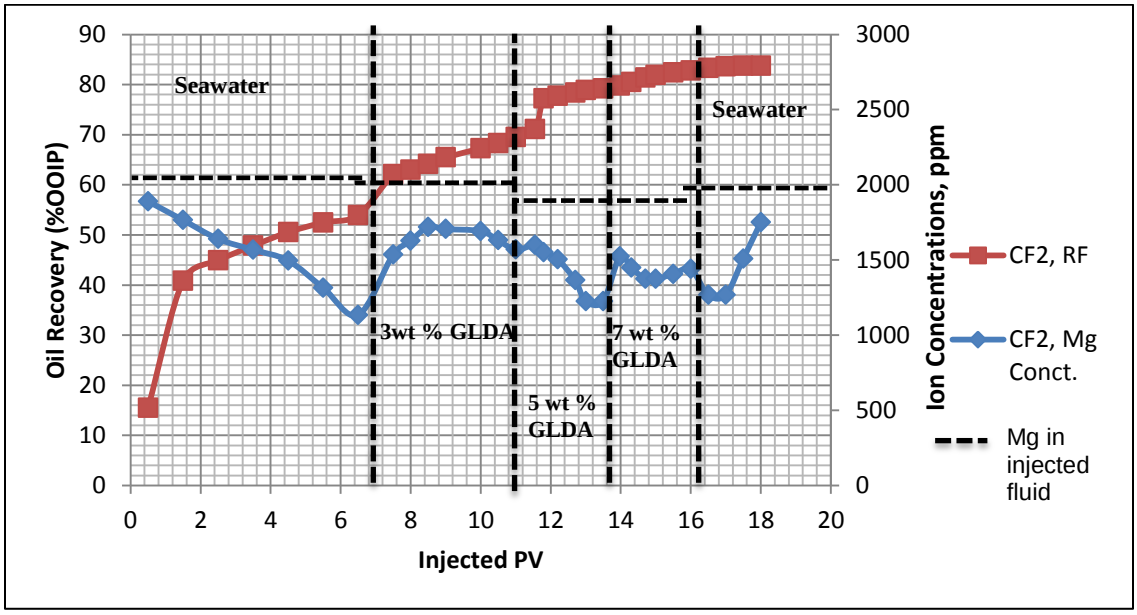

Figure 64: Oil Recovery and Mg^{+2} Concentration in the Produced Effluents from injection of Seawater (pH=7.7) followed by 3wt%, then 5wt% and 7wt% of GLDA at pH =4, Experiment 2.

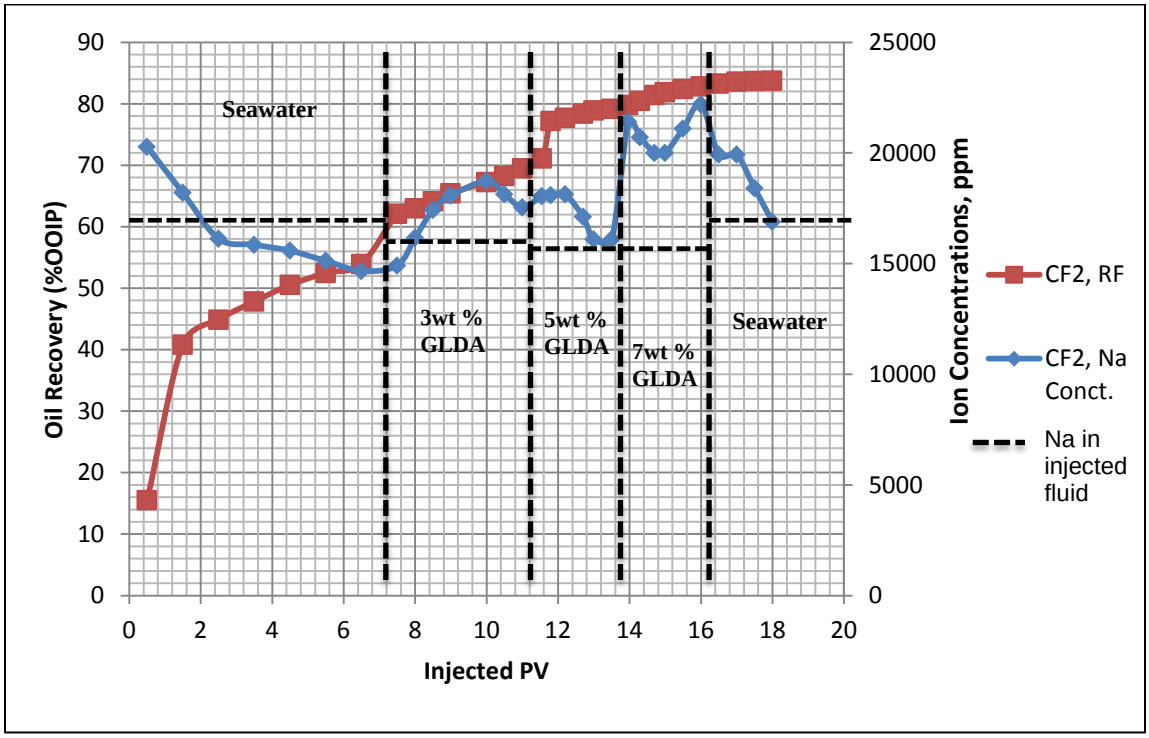

Figure 65: Oil Recovery and Na^+ Concentration in the Produced Effluents from injection of Seawater (pH=7.7) followed by 3wt%, then 5wt% and 7wt% of GLDA at pH =4, Experiment 2.

CHAPTER 5

CONCLUSIONS AND RECOMMENDATIONS

5.1 Conclusions

In this study, comprehensive zeta potential measurements were performed to investigate the effects of rock mineralogy and chelating agent solutions on the rock wettability condition. Interfacial tension was measured between different concentration of chelating agent and crude oil, to examine the alteration of IFT due to introduction of the chelating agents. In addition, core flooding experiments were conducted to investigate the use of chelating agents (EDTA and GLDA) as an EOR chemical fluid to improve oil recovery through in-situ generation of carbon dioxide in carbonate reservoirs. The following conclusions can be made from the interpretation of the obtained results:

- The compatibility between chelating agents and seawater was investigated, white precipitation was observed for pH less than 5.5. The precipitation increases as the pH value decreases and as the EDTA concentration increases. Increasing the pH value to 7 made the EDTA compatible with seawater and no precipitation was observed.
- Precipitation was occurred for all pH values less than 5 for samples prepared using 5 times diluted seawater. These observations show that, EDTA cannot be used with seawater or diluted seawater at low pH values. Moreover, the stability

of GLDA at high temperature was investigated; results show that, GLDA is compatible with seawater at high temperature conditions.

- Zeta potential measurements conclude that, using the chelating agent can alter the rock wettability to more water-wet then increase the ultimate oil recovery from carbonate reservoirs through wettability alteration mechanism. The comparison between deionized water, low salinity water and chelating agent solution shows that, more wettability alteration can be obtained with minimum cost by using chelating agent solutions instead of low salinity water. The presence of crude oil in the solution results in more negative values for the zeta potential, then improves the wettability alteration and therefore more oil recovery can be achieved.
- Interfacial tension for oil in DIW, oil in SW, and oil in chelating agent solution show that, chelating agent solutions can result in better oil recovery than DIW and SW due the lower IFT value, as low IFT means favorable flowing conditions; therefore more oil can be produced. Increasing the chelating agent concentration leads to lower IFT values.
- Slight changes in the pressure drop was observed during all core flooding experiments which implies that, there is no damage due to reaction between chelating agent and the core samples, and that was confirmed lately by using CT scan and permeability measurement for core samples after flooding.
- During all core flooding experiments, pH was changing in a small range and it stabilized at each phase which indicates that, the reactions between chelating agent solutions and the core samples reached the equilibrium state at each phase.

Solution pH has significant effect on the oil recovery, the lowest pH is the better since more CO_2 can be produced, however small concentrations should be used to avoid severe rock dissolutions.

- No carbon dioxide was observed during EDTA flooding with pH of 6, however in GLDA flooding with pH of 4, the reaction between the carbonate rock and GLDA solutions led to in situ CO_2 generation as it was observed in the effluent, and the amount of CO_2 was increasing with the GLDA concentration.
- The ultimate recovery in the second experiment (using GLDA solutions) is 83.76% while it is 65.5% in the first experiment (using EDTA solutions), which indicates that GLDA is more powerful than EDTA since same concentrations were used.
- Based on GLDA flooding, it is recommended to use GLDA with concentrations less than 10wt% because no more oil was recovered with 10wt% GLDA, and significant precipitation was observed in the effluent which implies that, severe rock dissolutions was occurred during core flooding. Moreover the CT scan results show that, channels/wormholes have been created inside the core samples which may lead to bypass more oil; then increase the residual oil saturation and reduce the ultimate oil recovery.
- The optimum concentration of EDTA and GLDA solutions to maximize the oil recovery without severe rock dissolution is the 3wt%, while the best sequential scenario for enhancing the oil recovery can be achieved by flooding with 3wt. % followed by 5wt%.

5.2 Recommendations

- Micro-CT scan could be used during core flooding to visualize the in-situ generation of carbon dioxide, then to better understand the mechanisms lead to more oil recovery.
- 3D reservoir simulation could be built to estimate the oil recovery from limestone reservoir due to in-situ CO_2 generation.
- Other types of chelating agents could be investigated to enhance the oil recovery from carbonate formation through in-situ generation of CO_2.

APPENDIX A: Fluid Characterization

Table A.1: Viscosity and Density of UTMN dead oil at different temperatures (p=14.7 psi)

Temperature (°C)	Viscosity (cP)	Density (g/cc)
36	10.263	0.869
41.5	9.609	0.864
42.2	8.554	0.865
55.4	5.508	0.855
72.2	3.727	0.8435
100 (extrapolation)	2.420	0.827

Table A.2: Viscosity and Density of Seawater at different temperatures (p=14.7 psi)

Temperature (°C)	Viscosity (cP)	Density (g/cc)
22	1.071	1.06
41.5	0.920	1.055
55.4	0.675	1.050
72.2	0.504	1.045
100 (extrapolation)	0.340	1.035

1. 3wt% GLDA Viscosity

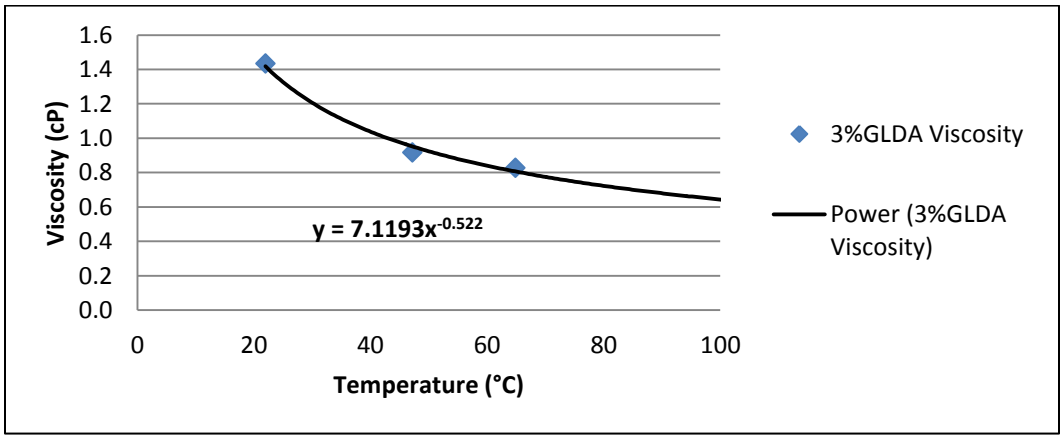

Figure A. 1: Viscosity of 3wt% GLDA as a function of temperature at atmospheric condition.

2. 3wt% GLDA Density

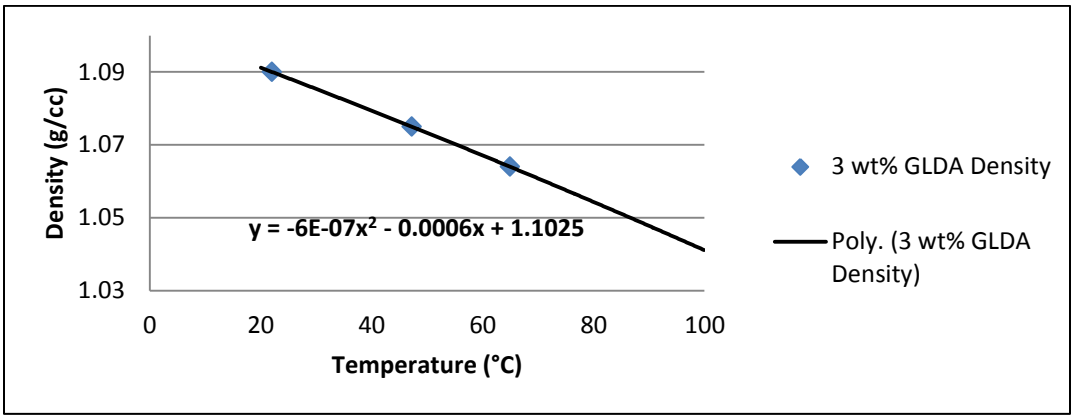

Figure A. 2: Density of 3wt% GLDA as a function of temperature at atmospheric condition.

Table A.3: Viscosity and Density of 3wt% GLDA at different temperatures (p=14.7 psi)

Temperature (°C)	Viscosity (cP)	Density (g/cc)
22	1.4336	1.09
47.2	0.9166	1.075
64.9	0.8277	1.064
100 (extrapolation)	0.6200	1.041

3. 5wt% GLDA Viscosity

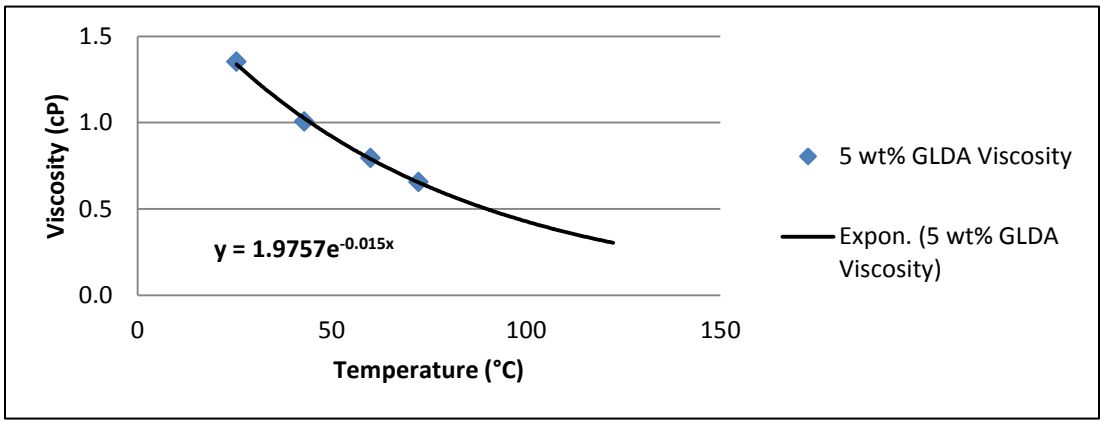

Figure A. 3: Viscosity of 5wt% GLDA as a function of temperature at atmospheric condition.

4. 5wt% GLDA Density

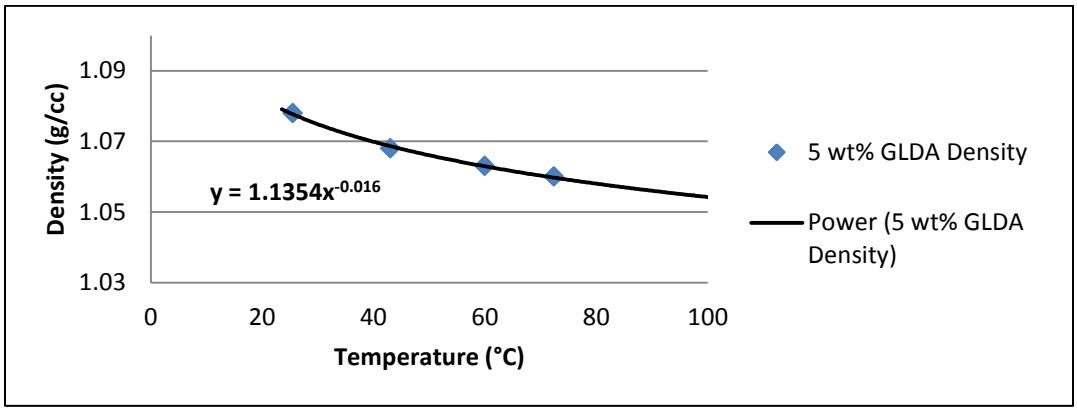

Figure A. 4: Density of 5wt% GLDA as a function of temperature at atmospheric condition.

Table A.4: Viscosity and Density of 5wt% GLDA at different temperatures (p=14.7 psi)

Temperature (°C)	Viscosity (cP)	Density (g/cc)
25.5	1.3512	1.078
43	1.0052	1.068
60	0.7932	1.063
72.4	0.6550	1.06
100 (extrapolation)	0.4200	1.055

5. 7wt% GLDA Viscosity

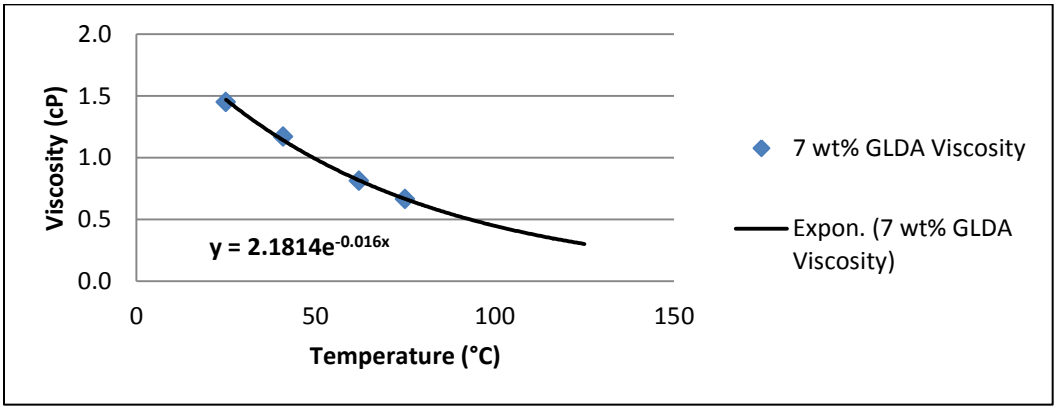

Figure A. 5: Viscosity of 7wt% GLDA as a function of temperature at atmospheric condition.

6. 7wt% GLDA Density

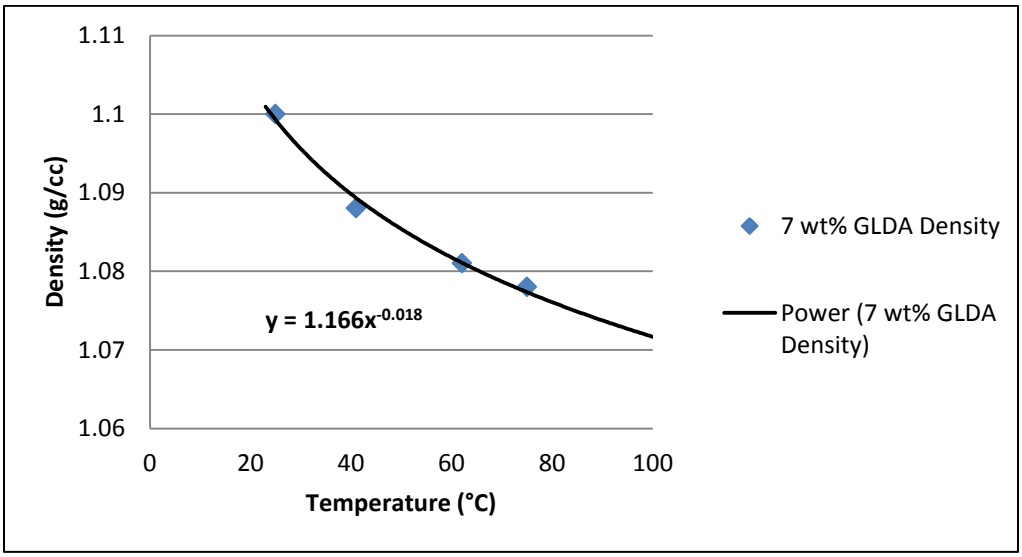

Figure A. 6: Density of 7wt% GLDA as a function of temperature at atmospheric condition.

Table A.5: Viscosity and Density of 7wt% GLDA at different temperatures (p=14.7 psi)

Temperature (°C)	Viscosity (cP)	Density (g/cc)
25	1.4481	1.1
41	1.1685	1.088
62.1	0.8114	1.081
75	0.6648	1.078
100 (extrapolation)	0.440	1.07324

APPENDIX B: Interfacial Tension with Temperature

1. IFT vs. Time for 5wt% GLDA at temperature of 23 °C and pH of 4

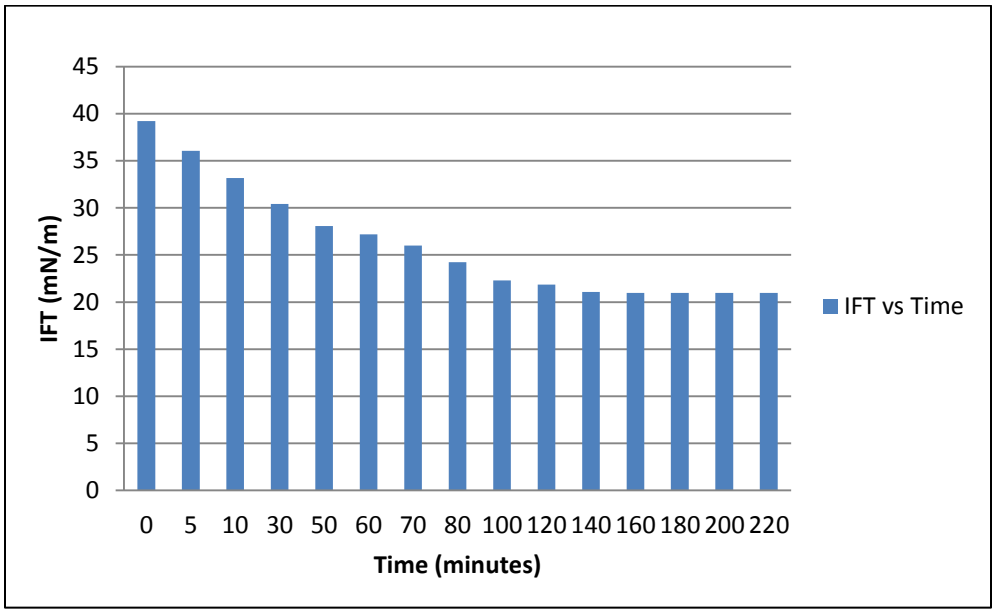

Figure B. 1: Interfacial tension of 5wt% GLDA at different times.

2. IFT vs. Temperature for DIW

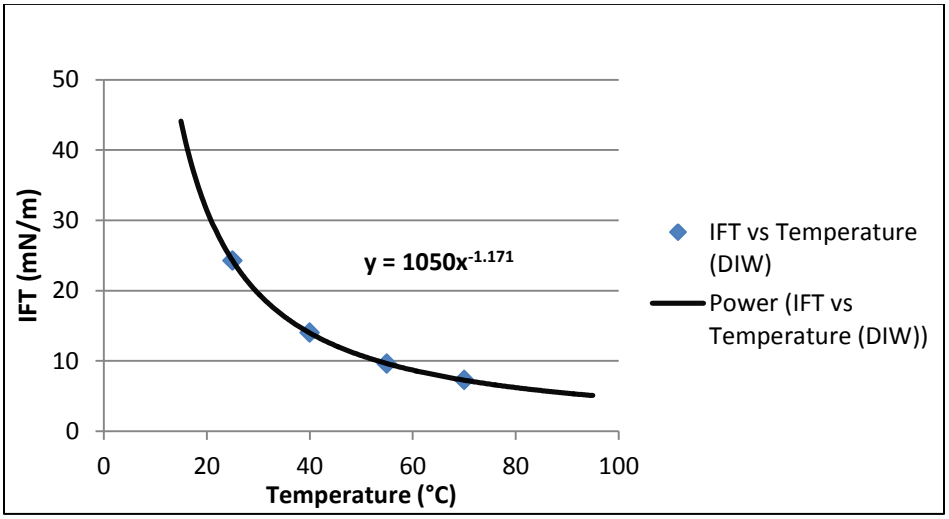

Figure B. 2: Interfacial tension of deionized water at different temperatures.

3. IFT vs. Temperature for SW.

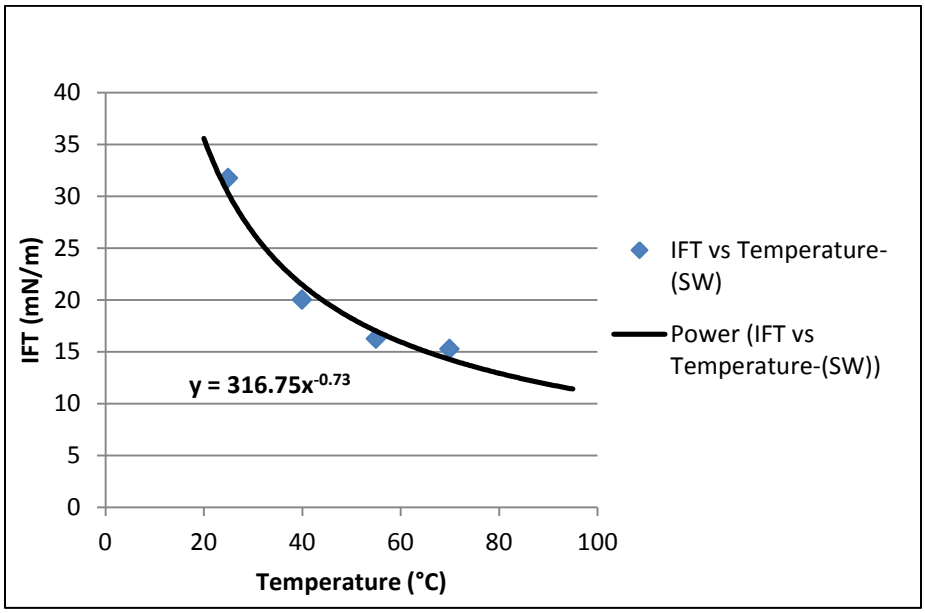

Figure B. 3: Interfacial tension of seawater at different temperatures.

4. IFT vs. Temperature for 3wt% GLDA at pH=4

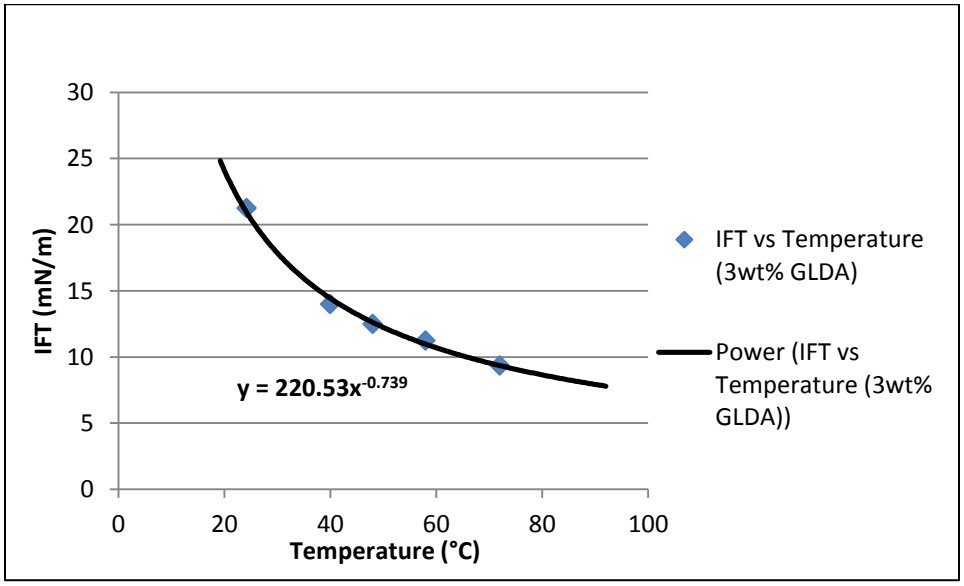

Figure B. 4: Interfacial tension of 3wt% GLDA at different temperatures.

5. IFT vs. Temperature for 5wt% GLDA at pH=4

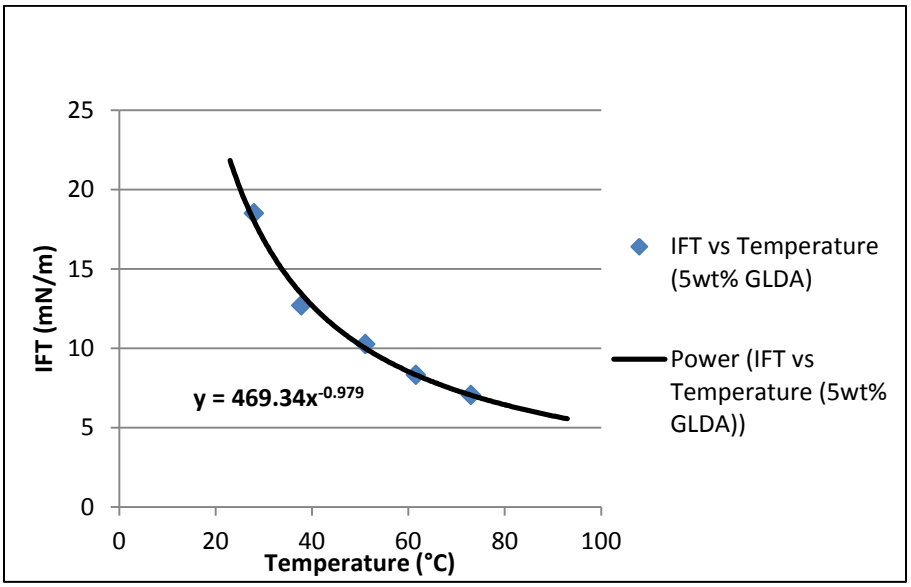

Figure B. 5: Interfacial tension of 5wt% GLDA at different temperatures.

6. IFT vs. Temperature for 7wt% GLDA at pH=4

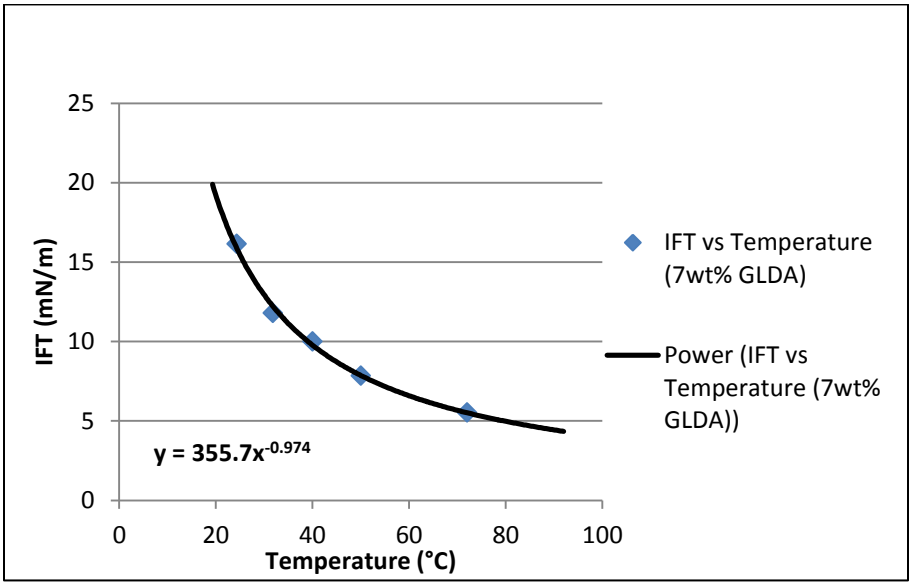

Figure B. 6: Interfacial tension of 7 wt. % GLDA at different temperatures.

APPENDIX C: Tabulated Data for Core Flooding Experiments

Table (C.1): Data for Oil Recovery, Pressure Drop and pH Curves, Experiment #1.

Injected Fluid	Cumulative PV Injected	Cumulative Oil Recovery (% OOIP)	Pressure drop(psi)	pH
Sea Water Flooding pH (7.70)	0.2523	13.585	8.31	7.52
	0.505	23.397	8.31	7.52
	0.757	28.680	8.31	7.52
	1.009	32.454	8.31	7.65
	1.262	35.851	8.33	7.65
	1.514	38.870	8.33	7.71
	1.766	41.134	8.33	7.77
	2.019	43.398	8.33	7.77
	2.271	44.908	8.33	7.77
	2.523	46.040	8.43	7.79
	2.776	46.794	8.43	7.79
	3.028	47.172	8.56	7.79
	3.280	47.776	8.69	7.80
	3.533	48.530	8.69	7.80
	3.785	48.530	8.69	7.82
	4.037	48.530	8.83	7.82
3 wt% EDTA at pH (5.53)	4.289	53.814	9.57	7.76
	4.542	54.568	9.57	7.76
	4.794	55.474	9.62	7.86
	5.046	55.700	9.62	8.05
	5.299	56.644	9.62	8.10
	5.551	56.833	9.743	8.15
	5.803	57.965	9.743	8.25
	6.056	58.719	9.743	8.30
	6.308	59.625	9.83	8.30
	6.560	59.738	9.83	8.35
	6.813	60.644	9.83	8.35
	7.065	61.248	9.83	8.35
	7.317	61.550	9.83	8.35
	7.570	62.403	9.83	8.35

Table (C.2): Cont. Data for Oil Recovery, Pressure Drop and pH Curves, Experiment #1.

Injected Fluid	Cumulative PV Injected	Cumulative Oil Recovery (% OOIP)	Pressure drop(psi)	pH
3 wt% EDTA at pH (5.53)	7.822	62.681	9.83	8.39
	8.074	62.682	9.9	8.39
	8.327	62.682	9.87	8.39
5 wt% EDTA, pH (6.73)	8.579	63.437	9.68	8.37
	8.831	63.927	9.53	8.37
	9.084	64.154	9.19	8.24
	9.336	64.229	9.12	8.2
	9.588	64.229	8.78	8.19
	9.841	64.229	8.52	8.19
7 wt% EDTA, pH (6.22)	10.093	64.305	8.30	8.59
	10.345	64.380	8.28	8.59
	10.598	64.448	8.25	8.69
	10.850	64.520	8.23	8.69
	11.102	64.591	8.23	8.75
	11.354	64.652	8.15	8.75
	11.607	64.690	8.12	8.75
	11.859	64.705	8.093	8.80
	12.111	64.705	8.093	8.80
	12.169	64.705	8.093	8.80
Final SW flooding pH (7.70)	12.421	64.780	8.43	8.72
	12.673	64.856	8.43	8.72
	12.926	64.871	8.43	8.64
	13.178	64.878	8.45	8.57
	13.430	64.954	8.45	8.41
	13.683	65.014	8.45	8.41
	13.935	65.074	8.48	8.28
	14.187	65.142	8.48	8.28
	14.440	65.203	8.48	8.20
	14.692	65.263	8.48	8.20
	14.944	65.331	8.51	8.20
	15.197	65.437	8.51	8.15
	15.449	65.437	8.51	8.15
	15.701	65.437	8.51	8.15

Table (C.3): Data for Oil Recovery, Pressure Drop and pH Curves, Experiment #2.

Injected Fluid	Cumulative PV Injected	Cumulative Oil Recovery (% OOIP)	Pressure drop(psi)	pH
Sea Water Flooding (7.70)	0.2500	15.480	7.09	6.9
	0.500	24.703	7.09	6.9
	0.750	31.290	7	6.9
	1.000	35.572	7	7.27
	1.250	38.536	7	7.27
	1.500	40.842	7	7.42
	1.750	42.028	7	7.42
	2.000	43.016	7	7.42
	2.250	43.905	7	7.71
	2.500	44.893	7	7.71
	2.750	45.750	7	7.71
	3.000	46.408	7	7.81
	3.250	47.166	7.18	7.81
	3.500	47.858	7.18	7.81
	3.750	48.549	7.18	7.81
	3.999	49.208	6.98	7.84
	4.249	49.880	7.1	7.84
	4.499	50.539	7.18	7.84
	4.749	51.131	7.18	7.84
	4.999	51.461	7.18	7.79
	5.249	52.153	7.18	7.79
	5.499	52.482	7.18	7.84
	5.749	52.712	7.18	7.84
	5.999	53.272	7.1	7.84
	6.249	53.743	7.1	7.84
	6.499	54.560	7.1	7.85
	6.749	54.853	7.1	7.85
	6.999	54.853	7.1	7.85
	7.249	54.853	7.1	7.85
3 wt% GLDA at pH (3.8)	7.499	62.099	6.95	7.74
	7.749	62.692	6.95	7.89
	7.999	62.989	6.97	7.89
	8.249	63.285	6.97	6.56
	8.499	64.142	6.97	6.56
	8.749	64.800	6.97	6.28
	8.999	65.459	6.96	6.28
	9.249	66.447	6.96	6.28

Table (C.4): Cont. Data for Oil Recovery, Pressure Drop and pH Curves, Experiment #2.

Injected Fluid	Cumulative PV Injected	Cumulative Oil Recovery (% OOIP)	Pressure drop(psi)	pH
3 wt% GLDA at pH (3.8)	9.499	67.271	6.96	6.20
	9.749	67.929	6.96	6.20
	9.999	68.885	6.96	6.35
	10.249	69.510	6.96	6.35
	10.499	70.367	6.95	6.29
	10.749	70.967	6.96	6.29
	10.999	71.223	6.96	6.29
	11.249	71.223	6.96	6.29
5 wt% GLDA pH (3.95)	11.550	77.152	6.97	6.25
	11.800	77.745	6.91	6.25
	12.050	78.074	6.85	6.13
	12.299	78.937	6.82	6.07
	12.549	79.135	6.82	6.07
	12.799	79.167	6.8	6.07
	12.947	79.418	6.8	6.05
	13.197	79.780	6.8	6.05
	13.447	80.030	6.8	6.00
	13.677	80.030	6.8	6.00
	13.718	80.030	6.8	6.11
7 wt% GLDA pH (3.95)	13.968	80.492	7.13	6.04
	14.218	81.051	7.159	5.99
	14.468	81.414	7.132	5.92
	14.718	82.184	7.127	5.92
	14.968	82.580	7.127	5.91
	15.217	82.777	7.125	5.91
	15.467	82.972	7.195	5.96
	15.717	83.028	7.233	5.95
	15.967	83.028	7.1	5.92
	16.217	83.028	7.159	5.92
Final SW flooding	16.447	83.245	7.112	6.04
	16.697	83.700	7.00	6.29
	16.947	83.733	7.031	6.76
	17.197	83.750	7.11	6.76
	17.447	83.760	6.850	7.20
	17.697	83.765	6.969	7.20
	17.947	83.765	6.979	7.23

Table (C.5): Data for Oil Recovery, Pressure Drop and pH Curves, Experiment #3.

Injected Fluid	Cumulative PV Injected	Cumulative Oil Recovery (% OOIP)	Pressure drop(psi)	PH
Sea Water Flooding pH (7.70)	0.2526	9.8	6.46	7.48
	0.505	17.9	6.26	7.48
	0.758	24.6	6.26	7.48
	1.010	29.9	6.28	7.51
	1.263	34.0	6.19	7.51
	1.516	37.1	6.19	7.51
	1.768	39.3	6.06	7.59
	2.021	41.1	6.06	7.59
	2.274	43.3	6.06	7.59
	2.772	45.6	5.99	7.52
	3.271	47.4	5.99	7.52
	3.770	49.1	5.99	7.52
	4.269	50.0	6.07	7.55
	4.768	50.5	6.07	7.64
	5.267	51.4	6	7.72
	5.766	51.8	6	7.86
	6.265	52.3	6	7.86
	9.416	52.4	5.94	7.86
	7.263	52.6	5.94	7.85
	7.762	52.7	5.98	7.84
	8.261	52.7	5.98	7.85
	8.760	52.7	6	7.95
	9.258	52.7	6	7.96
	9.416	52.7	6	7.95
5 wt% GLDA at pH (3.9)	9.606	54.5	6	7.72
	9.858	59.0	6	7.31
	10.111	63.0	6	6.9
	10.364	65.7	5.85	6.45
	10.616	67.9	5.96	6.21
	10.869	69.7	5.93	6.17
	11.122	71.2	6.01	5.99
	11.374	72.5	5.92	5.99
	11.873	73.4	5.95	5.99
	12.372	74.3	5.95	5.95
	12.871	75.0	6	5.95
	13.370	75.8	5.96	5.95
	13.869	76.2	5.85	5.92
	14.368	76.3	5.91	5.92
	14.867	76.3	5.92	5.93

Table (C.6): Cont. Data for Oil Recovery, Pressure Drop and pH Curves, Experiment #3.

Injected Fluid	Cumulative PV Injected	Cumulative Oil Recovery (% OOIP)	Pressure drop(psi)	pH
7 wt% GLDA pH (3.95)	15.119	76.4	5.55	5.81
	15.372	78.2	5.45	5.74
	15.625	80.9	5.4	5.69
	15.877	82.2	5.45	5.61
	16.130	83.1	5.4	5.61
	16.382	83.8	5.55	5.63
	16.635	84.3	5.5	5.56
	16.888	84.3	5.45	5.55
	17.140	84.4	5.5	5.56
	17.393	84.5	5.35	5.58
	17.892	85.1	5.4	5.58
	18.391	85.2	5.350	5.58
	18.890	85.3	5.300	5.58
	19.389	85.3	5.3	5.58
10 wt% GLDA pH (3.95)	19.641	85.3	5.15	5.5
	19.894	85.3	5.2	5.27
	20.146	85.3	5.2	5.19
	20.399	85.3	5.20	5.07
	20.652	85.3	5.2	5
	20.904	85.3	5.15	4.9
	21.157	85.3	5.100	4.95
	21.409	85.3	5.05	4.88
	21.908	85.3	5.05	4.86
	22.407	85.3	5.1	4.92
	22.906	85.3	5.1	4.94
Final SW flooding	23.159	85.3	5.300	4.910
	23.411	85.3	5.300	6.250
	23.664	85.3	5.350	6.900
	23.917	85.3	5.250	7.800
	24.416	85.3	5.400	7.810
	24.915	85.3	5.400	7.800
	25.414	85.3	5.350	7.810

Table (C.7): Data for Oil Recovery, Pressure Drop and pH Curves, Experiment #4.

Injected Fluid	Cumulative PV Injected	Cumulative Oil Recovery (% OOIP)	Pressure drop(psi)	pH
Sea Water Flooding at pH (7.7)	0.2500	8.651	6.7	7.52
	0.500	15.020	6.71	7.54
	0.750	20.533	6.71	7.61
	1.000	24.811	6.7	7.68
	1.250	28.614	6.72	7.73
	1.500	31.466	6.74	7.76
	1.750	34.317	6.75	7.8
	2.000	35.743	6.68	7.79
	2.250	37.169	6.66	7.800
	2.500	38.120	6.65	7.79
	3.000	39.071	6.66	7.82
	3.500	40.496	6.56	7.850
	4.000	41.447	6.6	7.86
	4.500	42.588	6.61	7.88
	5.000	43.443	6.6	7.89
	5.500	43.919	6.63	7.92
	6.000	44.299	6.6	7.92
	6.500	44.774	6.62	7.93
	7.000	45.250	6.6	7.94
	7.500	45.345	6.57	7.95
	8.000	45.915	6.55	7.97
	8.500	46.200	6.57	7.97
	9.000	46.295	6.55	7.97
	9.500	46.295	6.55	7.97
	10.000	46.295	6.55	7.97
	10.500	46.295	6.55	7.97
5 wt% EDTA at pH (6.38)	10.750	53.900	6.2	8.12
	11.001	57.227	6.3	8.3
	11.251	59.414	6.25	8.52
	11.501	61.315	6.1	8.73
	11.751	63.026	6.25	8.77
	12.001	63.501	6	8.8
	12.251	64.737	6	8.86
	12.501	65.973	5.9	8.85
	13.001	66.448	5.85	8.86
	13.501	66.639	6	8.85
	14.001	66.734	6	8.86
	14.501	66.829	6.05	8.8
	15.001	66.829	6	8.88

Table (C.8): Cont. Data for Oil Recovery, Pressure Drop and pH Curves, Experiment #4.

Injected Fluid	Cumulative PV Injected	Cumulative Oil Recovery (% OOIP)	Pressure drop(psi)	pH
7 wt% EDTA pH (6.1)	15.251	66.924	6	8.91
	15.501	66.924	6.05	8.95
	15.751	67.399	6	8.99
	16.001	67.399	6	9.1
	16.251	68.350	5.95	9.1
	16.501	68.350	5.97	9.11
	16.751	68.350	6	9.13
	17.251	69.300	6	9.1
	17.751	69.443	5.85	9.09
	18.251	69.538	6	9.09
	18.751	70.489	5.9	9.12
	19.251	70.584	5.9	9.11
	19.751	70.584	5.9	9.09
	20.251	70.584	5.9	9.1
	20.751	70.584	5.85	9.09
10 wt% EDTA pH (6.49)	21.001	70.584	5.9	9.12
	21.251	70.631	5.8	9.15
	21.501	71.106	5.85	9.2
	21.751	71.392	5.80	9.23
	22.251	72.152	5.7	9.21
	22.751	72.627	5.6	9.22
	23.251	72.818	5.500	9.21
	23.751	72.913	5.5	9.22
	24.251	72.913	5.6	9.21
	24.751	72.913	5.65	9.21
	25.251	72.913	5.6	9.21
	25.499	72.913	5.6	9.2
Final SW flooding at pH (7.7)	25.749	72.913	5.200	9.200
	25.999	73.008	5.250	9.120
	26.499	73.008	5.200	8.800
	26.999	73.008	5.150	8.500
	27.499	73.008	5.200	8.300
	27.999	73.008	5.200	8.270
	28.499	73.008	5.280	8.220
	28.999	73.008	5.280	8.220

APPENDIX D: Elemental Analysis Results

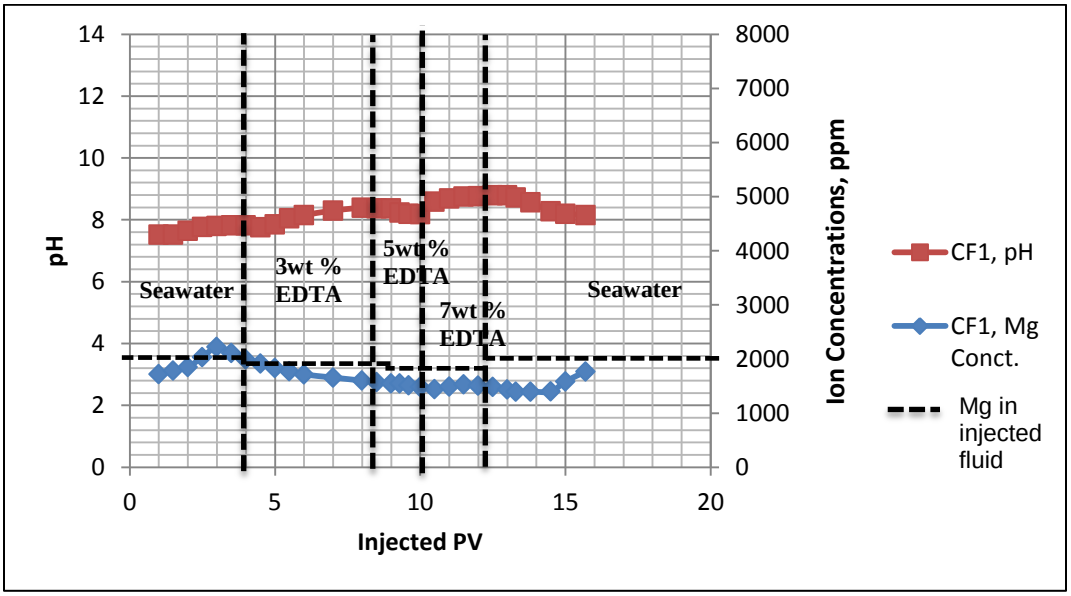

Figure D. 1: pH distribution and Mg^{+2} Concentration in the Produced Effluents from injection of Seawater (pH=7.7) followed by 3wt%, then 5wt% and 7wt% of EDTA at pH =6, Experiment 1.

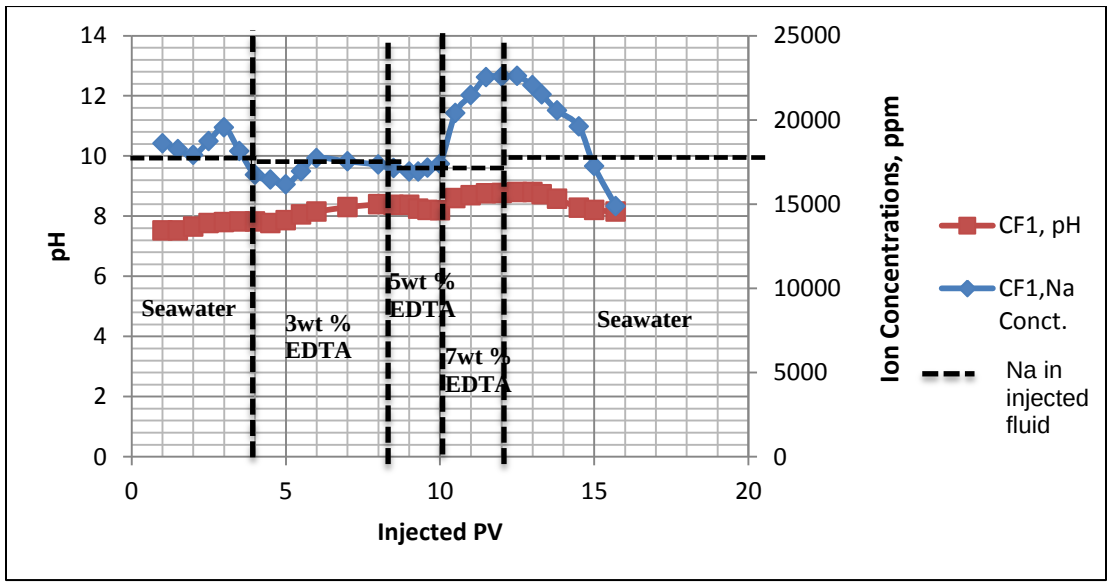

Figure D. 2: pH distribution and Na^{+} Concentration in the Produced Effluents from injection of Seawater (pH=7.7) followed by 3wt%, then 5wt% and 7wt% of EDTA at pH =6, Experiment 1.

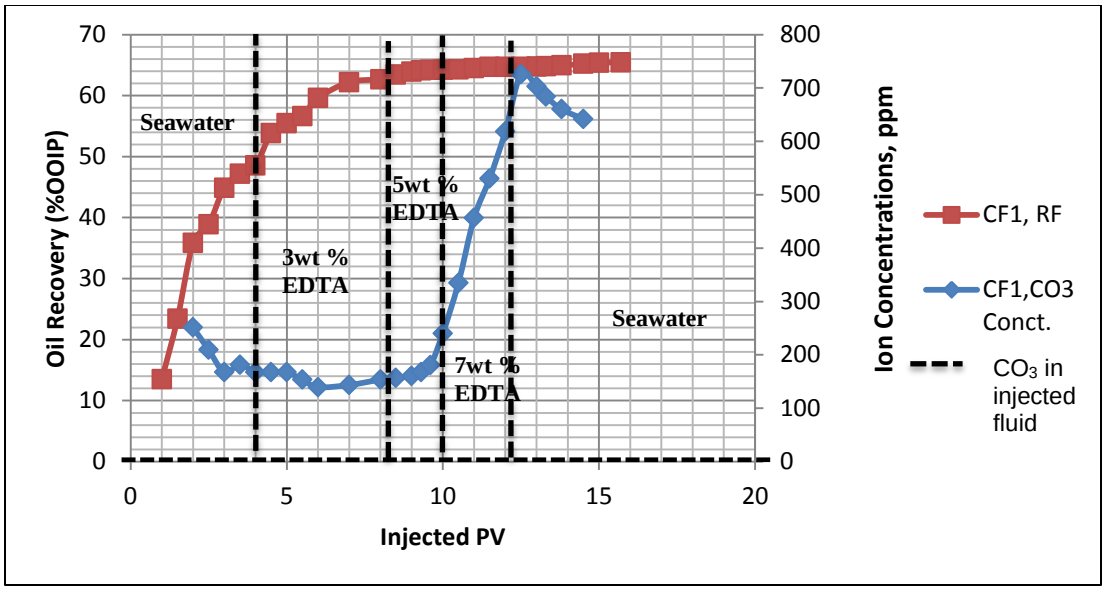

Figure D. 3: Oil Recovery and CO_3^{-2} Concentration in the Produced Effluents from injection of Seawater (pH=7.7) followed by 3wt%, then 5wt% and 7wt% of EDTA at pH =6, Experiment 1.

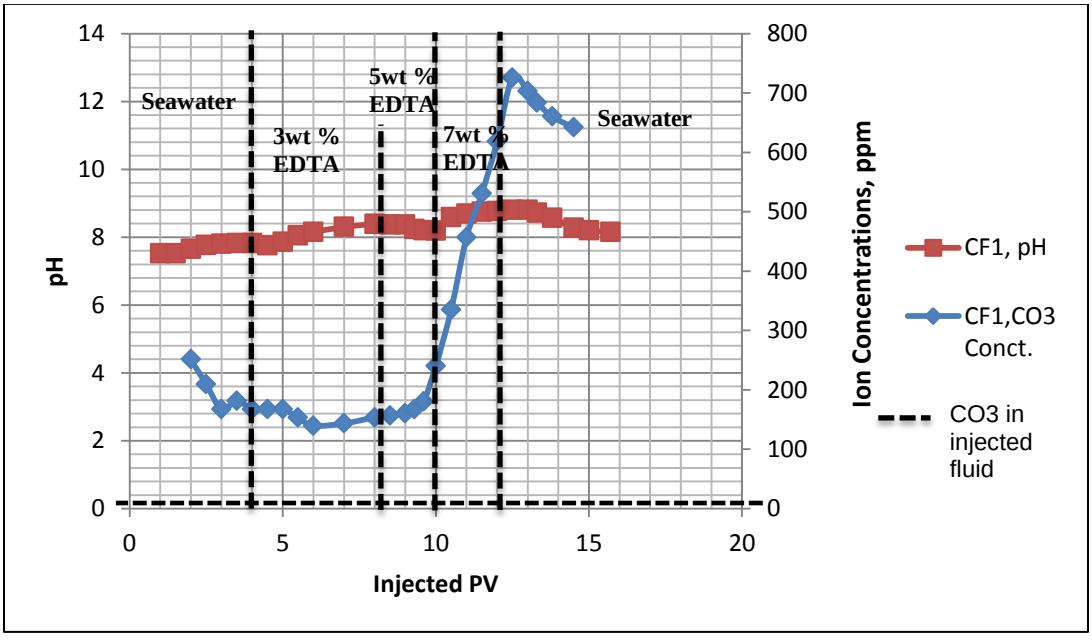

Figure D. 4: pH distribution and CO_3^{-2} Concentration in the Produced Effluents from injection of Seawater (pH=7.7) followed by 3wt%, then 5wt% and 7wt% of EDTA at pH =6, Experiment 1.

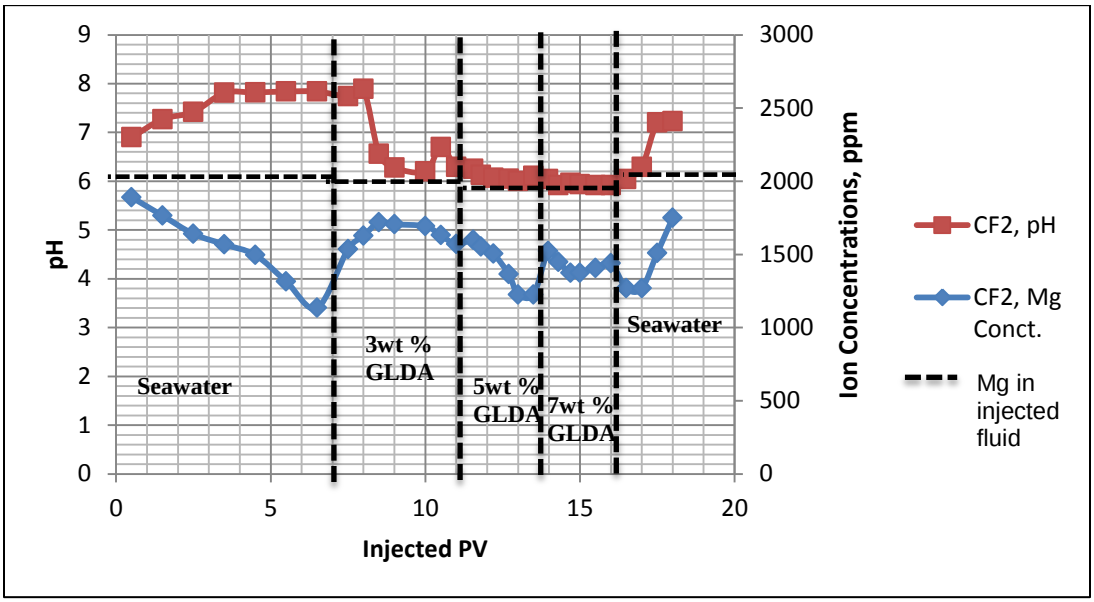

Figure D. 5: pH distribution and Mg^{+2} Concentration in the Produced Effluents from injection of Seawater (pH=7.7) followed by 3wt%, then 5wt% and 7wt% of GLDA at pH =4, Experiment 2.

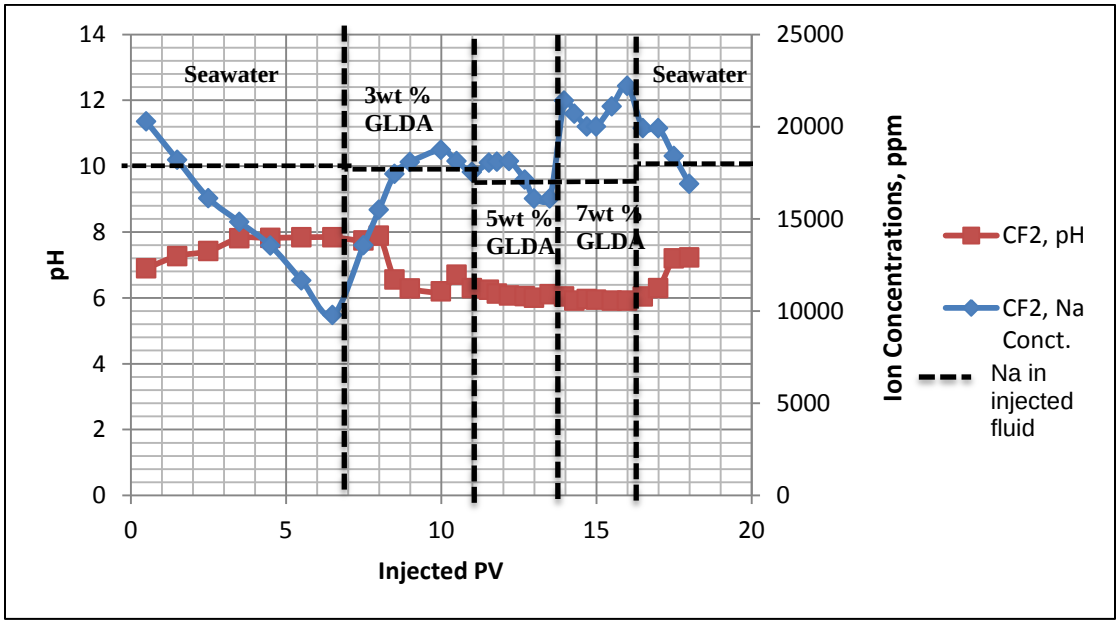

Figure D. 6: pH distribution and Na^{+} Concentration in the Produced Effluents from injection of Seawater (pH=7.7) followed by 3wt%, then 5wt% and 7wt% of GLDA at pH =4, Experiment 2.

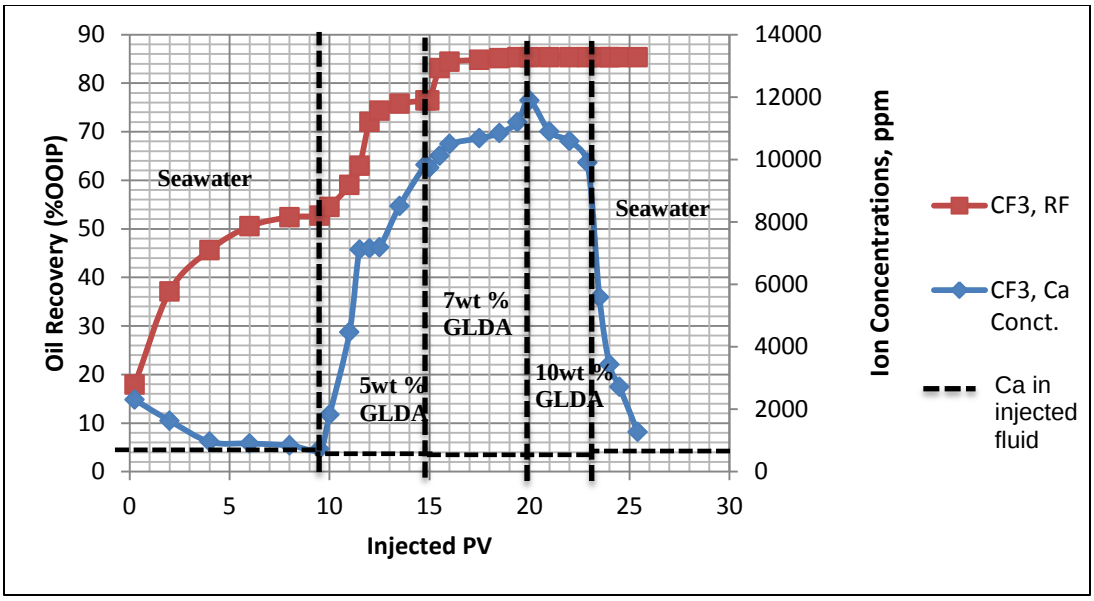

Figure D. 7: Oil Recovery and Ca^{+2} Concentration in the Produced Effluents from injection of Seawater (pH=7.7) followed by 5wt%, then 7wt% and 10wt% of GLDA at pH =4, Experiment 3.

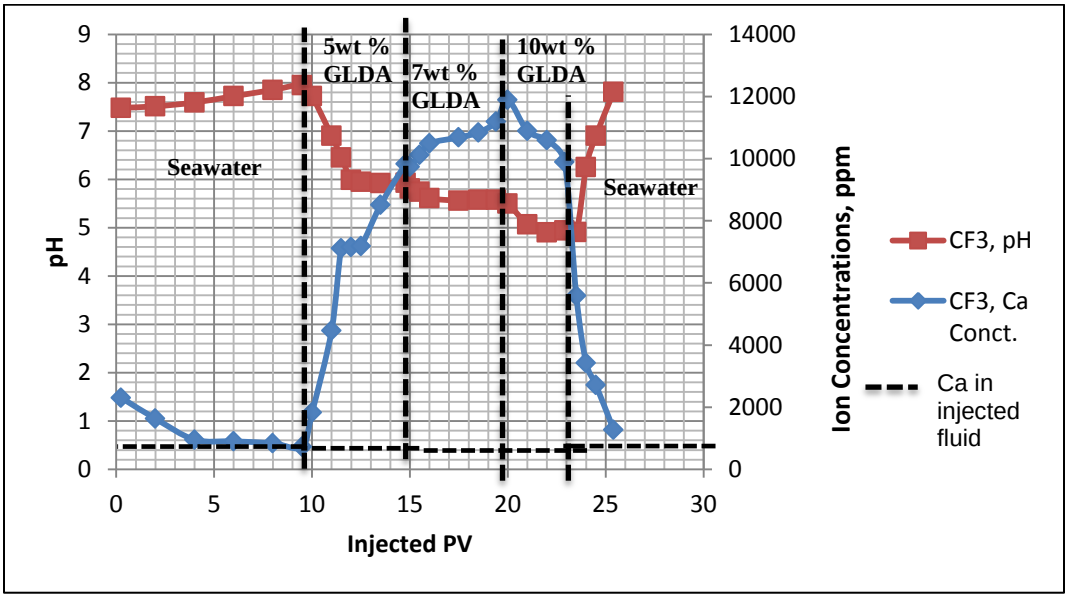

Figure D. 8: pH distribution and Ca^{+2} Concentration in the Produced Effluents from injection of Seawater (pH=7.7) followed by 5wt%, then 7wt% and 10wt% of GLDA at pH =4, Experiment 3.

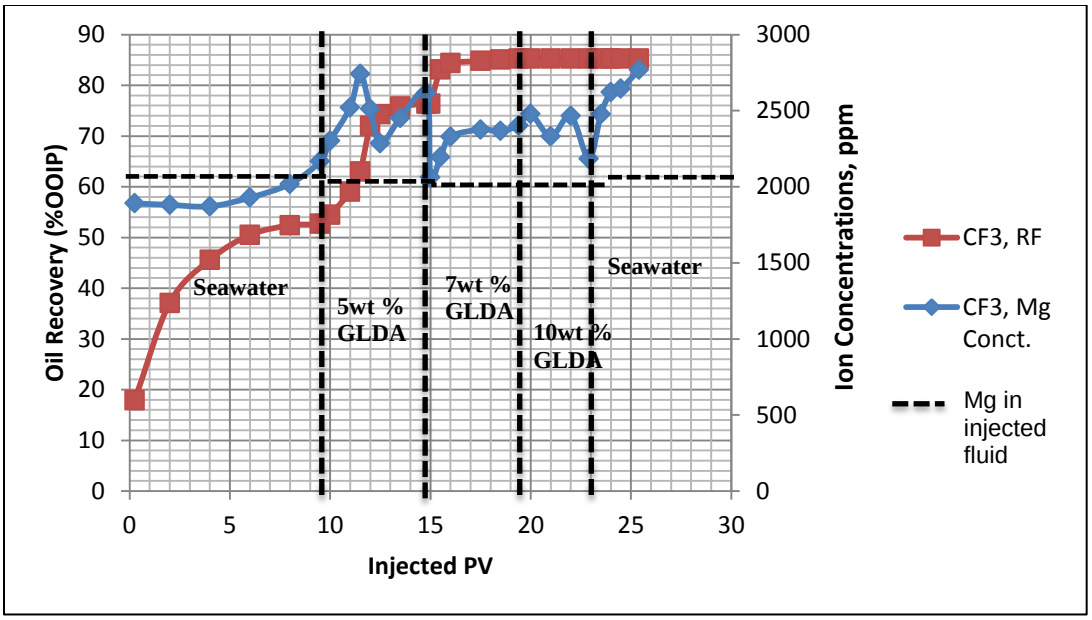

Figure D. 9: Oil Recovery and Mg^{+2} Concentration in the Produced Effluents from injection of Seawater (pH=7.7) followed by 5wt%, then 7wt% and 10wt% of GLDA at pH =4, Experiment 3.

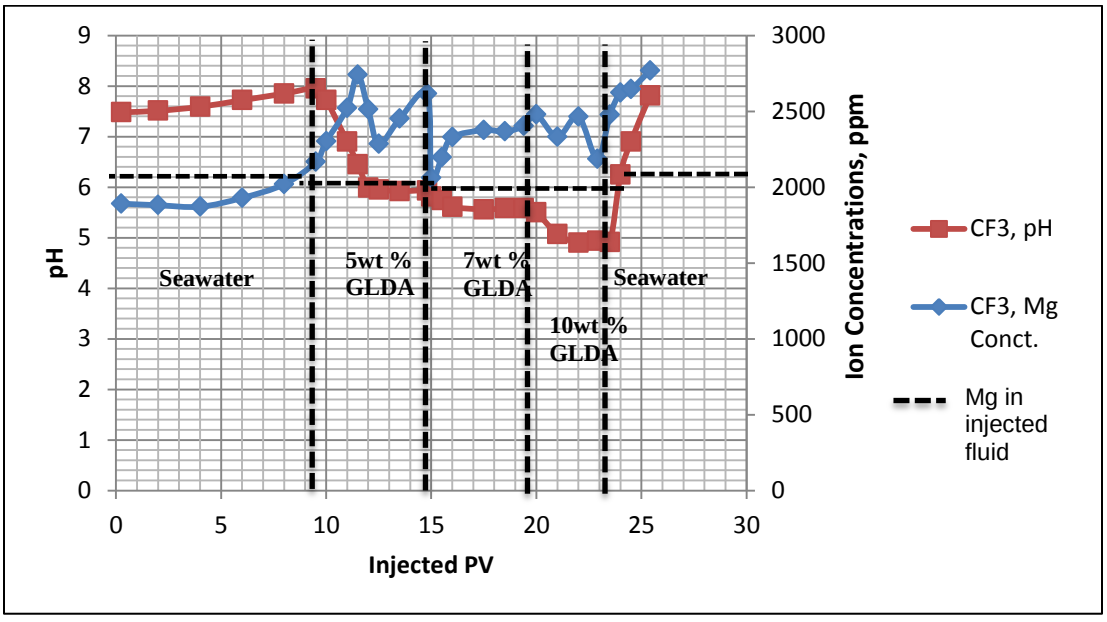

Figure D. 10: pH distribution and Mg^{+2} Concentration in the Produced Effluents from injection of Seawater (pH=7.7) followed by 5wt%, then 7wt% and 10wt% of GLDA at pH =4, Experiment 3.

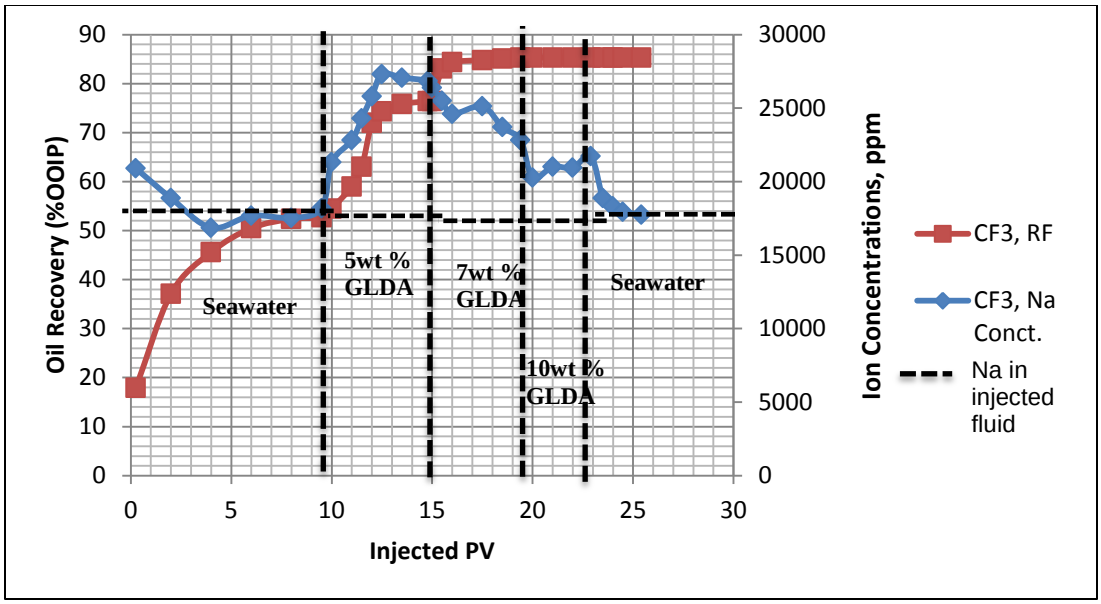

Figure D. 11: Oil Recovery and Na^+ Concentration in the Produced Effluents from injection of Seawater (pH=7.7) followed by 5wt%, then 7wt% and 10wt% of GLDA at pH =4, Experiment 3.

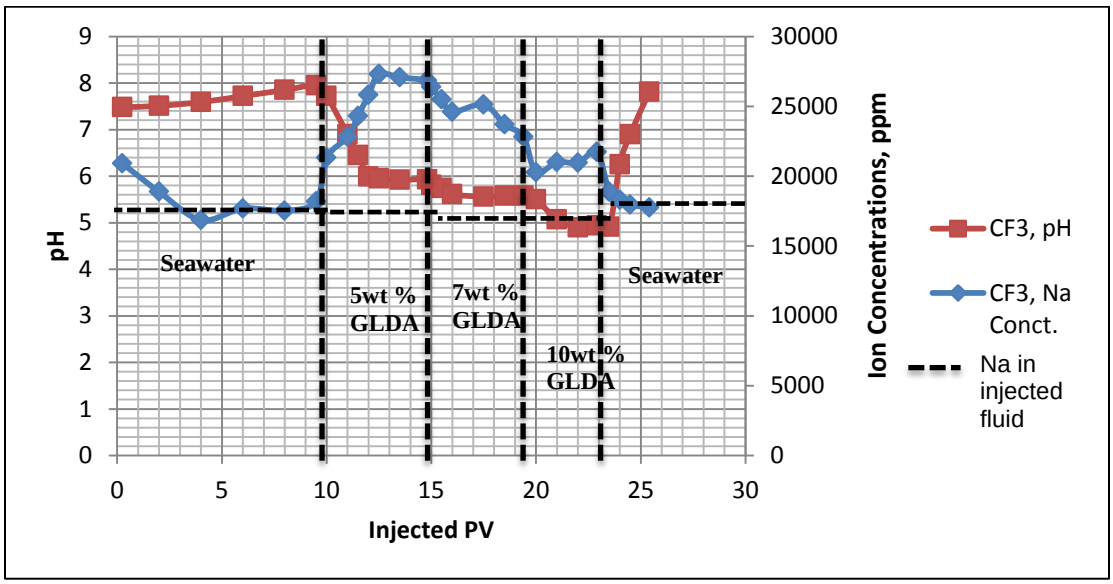

Figure D. 12: pH distribution and Na^+ Concentration in the Produced Effluents from injection of Seawater (pH=7.7) followed by 5wt%, then 7wt% and 10wt% of GLDA at pH =4, Experiment 3.

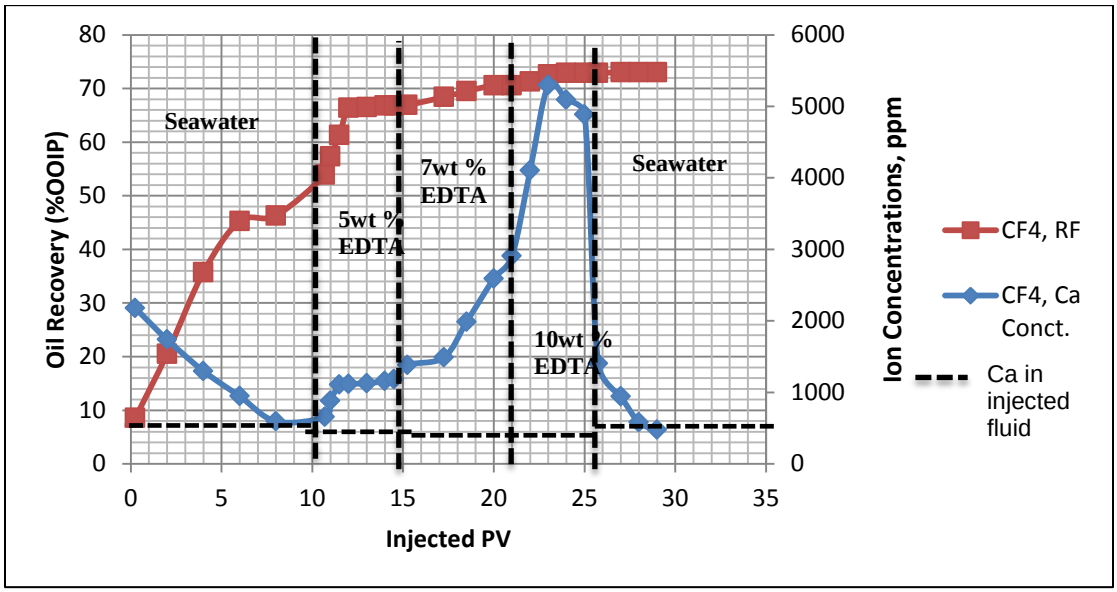

Figure D. 13: Oil Recovery and Ca^{+2} Concentration in the Produced Effluents from injection of Seawater (pH=7.7) followed by 5wt%, then 7wt% and 10wt% of EDTA at pH =6, Experiment 4.

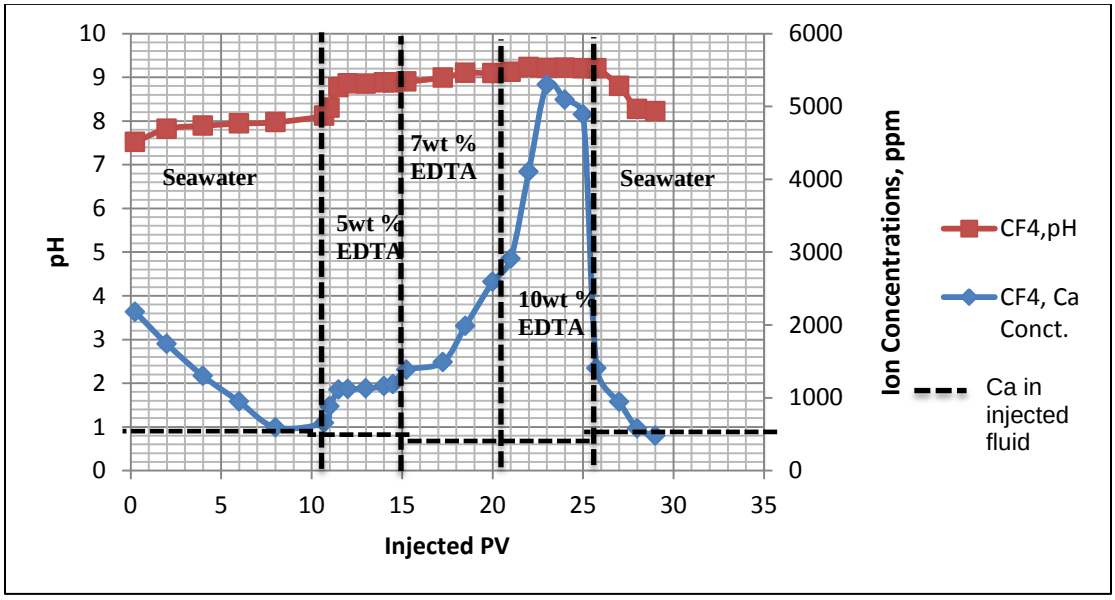

Figure D. 14: pH distribution and Ca^{+2} Concentration in the Produced Effluents from injection of Seawater (pH=7.7) followed by 5wt%, then 7wt% and 10wt% of EDTA at pH =6, Experiment 4.

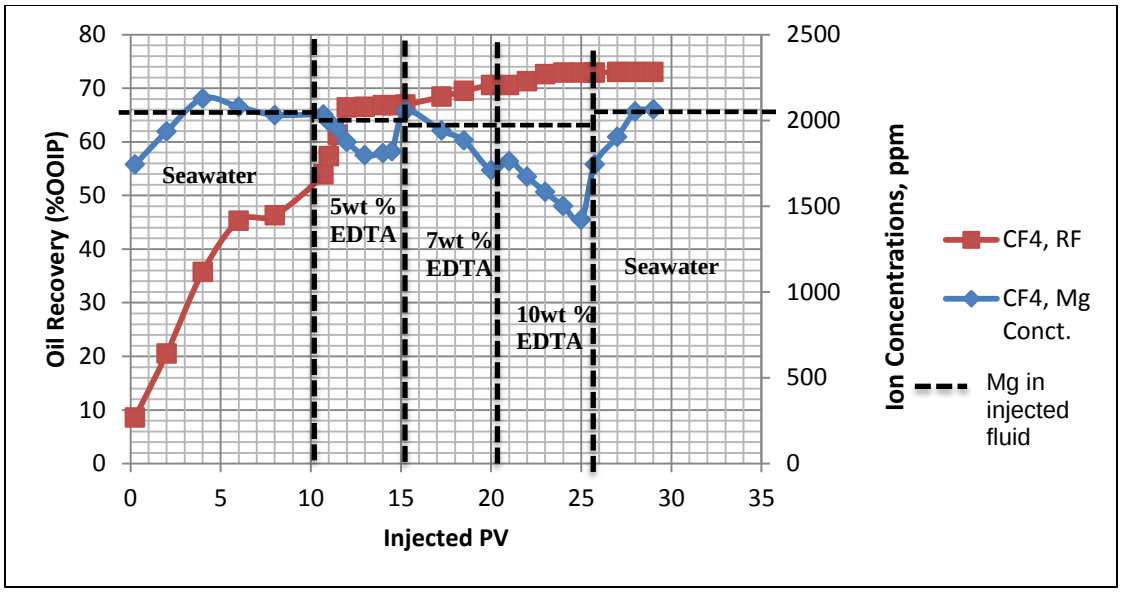

Figure D. 15: Oil Recovery and Mg^{+2} Concentration in the Produced Effluents from injection of Seawater (pH=7.7) followed by 5wt%, then 7wt% and 10wt% of EDTA at pH =6, Experiment 4.

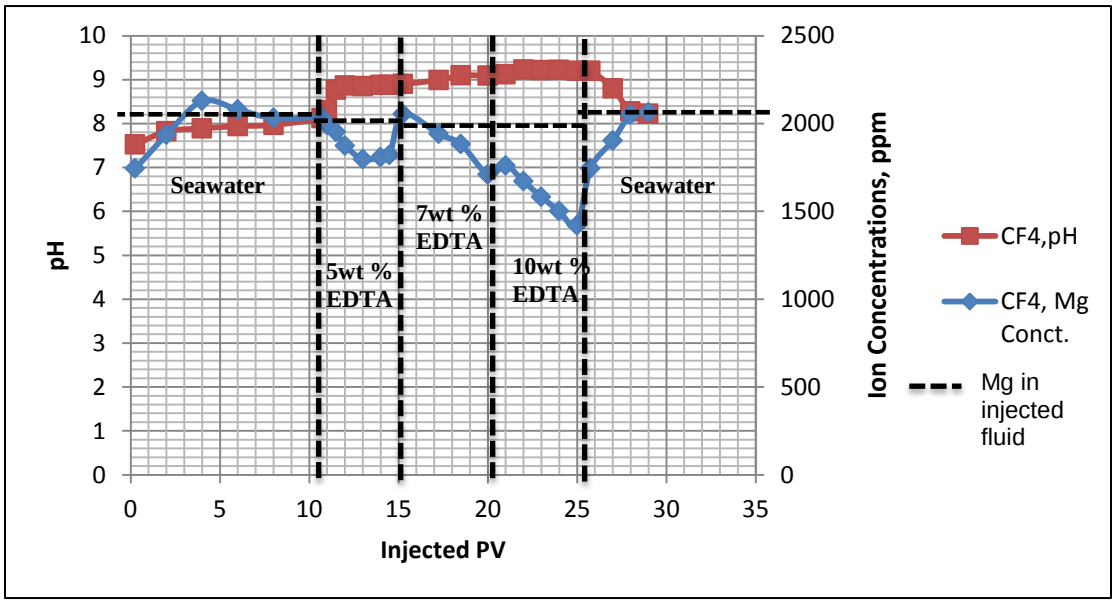

Figure D. 16: pH distribution and Mg^{+2} Concentration in the Produced Effluents from injection of Seawater (pH=7.7) followed by 5wt%, then 7wt% and 10wt% of EDTA at pH =6, Experiment 4.

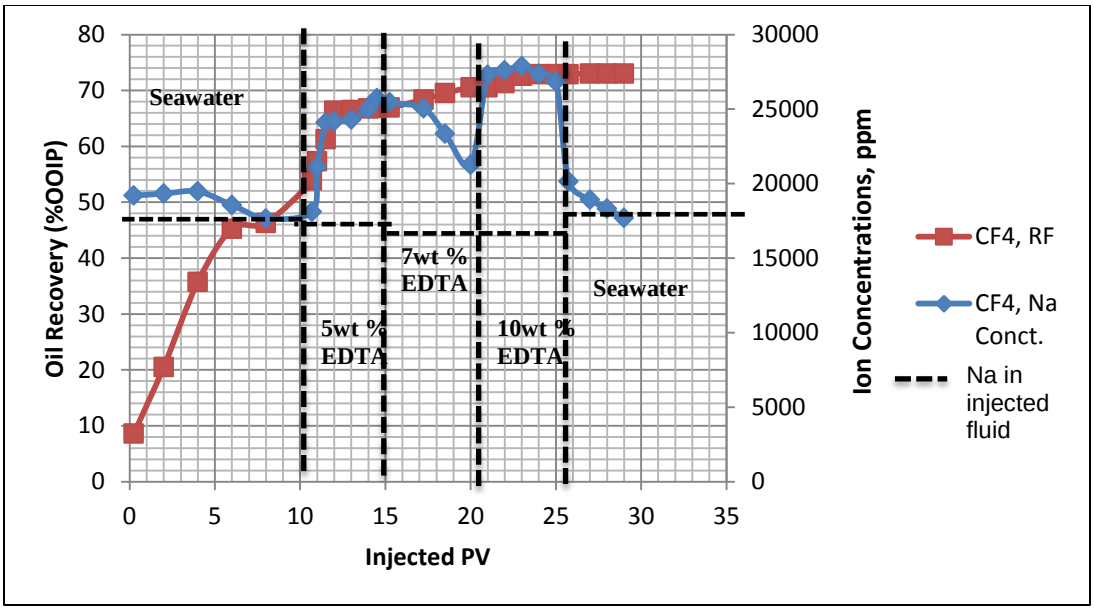

Figure D. 17: Oil Recovery and Na^+ Concentration in the Produced Effluents from injection of Seawater (pH=7.7) followed by 5wt%, then 7wt% and 10wt% of EDTA at pH =6, Experiment 4.

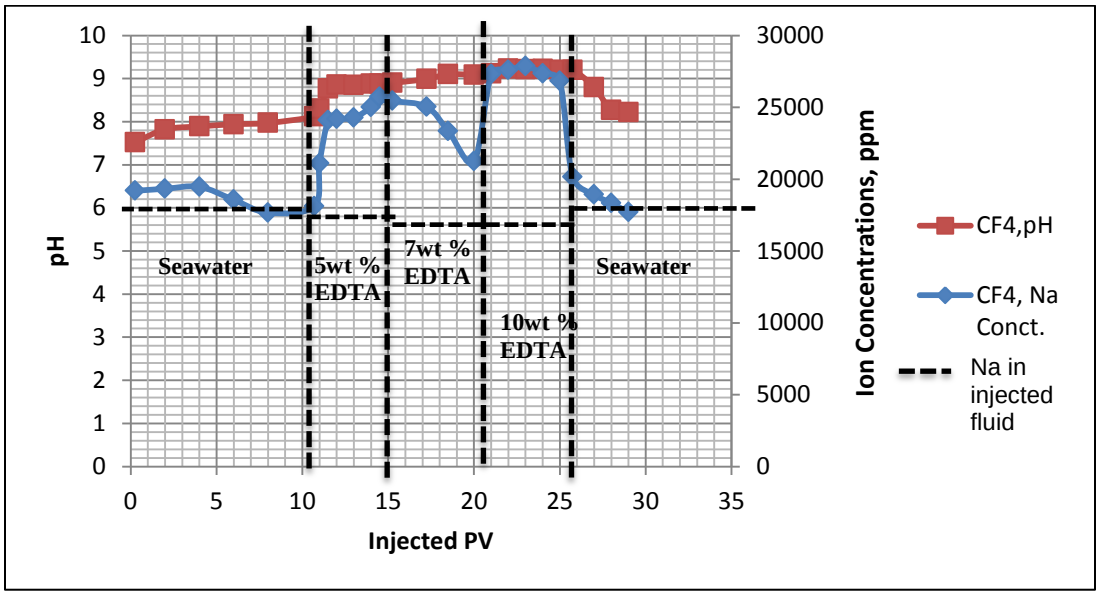

Figure D. 18: pH distribution and Na^+ Concentration in the Produced Effluents from injection of Seawater (pH=7.7) followed by 5wt%, then 7wt% and 10wt% of EDTA at pH =6, Experiment 4.

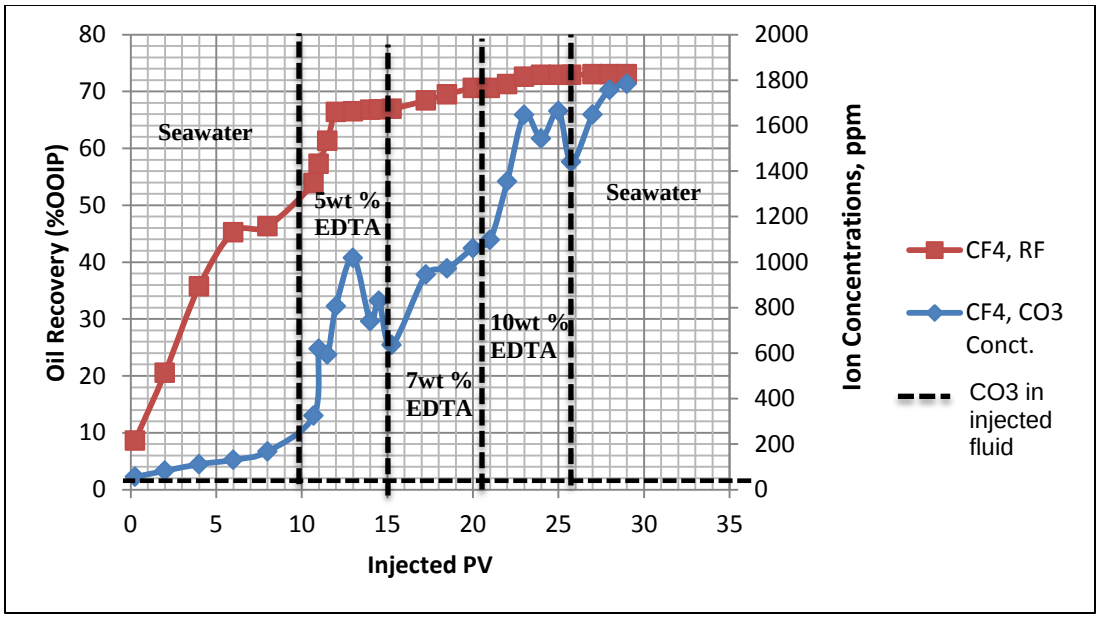

Figure D. 19: Oil Recovery and CO_3^{-2} Concentration in the Produced Effluents from injection of Seawater (pH=7.7) followed by 5wt%, then 7wt% and 10wt% of EDTA at pH =6, Experiment 4.

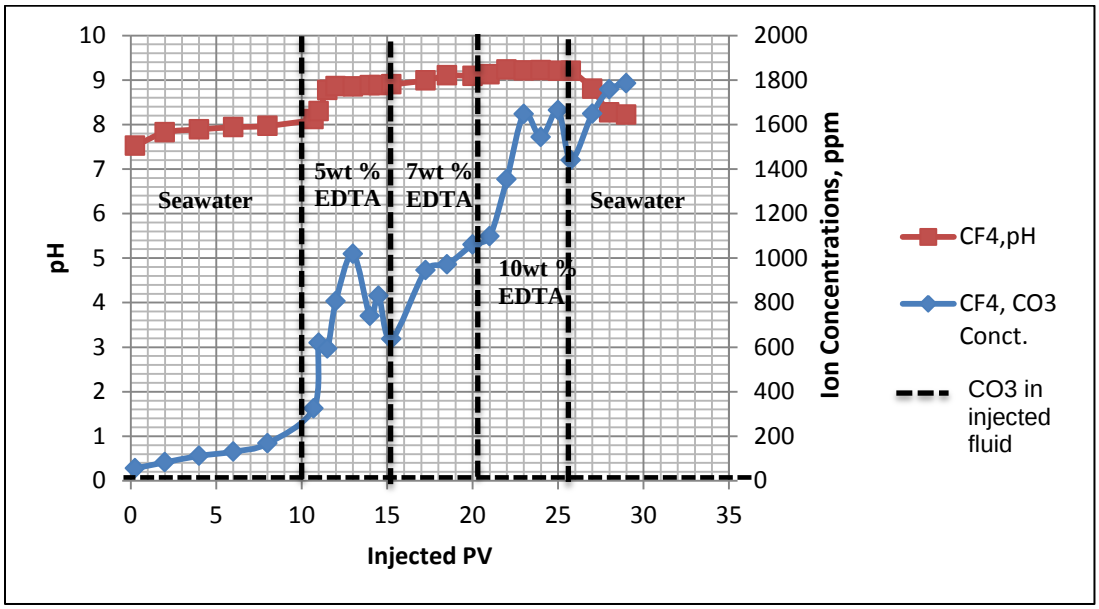

Figure D. 20: pH distribution and CO_3^{-2} Concentration in the Produced Effluents from injection of Seawater (pH=7.7) followed by 5wt%, then 7wt% and 10wt% of EDTA at pH =6, Experiment 4.

APPENDIX E: CT Scan Results

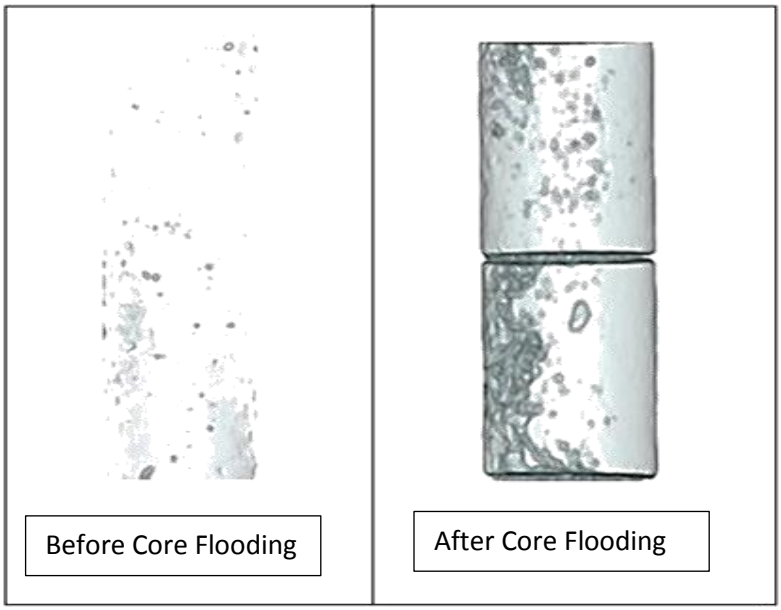

Figure E. 1: CT scan for core samples used in experiment 1, before and after core flooding.

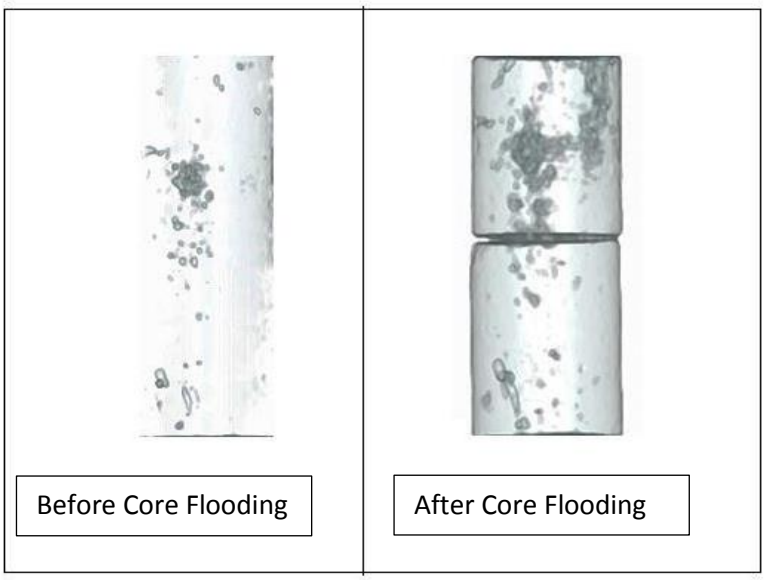

Figure E. 2: CT scan for core samples used in experiment 2, before and after core flooding.

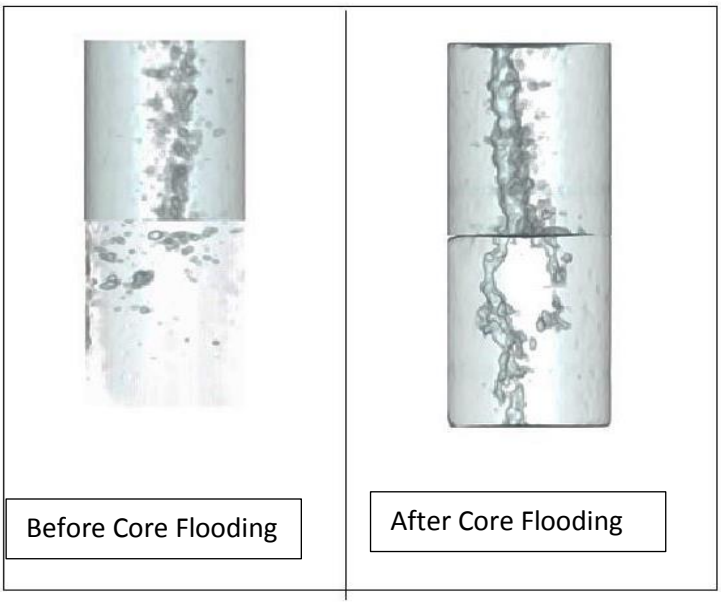

Figure E. 3: CT scan for core samples used in experiment 3, before and after core flooding.

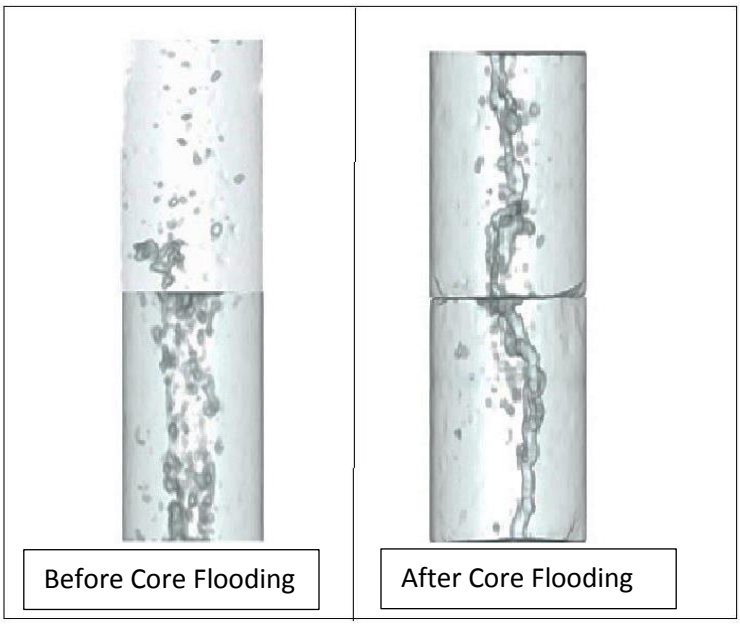

Figure E. 4: CT scan for core samples used in experiment 4, before and after core flooding.

APPENDIX F: Particle Size distributions for Zeta Potential Measurements

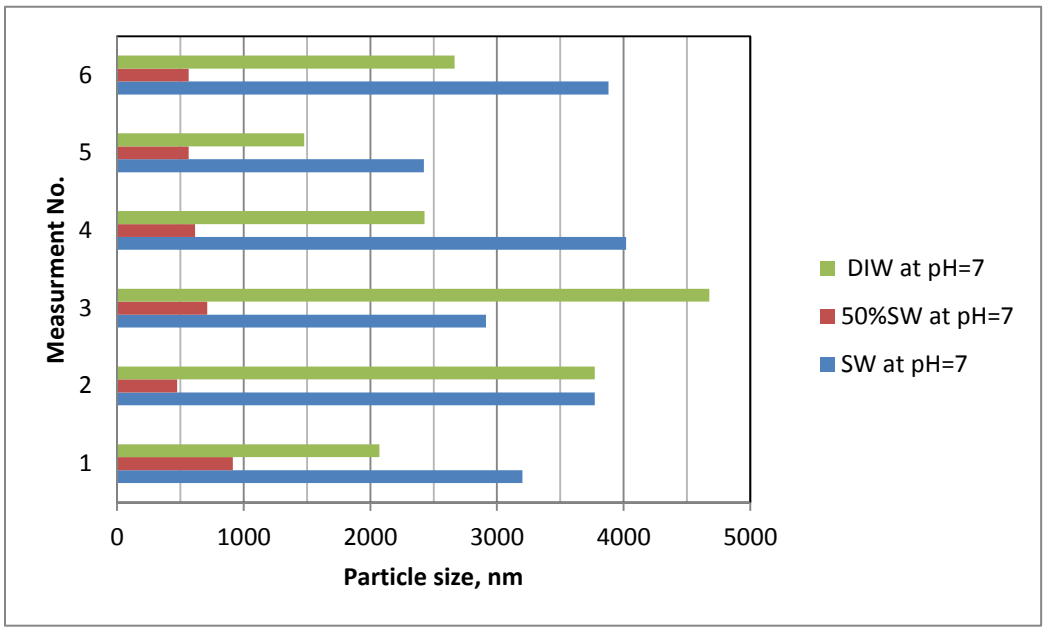

Figure F. 1: Particle size distributions for Limestone particles in DIW, in 50%SW, and in SW at pH=7, without EDTA.

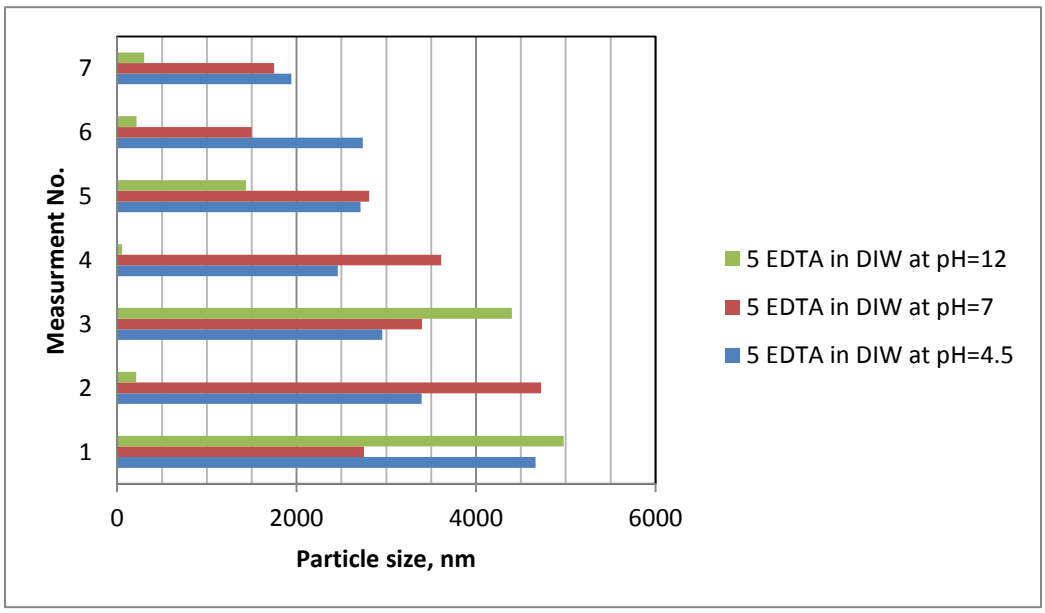

Figure F. 2: Particle size distributions for Limestone particles in 5wt%EDTA/DIW at pH= 4.5, 7, and 12.

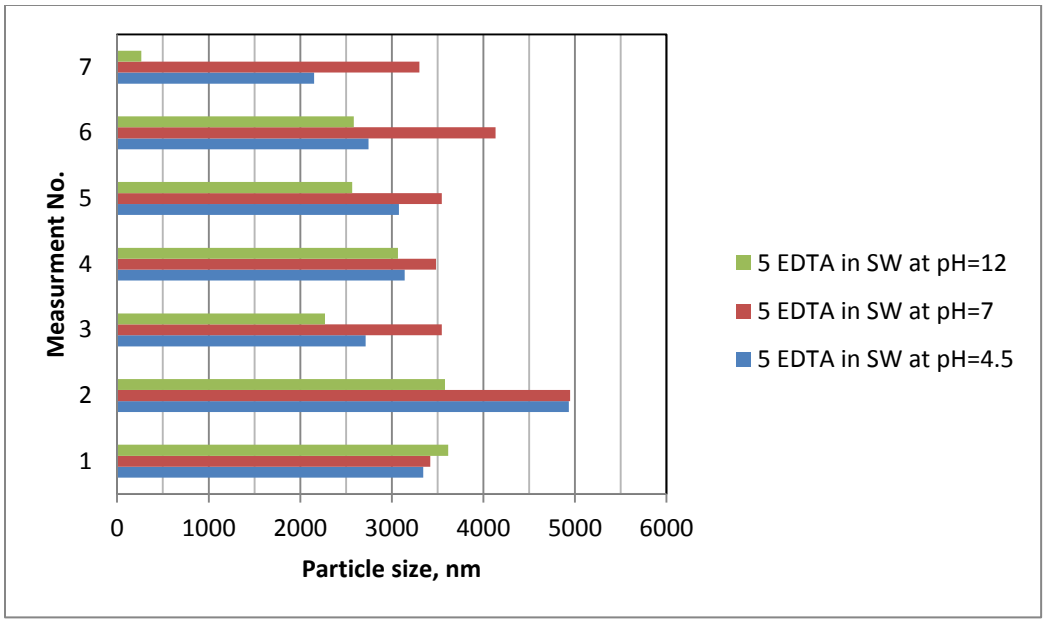

Figure F. 3: Particle size distributions for Limestone particles in 5wt%EDTA/SW at pH= 4.5, 7, and 12.

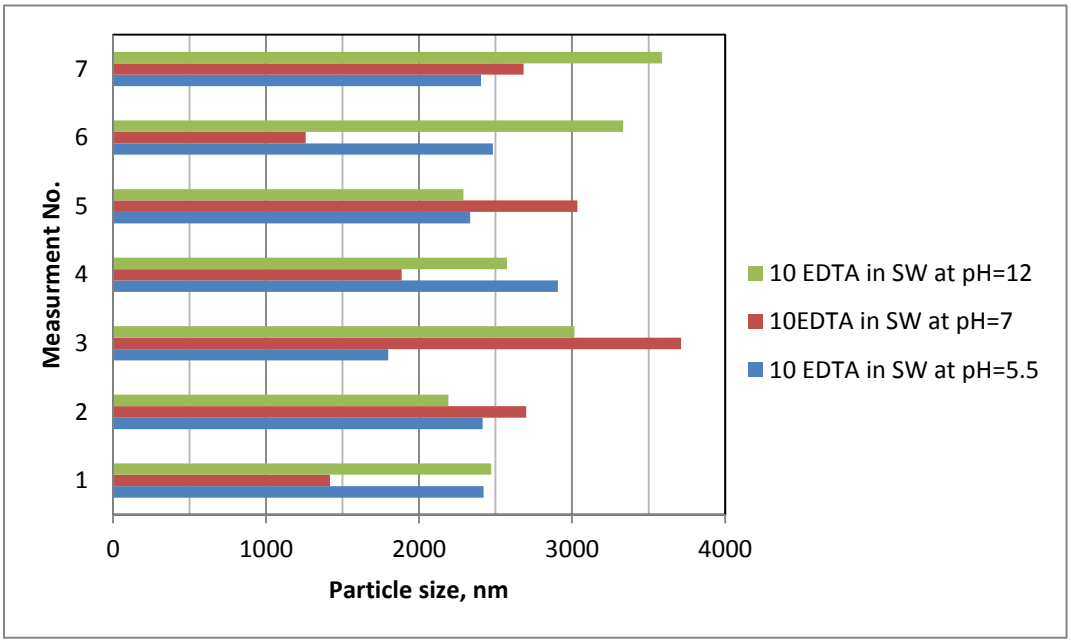

Figure F. 4: Particle size distributions for Limestone particles in 10wt%EDTA/SW at pH= 5.5, 7, and 12.

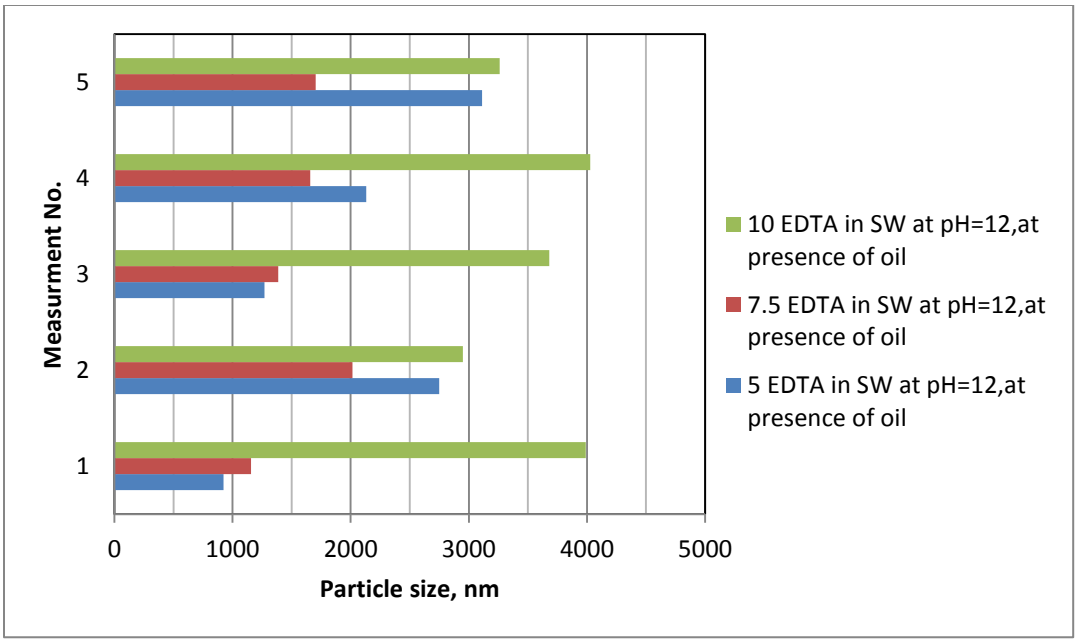

Figure F. 5: Particle size distributions for Limestone particles in 5, 7.5 and 10wt% of EDTA/SW at pH= 12, in the presence of crude oil.

REFERENCES

[1] Abdallah, W, Buckley, S, Carnegie, A, Edwards, J, Fordham, E 2007. "Fundamentals of Wettability.", oilfield review journal, page 44–61.

[2] Albert, A, Scheuerman, R , Templeton, C, Richardson, E 1983. "Higher-pH Acid Stimulation Systems.", Society of Petroleum Engineers of AIME, Journal Of Petroleum Technology,2175-84.

[3] Abu-Khamsin, S, Ahmad, S 2005. "Laboratory Study on Precipitation of Calcium Sulphate in Berea Sandstone Cores." , SPE106336 presented at the 2005 SPE Technical Symposium of Saudi Arabia Section held in Dhahran, Saudi Arabia, 14-16 May.

[4] AkzoNobel Functional Chemicals Product Stewardship Summary–Chelates: GLDA,2011

[5] Al-Khaldi, M, Nasr-El-Din, H, Sarma, H 2010. "Kinetics of the Reaction of Citric Acid With Calcite." SPE 118724 presented at the SPE International Symposium on Oilfield Chemistry, The Woodlands, Texas, USA, 20–22 April.

[6] Al-Khaldi, M, Nasr-El-Din, H, Blauch, M, Funkhouser, G 2005. "New Findings on Damage Potential, Geochemical Reaction Mechanisms, and Production Enhancement Applications for Citric Acid". SPE J. 10 (3): 267–275. SPE-82218-PA. doi: 10.2118/82218-PA.

[7] Al-Khaldi, M, Nasr-El-Din, H, Mehta, S, Al-Aamri, A 2007. "Reaction of citric acid with calcite". Chemical Engineering Science 62 (21): 5880–5896. doi: 10.1016/j.ces.2007.06.021

[8] Alotaibi, M, Naser-El-Din, H 2009. "Chemistry of Injection Water and its Impact on Oil Recovery in Carbonate and Clastic Formations." SPE 121565 presented at the 2009 SPE International Symposium on Oilfield Chemistry Held in the Woodlands, Texas, USA, 20-22 April.

[9] Alotaibi, M, Nasralla, R, Nasr-El-Din, H 2011. "Wettability Studies Using Low-Salinity Water in Sandstone Reservoirs." SPE 149942 Presented at the Offshore Technology Conference, Houston, USA, 3-6 May.

[10] Alotaibi, M, Nasr-El-Din, H 2011. 'Electrokinetics of limestone particles and crude-oil droplets in saline solutions' SPE Reservoir Evaluation & Engineering, vol. 14, no. 5, pp. 604–611.

[11] Alotaibi, M, Nasr-El-Din, H, Fletcher, J 2011, 'Electrokinetics of Limestone and Dolomite Rock Particles', SPE Reservoir Evaluation & Engineering, vol. 14, no. 5, pp. 594-603.

[12] Altunina, L, Kuvshinov, V, Stasyeva, L 2006, "Improved Cyclic-Steam Well Treatment With Employing Thermoreversible Polymer Gels." SPE 104330 Presented at Russian Oil and Gas Technical Conference and Exhibition held in Moscow, Russia, 3–6 October 2006.

[13] Anderson, W 1986, "Wettability Literature Survey — Part 1 : Rock /Oil/Brine Interactions and the Effects of Core Handling on Wettabiiity." SPE 13932 Journal of Petroleum Technology, October 1986, 1125-1144.

[14] Bernadlner, M, Thompson, K, Fogler, H 1992, "Effect of Foams Used During Carbonate Acidizing." SPE 21035 first presented at the 1991 SPE IntI. Symposium on Oilfield Chemistry held in Anaheim. CA, Feb. 20-22.

[15] Cayias, J, Schechter, R, Wade, W 1977, 'The utilization of petroleum sulfonates for producing low interfacial tensions between hydrocarbons and water.' J. Colloid Interface Sci. 59 (1): 31–38.

[16] Chang, S, Grigg, R 1999. "Effects of Foam Quality and Flow Rate on CO_2 - Foam Behavior at Reservoir Temperature and Pressure." SPE 56856 first presented at the 1998 SPE/DOE Improved Oil Recovery Symposium, Tulsa, Oklahoma, 19–22 April.

[17] Chen, P, Kishore M 2014 "Wettability Alteration in High Temperature Carbonate Reservoirs." SPE 169125 presented at the Eighteenth SPE Improved Oil Recovery Symposium held in Tulsa, Oklahoma, USA, 12–16 April.

[18] Craig, F 1971, 'The Reservoir Engineering Aspects of Waterflooding.' Second Edition. Society of Petroleum Engineers of AIME.

[19] Green, D, Willhite, P 1998, 'Enhanced Oil Recovery.' Society of Petroleum Engineers of AIME.

[20] Douglas, H, Walker, R 1950, 'The electrokinetic behavior of Iceland Spar against Aqueous Electrolyte Solutions.' Trans. Faraday Soc. 46: 559–568.

[21] Evertee, D 1994, 'Basic Principles of Colloid Science.' Royal Society of Chemistry, London, UK.

[22] Foster, W 1973 'A Low Tension Water flooding Process.' SPE-3803-PA, Journal of Petroleum Technology, vol. 25, no. 2, pp. 205-210.

[23] Fredd, C, Foglar, H 1997, "Chelating Agents as Effective Matrix Stimulation Fluids for Carbonate Formations." SPE 37212 presented at the 1997 SPE

international Symposium on oilfield Chemistry held in Houston,Texas, 18-21 February .

[24] Frenier, W, Fredd, C, Chang, F 2003, "A Biodegradable Chelating Agent Is Developed for Stimulation of Oil and Gas Formations." SPE80597 presented at the SPE/EPA/DOE Exploration and Production Environmental Conference held in San Antonio, Texas, U.S.A., 10–12 March.

[25] Frenier, W, Fredd, C, Chang, F 2001, "Hydroxyaminocarboxylic Acids Produce Superior Formulations for Matrix Stimulation of Carbonates." SPE 68924 presented at the SPE European Formation Damage Conference held in The Hague, The Netherlands, 21-22 May.

[26] Hirasaki, G, Miller, C, Puerto, M 2011, 'Recent Advances in Surfactant EOR.' SPE Journal, vol. 16, no. 4, pp. 889-907.

[27] Ghosh, P. 2009 'Colloid and Interface Science.' PHI Learning, New Delhi, Chapter 4

[28] Gumersky, K, Dzhafarov, I, Shakhverdiev, A Mamedov,Y 2000, 'In-Situ Generation of Carbon Dioxide : New Way To Increase Oil Recovery.' SPE 65170 presented at the SPE European Petroleum Conference held in Paris, France, 24–25 October.

[29] Hiemenz, P 1977, 'Principles of Colloid and Surface Chemistry.' Marcel Dekker Inc., New York, USA.

[30] Hill, H, Reisberg, J, Stegemeier, G 1973, 'Aqueous Surfactant Systems For Oil Recovery.', SPE-3798-PA ,Journal of Petroleum Technology 25 (2): 186–194.

[31] Jabbar, M, Al-Hashim, H, Abdallah, W 2013, 'Effect of Brine Composition on Wettability Alteration of Carbonate Rocks in the Presence of Polar Compounds', Paper SPE 168067 presented at the SPE Saudi Arabia Section Technical Symposium and Exhibition, SPE, 19-22 May, Al-Khobar, Saudi Arabia.

[32] Jankowski, D, Wolsky, A 1986, 'The Value of CO_2 to Today's Producer.' SPE 15036 presented at the Permian Basin Oil & Gas Recoveery Conference of the Society of Petroleum Engineers held in Midland, TX, March 13-14.

[33] Kasha, A 2014. 'Impact of Injection Water Chemistry on Zeta Potential of Carbonate Rocks.', M.S. Thesis, King Fahd University of Petroleum & Minerals, Saudi Arabia.

[34] Kassim, M 2012, 'The Role of Potential Determining Ions in Carbonate Rock - Seawater Interactions.', M.S. Thesis, King Fahd University of Petroleum & Minerals, Saudi Arabia.

[35] Khatere, S, Nasr-El-Din, H, De Wolf, C 2013, 'Thermal Decomposition of Chelating Agents and a New Mechanism of Formation Damage.' Paper SPE 165153 presented at the SPE European Formation Damage Conference and Exhibition held in Noordwijk, The Netherlands, 5–7 June 2013.

[36] Khatri, R, Chuang, S, Soong, Y, Gray, M 2006, 'Thermal and Chemical Stability of Regenerable Solid Amine Sorbent for CO_2 Capture.'Journal of Energy & Fuels 2006, Vol. 20,No.4, 1514-1520

[37] Hiorth, A, Cathles, L, Madland, M 2010,'The Impact of Pore Water Chemistry on Carbonate Surface Charge and Oil Wettability.' Transport in Porous Media, DOI 10.1007/s 11242-010-9543-6, 2010.

[38] Lindlof, J, Stoffer, K 1983, 'A Case Study of Seawater Injection Incompatibility.' Journal of Petroleum Technology 35(07):1256–62.

[39] Mahmoud, M, Abdelgawad, K 2013, 'Investigation of the Precipitation of Calcium Sulfate Scale during Low and High Salinity Water Injection in EOR Processes In Carbonate and Sandstone Reservoirs.' SPE 165162 presented at the SPE European Formation Damage Conference and Exhibition held in Noordwijk, The Netherlands, 5–7 June.

[40] Mahmoud, M, Abdelgawad, K 2014, 'A New Chemical EOR for Sandstone and Carbonate Reservoirs.' SPE 172183 presented at the SPE Saudi Arabia Section Annual Technical Symposium and Exhibition held in Al-Khobar, Saudi Arabia, 21-24 April.

[41] Mahmoud, M, Abdelgawad, K 2015, 'Chelating-Agent Enhanced Oil Recovery for Sandstone and Carbonate Reservoirs', SPE Journal, vol. 15, no. 2, pp. 483-495.

[42] Mahmoud, M, Abdelgawad, K 2014, 'High-Performance EOR System in Cabonate Reservoirs.' SPE 172182 presented at the SPE Saudi Arabia Section Annual Technical Symposium and Exhibition held in Al-Khobar, Saudi Arabia, 21-24 April.

[43] Mahmoud, M, Nasr-El-Din, H 2012. 'Modeling Flow of Chelating Agents during Stimulation of Carbonate Reservoirs.' SPE 150065 presented at the North Africa Technical Conference and Exhibition held in Cairo, Egypt, 20–22 February.

[44] Mahmoud, M, Nasr-El-Din, H, De Wolf, C, Lepage, J, Bemelaar, J 2011, 'Evaluation of a New Environmentally Friendly Chelating Agent for High-Temperature Applications.' SPE 127923 Presented at the International Fluid Dynamic Conference, Shiraz, Iran, 26–28 October.

[45] Moghadasi, J, Sharif, A, Kalantar, A, Motaie, E 2006, 'A New Model to Describe Formation Damage During Particle Movement and Deposition in

Porous Media.' SPE 99391 presented at the SPE Europec/EAGE Annual Conference and Exhibition held in Vienna, Austria, 12–15 June.

[46] Mohamed, I, He, J, Mahmoud, M, Nasr-El-Din, H 2010, 'Effects of Pressure , CO_2 Volume , and the CO_2 to Water Volumetric Ratio on Permeability Change during CO_2 Sequestration.' SPE 136394 presented at the Abu Dhabi International Petroleum Exhibition & Conference held in Abu Dhabi, UAE, 1–4 November.

[47] Rodríguez, K, Araujo, M 2006, 'Temperature and pressure effects on zeta potential values of reservoir minerals.' Journal of Colloid and Interface Science 300 (2): 788–794.

[48] Smani, M, Blazy, P, Cases, J 1975, 'Beneficiation of Sedimentary Moroccan Phosphate Ores—Part II: Electrochemical Phenomena at the Calcite/Aqueous Interface.' Trans. Soc. Min. Eng. (SME/AIME) 258: 174–176.

[49] Shiau, B, Hsu, T, Roberts, B, Harwell, J 2010, 'Improved Chemical Flood Efficiency by In Situ CO_2 Generation.' SPE 129893 presented at the 2010 SPE Improved Oil Recovery Symposium held in Tulsa, Oklahoma, U.S.A., 24-28 April.

[50] Szilágyi, P 2007, 'Study of Iron-Chelates in Solid State and Aqueous Solutions Using Mössbauer Spectroscopy.'

[51] Yarar, B. Kitchener, J 1970, 'Selective Flocculation of Minerals: 1- Basic Principles, 2- Experimental Investigation of Quartz, Calcite and Galena.' Trans. IMM C 79: 23–33.

[52] Yousef, A, Al-saleh, S, Al-Jawfi, M 2012, 'The Impact of the In Injection Water Chemistry on Oil Recovery from Carbonate Reservoirs.' Paper SPE 154077 presented at the SPE EOR Conference at Oil and Gas West Asia Held in Muscat,Oman, 16-18 April.

[53] Zahid, A, Shapiro, A, Skauge, A 2012, 'Experimental Studies of Low Salinity Waterflooding Carbonate: A New Promising Approach.' Paper SPE 155625, presented at the EOR conference at Oil and Gas west Asia, Muscat, Oman, April 16-18.

[54] Zhang, P, Austad, T 2006, 'Wettability and oil recovery from carbonates: Effects of temperature and potential determining ions', Colloids and Surfaces A: Physicochemical and Engineering Aspects, vol. 279, no. 1-3, pp. 179-187.

[55] Zhang, P, Tweheyo, M, Austad, T 2007, 'Wettability alteration and improved oil recovery by spontaneous imbibition of seawater into chalk: Impact of the potential determining ions Ca^{2+}, Mg^{2+}, and SO_4^{2-}'Colloids and Surfaces A: Physicochemical and Engineering Aspects **301** (1–3): 199–208.

VITAE

Name:	Amjed Mohammed Hassan Sheikh Mohammed
Nationality:	Sudanese
Date of Birth:	December 21, 1989
Email :	amjed.moh06@gmail.com
Address:	Al-Emtidad 3, Khartoum, Sudan.

Academic Background:

M.Sc. in Petroleum Engineering, December 2015
Department of Petroleum Engineering
College of Engineering
King Fahd University of Petroleum & Minerals,
Dhahran, Saudi Arabia.

B.Sc. in Petroleum Engineering, August 2011
Department of Petroleum and Natural Gas Engineering
Faculty of Engineering
University of Khartoum
Khartoum, Sudan.

Published Papers:

Hassan, A.M., Hossain, M.E. and Rammay, M.H., "Memory-based Diffusivity Equation: A Comprehensive Study on Variable Rock and Fluid Properties" Journal Nature Science and Sustainable Technology, 9(4), 2015, accepted on August 01, 2015, in press.
.https://www.novapublishers.com/catalog/product_info.php?products_id=57023.

Hassan, A.M., Hossain, M.E. and Rammay, M.H., "Investigation of Reservoir Heterogeneity Using Memory-Based Diffusivity" Journal Nature Science and Sustainable Technology, 9(4), 2015, accepted on August 01, 2015, in press.
https://www.novapublishers.com/catalog/product_info.php?products_id=57023.

Rammay, M.H., **Hassan, A.M.,** and Hossain, M.E., "A Comparative Study of Porosity and Permeability Variations Using Darcy and Memory-based Diffusivity Equations" Journal Nature Science and Sustainable Technology, 10(1), 2016, accepted on Sep 02, 2015, in press.